UNIVERSITA' DEGLI STUDI DI MILANO-BICOCCA

Facoltà di Scienze Matematiche, Fisiche e Naturali

Dipartimento di Biotecnologie e Bioscienze

DOTTORATO DI RICERCA IN BIOLOGIA – CICLO XXIV

SETTORE SCIENTIFICO DISCIPLINARE BIO-09

"FUNCTIONAL REGENERATION OF THE MESO-CORTICO-LIMBIC DOPAMINERGIC SYSTEM AS A MODEL TO STUDY NOVEL NEUROREPARATIVE STRATEGIES"

Dott.ssa Elena Dossi

Matricola: 055467

Coordinatore: Prof. Enzo Wanke

Tutor: Prof. Enzo Wanke

Anno Accademico 2011/2012

In collaboration with:

Prof. Peter Illes

Prof. Heike Franke

Dr. Claudia Heine

UNIVERSITÄT LEIPZIG

Rudolf-Boehm-Institut für Pharmakologie und
Toxikologie, Universität Leipzig
Härtelstrasse 16-18, D-04107 Leipzig, Germany

Supported by

fondazione cariplo

"Più affascinante della foresta vergine amazzonica: il Sistema Nervoso Centrale".

"A cento anni ho perso un po' la vista, molto l'udito. Alle conferenze non vedo le proiezioni e non sento bene. Ma penso più adesso di quando avevo vent'anni. Il corpo faccia quello che vuole. Io non sono il corpo: io sono la mente".

(Rita Levi Montalcini)

TABLE OF CONTENTS

1. INTRODUCTION

Dopaminergic neurons in the ventral mesencephalon send projections to different forebrain structures, forming a complex neuromodulatory system crucial for many cognitive processes and motor functions (Lapish et al., 2007). They are located in the substantia nigra (SN; A9 cell group) and in the ventral tegmental area (VTA; A10 cell group; Oades and Halliday, 1987). Prefrontal, orbitofrontal and cingulated cortices receive the most marked innervation from the VTA; projections from the VTA to the medial prefrontal cortex (mPFC) constitute a portion of the mesocortical dopamine system (Steketee et al., 2003). Much of this connectivity is bidirectional (Fuster, 2001): the mPFC receives dopaminergic afferents from the VTA and it sends glutamate projections to both the VTA and the nucleus accumbens. Furthermore, the mesocortical dopamine system is involved in a great variety of brain functions, such as working memory, attention selection and memory retrieval, because of its interconnections with brain areas processing external information as well as internal information (Miller et al., 2002).

Dopaminergic afferents from the mesencephalon seem to have a crucial role in the normal development of the PFC as well as in the regulation of neuronal activity in this brain area (Lewis et al., 1998). In fact, an abnormal maturation and alterations of the mesocortical projections to the PFC have been suggested to be involved in the development of psychostimulant-induced sensitization and in the

pathophysiology of several disorders, such as schizophrenia (Goldstein and Deutch, 1992), addiction (Steketee et al., 2003; Kauer, 2004; Van den Heuvel and Pasterkamp, 2008) or attention-deficit/hyperactivity disorder (Sullivan and Brake, 2003).

The analysis of the formation and development of functional connections in the Central Nervous System needs suitable model systems to understand the basic, functional mechanisms (Hofmann et al., 2004). We have reconstructed parts of the mesocorticolimbic dopaminergic system using the model of organotypic co-cultures of tissue slices from the VTA/SN-complex and the PFC (Franke et al., 2003; Heine et al., 2007). In fact, organotypic brain slices are closer to the *in vivo* situation than cell cultures; unlike acute slice preparation they are suitable for experiments over extended periods of time (Hofmann and Bading, 2006) and they represent the most intact culture system for studying cortex function in isolation (Gähwiler et al., 1997; Karpiak and Plenz, 2002; Stewart and Plenz, 2008); furthermore, by combining organotypic cultures with microelectrode array (MEA) recordings, it is possible to simultaneously and repeatedly perform extracellular, non-invasive, multi-site recordings from electrodes covering the whole preparation, and to monitor long-term processes of neurite outgrowth and development and synapse formation at a functional level (Egert et al., 1998; Beggs and Plenz, 2003 and 2004; Hofmann et al., 2004).

The aim of the present study was to characterize the developmental features of the VTA/SN-PFC co-cultures maintained on multielectrode array platforms, in order to study the functionality of

the neuronal projections which have been demonstrated to grow *in vitro* between the two areas of the cultures (Franke et al., 2003; Heine et al., 2007). Furthermore, we validated the system as an useful pharmacological tool to study the effects of different neuromodulatory substances.

2. THE MESOCORTICOLIMBIC SYSTEM

Two major ascending dopaminergic pathways can be identified in the mammalian Central Nervous System (CNS): the nigrostriatal system, which originates in the substantia nigra and projects predominantly to the striatum, and the mesocorticolimbic system, whose projections arise from the ventral tegmental area (VTA) and reach the prefrontal cortex (PFC), hippocampus, amygdala and nucleus accumbens. This latter system can be further subdivided into two subsystems involved in different neurological functions: the mesolimbic and the mesocortical systems, according to the localization of the cell bodies in the VTA and their projection areas (Williams and Goldman-Rakic, 1998; Adell and Artigas, 2004).

2.1 - THE VENTRAL TEGMENTAL AREA (VTA)

Dopaminergic cells in the ventral midbrain have a fundamental role for the control of cognitive and motor behaviours and are associated with multiple neurodegenerative diseases and psychiatric disorders (Van den Heuvel and Pasterkamp, 2008). These cells have been divided into three anatomically and functionally distinct subgroups: the ventral tegmental area (VTA, A10 group) consists of a few heterogeneous groups of cells, lying together close to the midline on the floor of the midbrain (mesencephalon) (Oades and Halliday, 1987); laterally to the VTA, the A9 group corresponds to the neurons

of the substantia nigra pars compacta (SNc), involved in the control of voluntary movement, while the A8 group defines the retrorubal field (RRF), which has a role in the regulation of emotions and reward (Van den Heuvel and Pasterkamp, 2008).

2.1.1 – ANATOMY OF THE VTA

The group of cells which constitutes the VTA can be divided into different nuclei. The cells, which are located on the lateral borders of the A10 area, constitute the *Nucleus paranigralis* (Npn). According to an immunocytochemical study of tyrosine hydroxylase, performed by Pearson et al. (1983), this nucleus results clearly distinguishable from another closely packed group of small, round, oval or stellate cells, located below the exits of the third nerve and named *N. parabrachialis pigmentosus* (Npbp). Rostrally the VTA borders on the diencephalon with the *N. interfascicularis* (Nif), containing small, tightly packed cells, while it distributes dorsally in the *N. linearis* (Nln) *caudalis and rostralis*, characterized mainly by medium sized and oval or fusiform cells (Oades and Halliday, 1987). The estimated number of neurons in the adult mesodiencephalic dopamine system ranges from 20,000-30,000 in mice (with different proportion of dopaminergic cells in Npn and Npbp) to 400,000-600,000 in humans; these neurons form forebrain projections and receive inputs from various brain regions (Adell and Artigas, 2004; Van den Heuvel and Pasterkamp, 2008).

2.1.2 – CELLULAR ORGANIZATION IN THE VTA

Ascending dopaminergic (DAergic) projections from the VTA, which originate from VTA principal neurons, have important roles in different neural functions as motivation, attention, reward, learning and memory. Furthermore, in the VTA there is also a substantial number of non-DAergic projection neurons, or secondary neurons, which are γ-aminobutyric acidergic (GABAergic; Fig. 1; Johnson and North, 1992). This latter class of cells represents 15-20 % of the total neuronal population and contributes to the same functions as DAergic neurons (Carr and Sesack, 2000a). DAergic and GABAergic neurons in the VTA and SN form subpopulations, which differ for their electrophysiological properties, regulation by neuropeptides and vulnerability (for DAergic cells) to neurodegeneration, and this diversity is at least partly linked to the anatomical organization of these two regions and their inputs and outputs (Korotkova et al., 2004).

DOPAMINERGIC NEURONS. Electrophysiological properties of DAergic cells in the VTA and SN have been studied extensively. This population represents the VTA principal neurons and they have been reported to have slower firing frequencies (1-8 Hz) and a longer action potential (AP) duration (2-4 ms; Fig. 2) than VTA secondary cells; they are sensitive to opioids and stain positive for tyrosine hydroxylase (TH) (Johnson and North, 1992). Morphologically, VTA DAergic neurons show a large or a fusiform soma with multi- or bipolar dendrite arborizations; they project their axons mainly to the nucleus accumbens (NAcc; mesolimbic projection) and the PFC

(mesocortical projection) (Oades and Halliday, 1987; Grace and Onn, 1989).

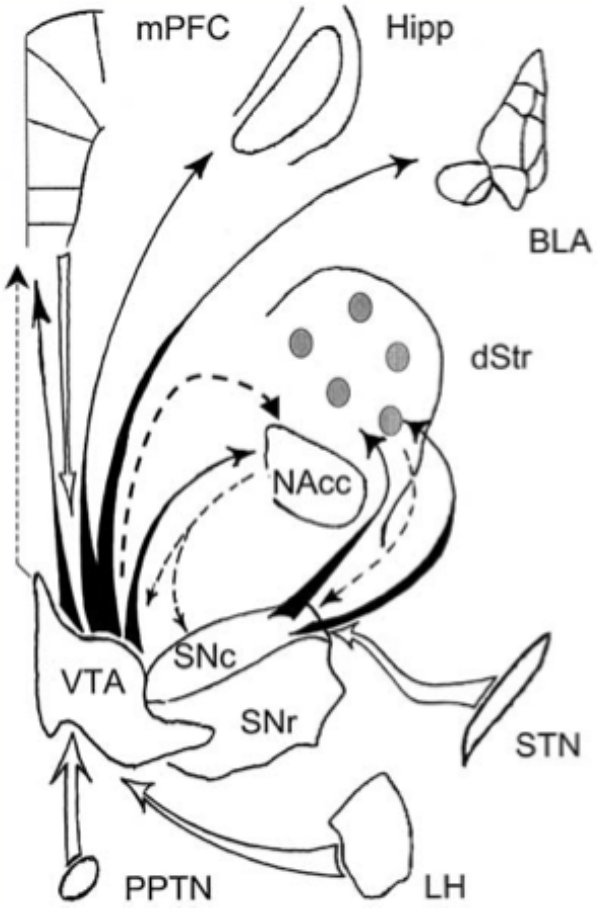

Figure 1. A simplified scheme of the connectivity profile of VTA and SNc. Filled arrows indicate dopaminergic projections; dashed arrows, GABAergic; white arrows, glutamatergic pathways. Ventral portion of SNc projects to striatal patches (grey circles), while dorsal SNc, to striatal matrix. mPFC, medial prefrontal cortex; hipp, temporal hippocampus; BLA, basolateral complex of the amygdala; NAcc, nucleus accumbens; dStr, dorsal striatum; STN, subthalamic nucleus; PPTN, peduncolopontine tegmental nucleus; LH, lateral hypothalamic area (from Korotkova et al., 2004).

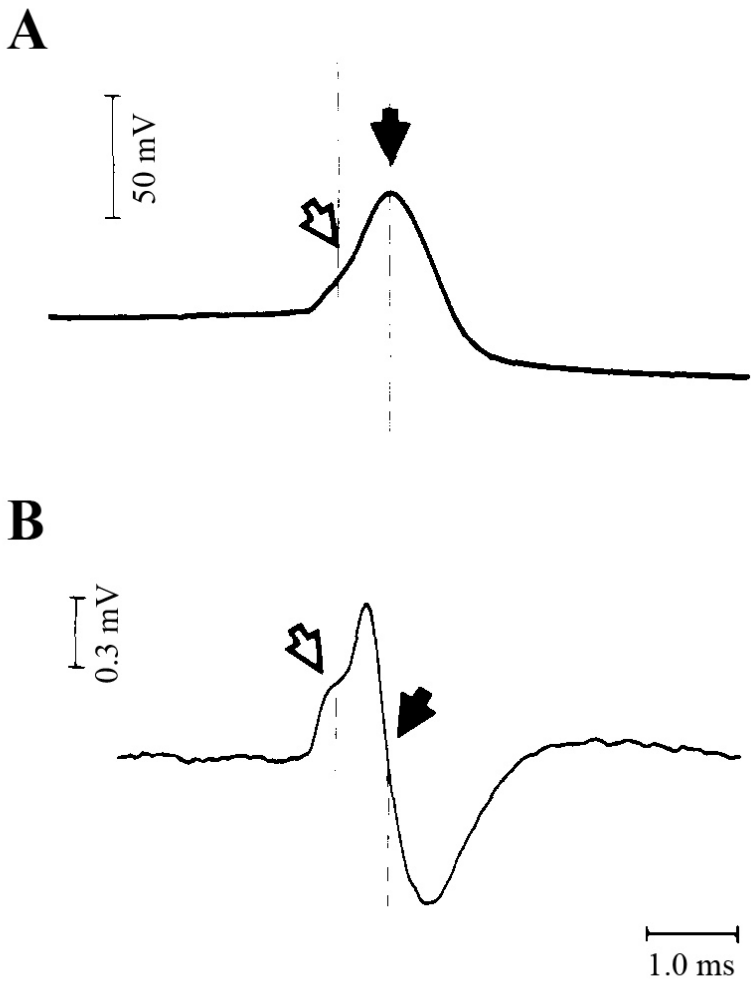

Figure 2. Comparison of extracellularly and intracellularly recorded spontaneously occurring action potentials from dopamine midbrain neurons. A) Spontaneously occurring DA action potential recorded intracellularly, demonstrating an inflection in the rising phase (open arrow). B) Extracellular recording of a DAergic neuron action potential. A notch is commonly observed in the positive phase (open arrow). There is a correspondence between the inflection in the rising phase of the intracellular action potential and the notch in the positive phase of the extracellular one. The zero crossing of the extracellular record occurs at the peak of the intracellular action potential (black filled arrows): thus, the long negative extracellular component is a consequence of the long falling phase of the intracellularly recorded action potential (adapted from Grace and Bunney, 1983a).

DAergic neuron dendrites show spinule-like protrusions at irregular intervals, with the dendrites terminating in forks or tufts; these dendritic terminals consist of 2-3 fine processes, which are able to wrap around another terminal (in the VTA or SN), similar to what has been described for the basket-like terminations of axons around the base of cortical pyramidal cells (Grace and Bunney, 1983b). This organization could serve as dendritic release sites of DA on non-DAergic neurons (Grace and Onn, 1989).

DAergic neurons can exhibit two different modes of spike firing: tonic single spike activity and burst spike firing (Grace and Bunney, 1984 a and b; Koyama et al., 2005; Goto et al., 2007).

Tonic firing (Fig. 3A) consists of spontaneously occurring baseline spikes, driven by pacemaker-like membrane currents of DAergic cells (Grace and Bunney, 1984a and 1984b). In fact, pacemaking in VTA DAergic neurons depends primarily on two sodium-permeable conductances: a voltage-independent background sodium leak current, which is the largest depolarizing current during most of the inter-spike interval (between ≈ -65 mV and ≈ -55 mV), and a TTX-sensitive, voltage-dependent sodium current, which activates at approximately -60 mV and becomes the dominant inward current from ≈ -55 mV to the spike threshold near -45 mV (Khaliq and Bean, 2010). However, not all DAergic neurons fire spontaneously, because they are under the influence of GABA inhibition, generated by pathways intrinsic and extrinsic to the midbrain (Johnson and North, 1992; Goto et al., 2007). Tonic firing of DAergic cells is responsible for the baseline level of DA concentration: this is mediated by an escape of DA from

the synapses into the extracellular space. Therefore, the concentration of tonic extracellular DA is dependent on the number of DAergic neurons displaying spontaneous tonic spike activity (Floresco et al., 2003).

Burst spike firing pattern (Fig. 3B) represents a phasic activation of the DA system, which is dependent on glutamatergic excitatory synaptic input onto DAergic neurons from different areas, such as the PFC and the peduncolopontine tegmentum (Johnson and North, 1992; Floresco et al., 2003). The burst firing consists of a repetitive occurrence of groups of action potentials (APs, 2 to 6 or even more) with short inter-spike intervals, progressively decreasing amplitude and increasing duration, which trigger a high amplitude (hundreds of μM to mM levels), transient, phasic DA release from both terminals and soma/dendrites, intrasynaptically within the target areas, in a more efficient way than does regular tonic firing (Grace and Bunney, 1983a; Floresco et al., 2003; Korotkova et al., 2004; Goto el al., 2007). This phasic DA release acts transiently in the synaptic cleft and in very close proximity to the synapse, because of the immediate re-uptake into pre-synaptic terminals via DA transporters (Chergui et al., 1994).

Tonic and burst firing have been studied through different approaches, such as in awake and in anesthetized animals and with *in vitro* models. *In vivo*, using extracellular single-unit recordings, classic midbrain DAergic neurons have been identified through their long APs (>1 ms), which present a multiphasic shape, and their inhibition with

pharmacological D2 autoreceptor activation (Dopamine Handbook, Oxford University Press, 2010).

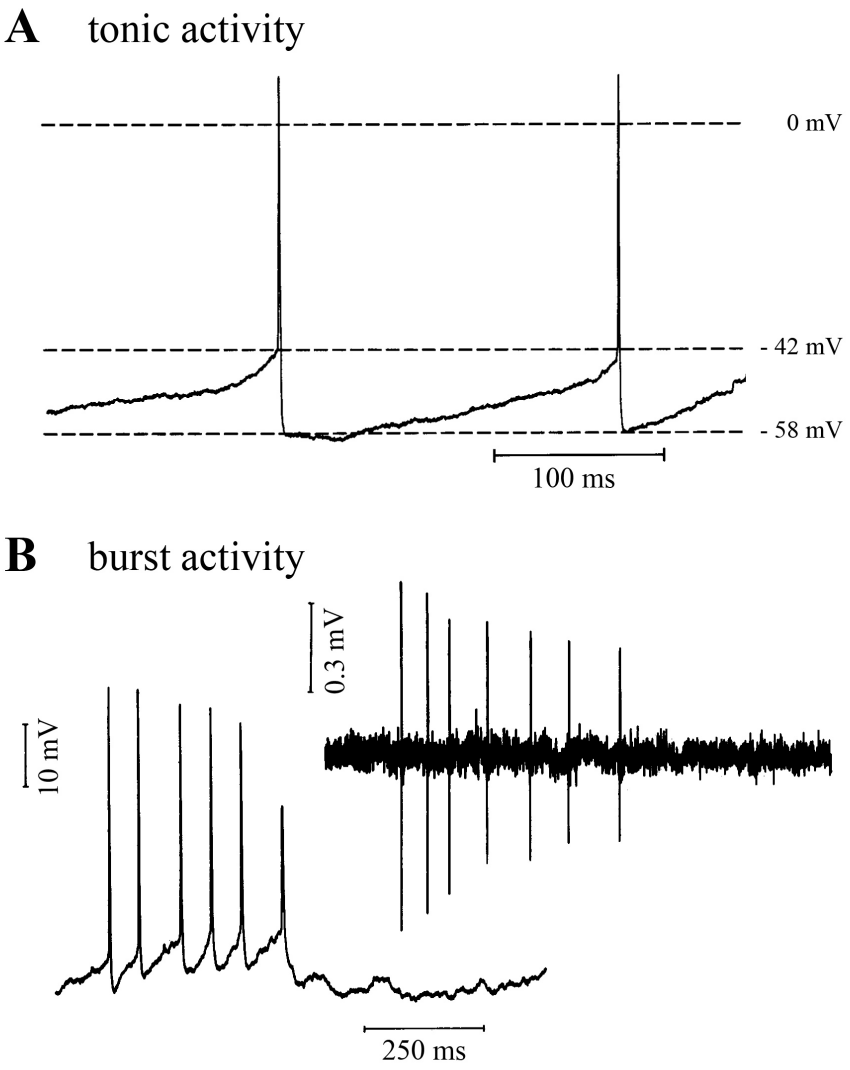

Figure 3. Classic dopamine midbrain neurons recorded *in vivo* in anesthetized rats. In A, an intracellular recording of tonic activity mode is shown. In B, an intracellular recording, on the left, and an extracellular *in vivo* recording, on the right, of burst activity mode (adapted from Grace and Bunney, 1984a and 1984b).

When an animal (mostly rodents or primates) is not actively engaged in a behavioural task, DAergic midbrain neurons show a tonic firing in the form of single APs in a frequency range of about 0.1-10 Hz, which appears very regular in rodents (Schultz, 1986; Bayer et al., 2007). This frequency (mean 3-6 Hz) is only about two-fold higher than those recorded from isolated DA cells in *in vitro* preparations. This tonic firing is replaced in both rodents and primates by bursts of APs (20-80 Hz, with instantaneous firing rates up to 100 Hz) in behavioural contexts, as a consequence of the presentation of a novel, salient, rewarding or reward-predicting sensory stimulus (Schultz, 1986). It has also been noted by Bayer et al. (2007) that the burst sizes (such as the number of intra-burst APs) and the firing rate during the post-reward interval correlate well with the amplitude of the positive reward prediction errors (Grace and Bunney, 1984b).

Also in anesthetized animals DAergic midbrain neurons show a long AP (2-3 ms) with a relative high AP threshold at around -40 mV and a prominent afterhyperpolarization (AHP), sensitive to potassium channel blockers (Grace and Bunney, 1984a). Furthermore, the single-spike tonic discharge mode and the burst mode appear to be fairly similar in anesthetized compared to those in awake animals: A10 DA cells of rats anesthetized with chloral hydrate discharge APs as irregular single spikes or bursts of spikes; the bursting pattern is exhibited by 73 % of VTA cells, but this percentage is influenced by the type and level of anesthesia (Grenhoff et al., 1988; Overton and Clark, 1997).

Finally, the use of *in vitro* brain slice preparations in combination with intracellular recording techniques has led to a large increase in the amount of information on DAergic neuron function and the electrical properties of acutely isolated and cultured DA midbrain neurons have been studied (Dopamine Handbook, Oxford University Press, 2010). In addition to identifying the AP properties, these studies have shown that the broad action potential is able to back-propagate along the dendrites and trigger the Ca^{2+}-dependent DA release from the same dendrites (Hausser et al., 1995; Gentet and Williams, 2007). Differently from *in vivo* preparations, DAergic neurons studied through *in vitro* approaches show a pacemaker activity, while the bursts are absent, but can be induced through pharmacological modulation of ion channels (such as blockade of small conductance Ca^{2+}-activated potassium (SK) channels and T-type calcium channels, whose inhibition elicits burst firing because they are the primary calcium sources for activation of SK channels, or activation of NMDA receptors) (Overton and Clark, 1997; Korotkova et al., 2004). Furthermore, a hyperpolarization-activated non-selective cation current (I_h) underlies time-dependent inward rectification and a rapidly inactivating A-type K^+ current (I_A), activated during the phase between the AHP and the subsequent AP, regulates spike firing frequency (Liss et al., 2001; Neuhoff et al., 2002)

Even if the properties of DAergic neurons, firstly evaluated in the SN, are broadly conserved in the VTA, different studies have shown that VTA DAergic neurons comprise subpopulations of cells, which differ in some of their firing properties and modulation. Margolis et al. (2008) have demonstrated that some VTA neuronal properties

correlate better with projection targets than with neurotransmitter content. In fact, in the rat AP duration of VTA DAergic neurons correlates with projection targets: the briefest AP durations (mean ≈ 1.7 ms) are exhibited by cells projecting to the amygdala, followed by PFC- (mean ≈ 2.2 ms) and then NAcc-projecting cells (≈ 3 ms); furthermore, while AMYG-projecting neurons are not inhibited by D_2 receptor activation, most PFC- and NAcc-projecting cells exhibit a significant hyperpolarization in response to a D_2 receptor agonist (Margolis et al., 2008). Besides, the properties of different populations of VTA DAergic neurons do not generalize between species. In the mouse, in fact, DAergic neurons, which project to mPFC, are unique due to the absence of functional somatodendritic D_2 receptors and D_2 receptor-mediated hyperpolarization (Lammel et al., 2008). Furthermore, mesocorticolimbic DAergic neurons, which selectively project to the mPFC, the basolateral amygdala, the core and the medial shell of NAcc, are able to fire APs at significantly higher frequencies compared to "conventional" SN DAergic neurons (< 10 Hz); additionally, mesocortical neurons show the lowest DA transporter (DAT) mRNA expression and the lowest DAT/TH and DAT/VMAT2 mRNA expression ratios, contributing to the 10-fold slower decay of extracellular DA concentrations in cortical areas compared to those in the striatum (Lammel et al., 2008). Finally, the I_h is absent in mouse PFC-projecting DAergic neurons (Lammel et al., 2008), but is large in those of the rat (Margolis et al., 2006a). Therefore, the attribution of properties to VTA DAergic neurons is complex and difficult, because of the presence of heterogeneous

neural responses, observed in this brain region (Margolis et al., 2006b).

GABAERGIC NEURONS. The second class of neurons identified in the VTA (and SN) consists of GABAergic neurons (which constitute 15-20% of the total neuronal population in this area), whose importance has been underestimated for a long time due to the idea that their main role was only to inhibit DAergic neurons. On the contrary, they also contribute to mesoprefrontal and mesoaccumbal connections (Carr and Sesack, 2000b; Adell and Artigas, 2004; Korotkova et al., 2004): a substantial population of GABA-containing neurons (also called secondary cells) in the VTA sends axons to the PFC, where they form symmetric synapses on the distal processes of both pyramidal and GABAergic local circuit neurons and provide a substrate for inhibitory and disinhibitory influences on PFC activity (Carr and Sesack, 2000a). At the same time, they receive excitatory inputs from prefrontal cortical neurons and inhibitory synapses, thus being subjected to GABA inhibition (Steffensen et al., 1998). The excitatory synapses on DAergic and GABAergic neurons are different, because while those on DAergic cells show depression as a consequence of repetitive activation, NMDA-dependent long-term potentiation (LTP) and are minimally affected by baclofen ($GABA_B$ receptor agonist), the excitatory synapses on GABAergic neurons show a facilitation upon repetitive activation and a baclofen-mediated depression and do not present NMDA-dependent LTP (Bonci and Malenka, 1999). The presence of GABAergic projection neurons inside a DAergic pathway is not only typical of the mesocortical pathway, but it is common to several major ascending DA systems,

such as the nigrostriatal and the mesolimbic pathways, whose function is mainly neuromodulatory (Carr and Sesack, 2000a).

Two different subpopulations of GABAergic cells, which do not stain for TH, have been identified in the VTA, according to their firing rates: one group is characterized by a relatively high frequency firing, similar to SN GABAergic neurons (≈ 8 Hz), while the second cluster consists of slow-firing cells (≈ 0.7 Hz). Furthermore, they also differ in AHP amplitude (larger in slow-firing cells) and spike threshold, which is more negative in fast-firing ones (Korotkova et al., 2003; Korotkova et al., 2004). On the contrary, both subpopulations of cells are large (30 μm diameter or larger) multipolar cells with few dendritic processes (Fig. 4A), they respond to depolarizing current steps with a high frequency (> 30 Hz) activity, which does not present accommodation (Fig. 4B), and they show a shorter spike duration (< 1.5 ms) and a smaller I_h than DAergic neurons and are responsive to opioids (Grace and Onn, 1989; Johnson and North, 1992; Steffensen et al., 1998; Korotkova et al., 2003).

The firing rate of VTA GABAergic neurons is a function of afferent inputs, which play a fundamental role in modulating the firing pattern: in fact, they present fast firing rates and a phasic activity, characterized by alternating 0.5-2 sec ON and 0.5-2 sec OFF periods, in animals under halothane anesthesia, a regular activity which is contingent on cortical arousal in freely behaving rats, while they are quiescent in the *in vitro* slice preparations (Steffensen et al., 1998).

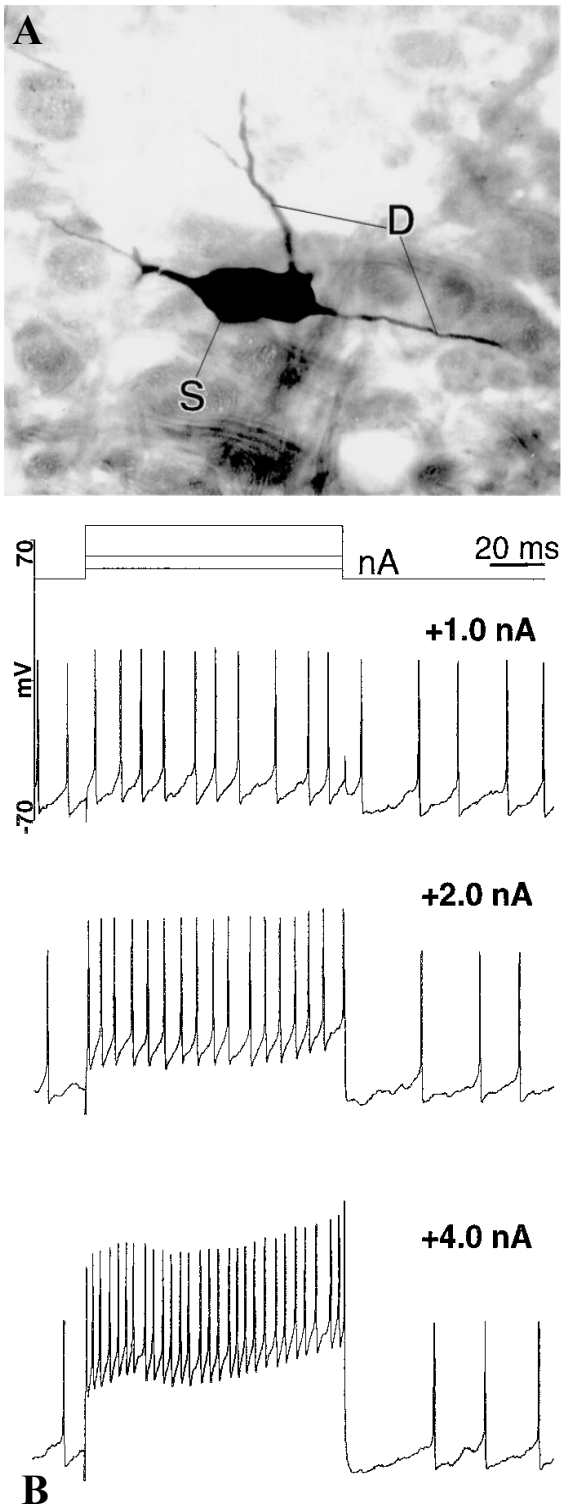

Figure 4. GABAergic neurons in the VTA. A) Light micrograph of a neurobiotin-labeled non-DAergic neuron in the VTA *in vivo*. This neuron is a characteristic neuron, electrophysiologically identified as VTA non-DAergic neuron, and it is multipolar in shape with few dendritic processes (D) branching from its soma (S). B) Lack of accommodation in VTA non-DAergic neurons. The neuron shown here has a resting potential of -64 mV. Increasing levels of depolarizing current (shown above the traces) produce multiple spikes, which are not related to DAergic neurons (from Steffensen et al., 1998).

GLUTAMATERGIC NEURONS. Recent electrophysiological and anatomical findings indicate that in the VTA there is a third population of cells, which are neither DAergic nor GABAergic; through the detection of mRNA encoding vescicular glutamate transporters (VGluT1, VGluT2, considered one of the most reliable markers for glutamatergic neurons, and VGlut3), which transport glutamate into synaptic vesicles for release at presynaptic sites, VTA glutamatergic neurons have been identified (Kawano et al., 2006; Yamaguchi et al., 2007). Some VTA VGluT2-expressing neurons establish local glutamatergic synapses on DAergic and GABAergic neurons, providing local excitatory neurotransmission, which can counterbalance the intrinsic inhibition of GABAergic neurons, contrary to the notion that all glutamatergic regulation to the A10 region is from extrinsic neurons (Yamaguchi et al., 2007; Dobi et al., 2010). Thus, VTA glutamatergic and GABAergic neurons provide synaptic inputs to DAergic, GABAergic and glutamatergic neurons within the VTA (Dobi et al., 2010). Furthermore, given that it has been demonstrated that VTA glutamatergic neurons project to the PFC, this population of cells may regulate the activity of DAergic neurons both directly through local synaptic connections and indirectly by signalling on PFC neurons that project back to the VTA and provide feedback to VTA DAergic neurons (Hur and Zaborszky, 2005; Dobi et al., 2010).

Two subpopulations of neurons expressing VGluT2 mRNA and not homogeneously distributed in the VTA have been identified in the A10 region: i) VGluT2-only neurons, which express VGluT2 mRNA but not TH and GABA markers and are the prevalent cell type in

Npbp and Npn of the VTA, following a lateromedial increasing gradient of distribution (72-79 % of VGluT2-positive cells; Yamaguchi et al., 2007; Yamaguchi et al., 2011), and ii) VGluT2-TH neurons, which co-express VGluT2 mRNA and TH and are present in the medial aspects of A10 nuclei (about half of TH-positive cells; Kawano et al., 2006; Yamaguchi et al., 2007). The differential distribution of VGluT2-only, VGluT2-TH and TH-only (mainly in the lateral aspects of the VTA) neurons within the VTA suggests a differential compartmentalization of cells with different signalling phenotype within the A10 region; thus, there exists a substantial mesocortical glutamate pathway in parallel to the well-known mesocortical DAergic and GABAergic pathways (Gorelova et al., 2011; Yamaguchi et al., 2011).

2.1.3 – CORELEASE OF DOPAMINE AND GLUTAMATE

DAergic neurons are endowed with asynaptic as well synaptic axon varicosities; this observation raises the hypothesis that the synaptic junctions established by DAergic neurons are the sites where glutamate is released as a co-transmitter (Descarries et al., 2008). The first indirect evidence for the corelease of glutamate and DA was the demonstration that a subset of DAergic neurons are immunopositive for glutamate, both in rat and monkey, and that they are also immunopositive for the glutamate biosynthetic enzyme, the phosphate-activated glutaminase (Kaneko et al., 1990; Sulzer et al., 1998). However, a more convincing and conclusive evidence is represented by the finding that a subpopulation of midbrain DAergic

neurons (limited compared to the total number of midbrain DAergic cells) contains mRNA for VGluT2, thus having at least the potential to package glutamate into vesicles for release (Fig. 5; Dal Bo et al., 2004; Kawano et al., 2006; Yamaguchi et al., 2007).

Even if VGluT2 may be present on synaptic vesicles to promote DA storage (Hnasko et al., 2010), there are also electrophysiological evidences for a functional corelease of glutamate from DAergic neurons in the mesocortical pathway. In fact, Lavin et al. (2005) have demonstrated that electrical or chemical activation of the VTA can evoke a short-latency excitatory post-synaptic potential (EPSP) in the PFC, that lasts tens of milliseconds and is blocked by lesions in the VTA (suggesting that it requires the integrity of DAergic neurons) and by administration of glutamate receptor antagonists, but not of DA receptor ones. This suggests that the PFC receives a fast non-DA-mediated signal from the VTA and a slower DA-mediated signal, which differentially affects spontaneous and evoked firing (Lavin et al., 2005). Furthermore, cultured DAergic neurons producing autapses, if stimulated, are able to evoke Ca^{2+}-dependent EPSPs mediated by both NMDA and AMPA receptors, indicating that glutamate is synaptically released (Sulzer et al., 1998). Likewise, glutamatergic EPSPs can be evoked in NAcc neurons by VTA stimulation in a VTA-NAcc acute slice preparation and this depolarizing event is removed with the selective elimination of VGluT2 from DAergic neurons using DAT-Cre/VGluT2Lox knockout mice (Hnasko et al., 2010). Finally, Stuber et al. (2010) have demonstrated that, activating DAergic neurons selectively through

optogenetic techniques, excitatory post-synaptic currents (EPSCs) are produced in the vast majority of medial NAcc neurons.

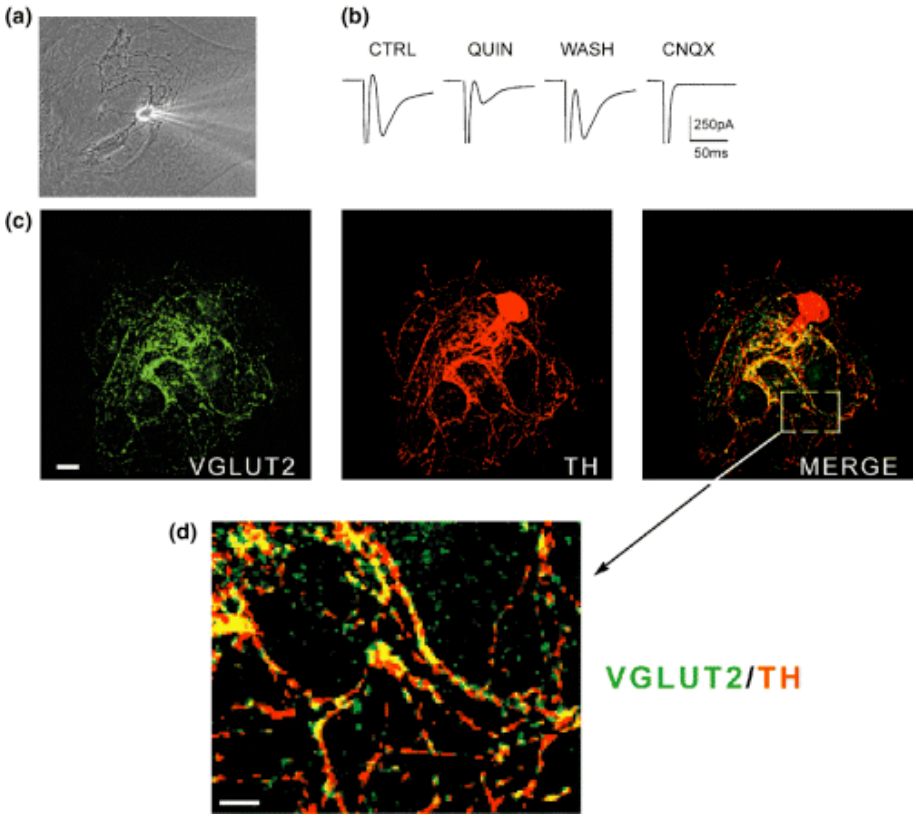

Figure 5. Expression of VGluT2 by isolated DAergic neurons in culture. (a) Phase contrast image of an isolated mesencephalic neuron. Note the presence of a patch pipette on the right. (b) A single DAergic neuron was recorded by whole-cell patch-clamp. From a holding potential of -70 mV, a brief depolarization to +20 mV induced an unclamped AP (clipped) followed by a rapid EPSC, which was inhibited by quinpirole (D2 receptor agonist) and completely blocked by CNQX (5 μM; AMPA/kainate glutamate receptor antagonist). (c) Confocal images showing VGluT2 immunolabeling (green) in a TH-positive (red) DAergic neuron in culture. The merged image (right) shows that most of the VGluT2 staining is found on TH-positive processes (yellow) [Scale bar: 15 μm]. (d) Enlargement from the merged image in (c). Note that although most VGluT2-positive structures were TH-positive (yellow), a number of TH-positive varicosities were VGluT2-negative (red puncta) [Scale bar: 4 μm] (from Dal Bo et al., 2004).

Thus, considering that DAergic neurons have a fundamental role in the transmission of information about the mismatch between expected and actual rewards (prediction errors) that serve as a learning signal in efferent regions, and given the fact that DA acts as a relatively slow modulator of cortical neurotransmission, corelease of glutamate from DAergic neurons in the VTA could serve to transmit this temporally precise signal. In this way, the mesocortical DA system optimizes the characteristics of glutamate, GABA and DA neurotransmission within the midbrain and the cortex to convey temporally precise information and to modulate the activity of the network on longer timescales (Lapish et al., 2007).

2.1.4 – CORELEASE OF DOPAMINE AND GABA

In contrast with the well identified corelease of dopamine and glutamate from neurons in the VTA which project to the PFC, there is little evidence for a corelease of DA and GABA from the same population of cells. The only evidence of a DA/GABA coexpression has been reported by González-Hernández et al. (2001) for mesostriatal neurons, projecting from the medial region of SNc and A10 to the striatum: in fact, 10 % of DAergic nigrostriatal neurons also contain the GABA synthetic enzyme glutamic acid decarboxylase (GAD65) mRNA. It has been hypothesized that GABA released from DAergic/GABAergic cells can exert a short auto-regulatory mechanism on the mesostriatal system; in the DAergic cells, GABA cotransmission could play a modulatory role, protecting these neurons

from excessive activity, and having neuroprotective effects (González-Hernández et al., 2001).

2.1.5 – VULNERABILITY TO NEURODEGENERATION

It is well known that DAergic neurons of the midbrain not only show distinct functions and different activity patterns, but they also display differential vulnerability to neurodegeneration, with certain subpopulations being more vulnerable than others (Liss and Roeper, 2008). One example is constituted by Parkinson's disease (PD) and its chronic animal models, where it is evident that DAergic neurons in the SN projecting to the striatum are almost completely lost, while DA midbrain neurons of the VTA, which are part of the mesocortical and mesolimbic pathways, are less affected by degeneration during the course of the disease (Dopamine Handbook, Oxford University Press, 2010) and they might also display a form of hyperactivity at the early stages of PD (Liss and Roeper, 2008). Candidate determinants for such a diversity in the resistance to neurodegeneration have been identified using models of neurodegeneration induced by neurotoxins MPTP (1-methyl-4-phenyl-1,2,3,6-tetrahydropyridine), 6-OHDA (6-hydroxydopamine) and rotenone, and include differences in the electrophysiological properties and activity of ion channels (L-type Ca^{2+} channels and K-ATP channels) and in gene expression (Korotkova et al., 2004; Dopamine Handbook, Oxford University Press, 2010).

Mitochondrial dysfunction plays a critical role in the pathogenesis of idiopathic, toxin-induced cases and several familial forms of PD. Liss et al. (2005) have demonstrated that the Kir6.2-containing K-ATP channels (physiologically closed at high ATP and low ADP levels and open in the presence of a decreased ATP/ADP ratio; Korotkova et al., 2004), expressed in all midbrain DAergic neurons but at about two-fold higher levels in vulnerable mesostriatal SN DAergic neurons, are causally linked to the differential degeneration of DAergic neurons *in vivo* in response to mitochondrial complex I inhibition. In fact, the presence of functional K-ATP channels promotes cell death of SN DAergic but not of VTA DAergic neurons, because these channels are selectively activated in the former cell population, causing the hyperpolarization of the membrane potential and preventing the generation of APs, but not in the latter (Liss et al., 2005; Liss and Roeper, 2008). However, the selective activation of K-ATP channels in SN DAergic neurons is controlled by oxidative mechanisms, such as differential degrees of uncoupling of mitochondrial respiratory chain and different levels of uncoupling protein UCP-2 (Liss et al., 2005; Dopamine Handbook, Oxford University Press, 2010).

A second channel-based mechanism for the differential vulnerability among DAergic midbrain neurons has been identified by Chan et al. (2007), whose work pointed out the role of $Ca_v1.3$ L-type Ca^{2+} channels. In fact, while pacemaking in VTA DAergic neurons is based on sodium entry through voltage-dependent Na^+ channels, SN DAergic neurons rely on $Ca_v1.3$ L-type Ca^{2+} channels to drive their maintained, rhythmic pacemaking. This unusual and unrelenting Ca^{2+} entry can act as an energetic stress that makes SN neurons particularly

susceptible to oxidative damage and death (Bean, 2007; Sulzer and Schmitz, 2007). Furthermore, finding that pacemaker activity in $Ca_v1.3$ knockout mice persists in SN DAergic neurons due to a switch from calcium- to sodium-based pacemaking, Chan et al. (2007) have shown that a corresponding drug-induced (with a Ca^{2+} channel blocker) pacemaker-switching (also called 'rejuvenation') of SN DAergic neurons is able to reduce their vulnerability to a level comparable to that of VTA DAergic neurons, in a PD mouse model (Liss and Roeper, 2008). In fact, it has been previously demonstrated that the electrical activity and the associated influx of Na^+ and Ca^{2+} are necessary for the survival of DAergic neurons, at least *in vitro* (Salthun-Lassalle et al., 2004). In this way, inducing the SN DAergic neurons to switch to a metabolically less demanding sodium-based pacemaking would manage to keep their K-ATP channels closed and to maintain them alive throughout the disease, as it happens for VTA DAergic neurons (Liss and Roeper, 2008).

Finally, differences in gene expression are also involved in determining the differential vulnerability to neurodegeneration, identified between SN and VTA DAergic neurons. In this context, calbindin D28K is expressed in a relevant fraction of resistant VTA DAergic neurons and in a small subset of SNc neurons (Simeone et al., 2011); on the contrary, the G-protein-gated inwardily rectifying K^+ channel (Girk2) is expressed in many SN neurons and in the dorsal-lateral VTA, together with the glycosilated active form of DAT, whose distribution correlates with the neurodegeneration map caused by toxin-induced PD (Afonso-Oramas et al., 2009). Another gene, which has a specific expression profile, is Otx2, a transcription factor

expressed exclusively in a relevant fraction of VTA neurons and absent in SN cells, particularly in those neurons which show Girk2 and high level of DAT; mouse models with loss or gain of function of this gene have revealed that Otx2 is able to control neuron subtype identity antagonizing Girk2 and DAT expression (which are typical features of dorsal-lateral VTA) as well as vulnerability to toxin-induced PD (Simeone et al., 2011).

2.2 - THE PREFRONTAL CORTEX (PFC)

The functioning of the cerebral cortex is organized in a hierarchical manner. At the bottom of the organization there are sensory and motor areas, which are involved in sensory and motor functions; higher areas, which are those displaying a later phylogenetic and ontogenetic development, participate to progressively more integrative functions. The prefrontal cortex represents the highest level of the cortical hierarchy involved in the representation and execution of actions (Fuster, 2001) and it is fundamental for top-down control over higher-order executive functions (Lodge, 2011).

The most important function of the PFC is represented by the "working memory", which is the type of memory that is active and relevant only for a short period of time (usually on the scale of seconds) and keeps events "in mind" for brief time windows (Goldman-Rakic, 1995). It has been demonstrated that cells in the PFC of the monkey fire persistently at high rates while the animal retains an item of visual information in short-term memory; in

delayed-response tasks, this type of 'memory cells' fire more frequently during the delay periods, which are the periods when short-term memory is required, than during baseline periods (Goldman-Rakic, 1995; Fuster, 2001). The involvement of prefrontal cells in working memory is related to the need to retain information for an impending action that is in some way dependent on that kind of information (Fuster, 2001).

2.2.1 – ANATOMY OF THE PFC

The PFC is the association cortex of the frontal lobe, located rostrally to the motor and premotor cortices. Phylogenetically, the PFC is one of the latest cortices to develop, with the maximum relative growth in the human brain, where it is the most extensive cortical area of the cerebral hemisphere because it constitutes nearly one-third of the neocortex (Groenewegen and Uylings, 2000; Fuster, 2001). Furthermore, in the course of ontogeny, the PFC undergoes late development, because in humans it is a late-maturing cortex, which reaches full maturity only during adolescence, when higher cognitive functions, such as propositional speech and reasoning, develop (Fuster, 2001).

The PFC can integrate a variety of information due to the profuse variety of its connections and thus it is well suited for a role as brain's "executive"; it is able to synthesize information from various brain systems and exert control over behaviour (Miller et al., 2002). The PFC has interconnections with brain areas processing external

information (with all sensory systems and cortical and subcortical motor system structures) as well as with those processing internal information (limbic and midbrain structures) (Fuster, 2001; Miller et al., 2002). In this way the PFC is involved in many parallel and functionally segregated cortical-subcortical circuits, which are essential for sensorimotor, cognitive, emotional/motivational behavioural and visceral functions (Groenewegen and Uylings, 2000).

The PFC can be subdivided in three major regions: orbital, medial and lateral (Van de Werd et al., 2010). The orbital region is involved in emotional behaviour through an inhibitory control exerted via its afferents to hypothalamus, basal ganglia and other neocortical areas; in fact, it is known, from the famous case of Phineas Cage, that lesions of the orbital PFC cause changes of personality and disorder of attention (Fuster, 2001). The medial portion of the PFC (including the infralimbic, prelimbic, dorsal and ventral anterior cingulated and medial precentral areas) receives a strong dopaminergic innervation from the VTA, it is a component of the motive circuits involved in reward-oriented behaviours and drug abuse, but it also controls general motility, attention and emotion; loss of spontaneity and difficulty in the initiation of movements and speech appear when the medial PFC is lesioned (Fuster, 2001; Steketee, 2003). Finally, the lateral PFC plays a crucial role in the organization and execution of behaviour, speech and reasoning; in fact a lesion to this area causes deficit in planning and attention and the so called “dysexecutive syndrome” (Groenewegen and Uylings, 2000; Fuster, 2001).

2.2.2 – DOPAMINERGIC AFFERENTS

In the PFC DAergic projections from the mesencephalon follow a bilaminar distribution pattern in the upper (layer I) and deeper (layers V and VI) layers and rarely ramify, in the way that DAergic varicosities are organized along the unmyelinated axon (Goldman-Rakic et al., 1992). The synaptic nature of the DAergic mesocortical pathway has been the subject of a long debate; it has been estimated that almost 40% of DAergic axon varicosities in the PFC forms clear symmetric synapses, while the remaining ones are likely to contribute to extrasynaptic DA release (Smiley and Goldman-Rakic, 1993). It is now accepted that DA in the PFC has a synaptic as well as a non-synaptic signalling component (Dopamine Handbook, Oxford University Press, 2010).

DAergic afferents forming symmetric synapses mainly release DA on the spines and thus selectively target the distal dendritic field of pyramidal neurons (Smiley and Goldman-Rakic et al., 1993); these same spines are often the targets of an asymmetric bouton, which is typical of axons containing excitatory amino acids. Given the fact that the spine synapses are the structures through which pyramidal neurons receive the major sensory inputs and are the sites of pyramid-to-pyramid communication, which represents the cellular basis of working memory, these three-way synaptic complexes, known as "synaptic triads" (Fig. 6), allow a direct DAergic modulation of local spine responses to excitatory inputs. In this way, DAergic terminals can regulate the integration of inputs performed by a pyramidal neuron and directly alter the output of the cortex through axonal

projections to different cortical structures (Goldman-Rakic et al., 1989; Goldman-Rakic et al., 1995; Goldman-Rakic et al., 2000). However, DAergic synapses can also target pyramidal and non-pyramidal dendritic stems: specifically, it has been demonstrated the specificity of DAergic axodendritic synapses for parvalbumin (PV)-expressing interneurons (Fig. 7; Sesack et al., 1998). This population of local circuit neurons includes chandelier and wide-arbor cells, which contact the soma and the axon initial segments of pyramidal neurons, exerting a strong inhibition. Thus, synaptically released DA modulates pyramidal neurons directly, through distal axospinous and to a lesser extent axodendritic synapses, and indirectly, through perisomatic interneuron-mediated inhibition (Sesack et al., 2003).

Extrasynaptically released DA or DA escaping from synapses could also play an important role in the modulation of PFC activity and functionality. Different indirect anatomical evidences support a function of DA as a volume transmitter: some varicosities do not form morphologically identified synapses, DATs are localized at a distance from DAergic synapses and varicosities and they are expressed at low levels in the PFC (Sesack et al., 2003), and DAergic receptors are positioned at extrasynaptic locations (Pickel et al., 2002).

Thus, DA signals target neurons through a synaptic mode, with a degree of specificity in cell types and dendritic compartments innervated, and through an extrasynaptic mode, which is less specific. Extrasynaptic DA release and diffusion produce a background tone of receptor activation that boosts synaptic DA inputs and raises the

probability of target neuron response to ensuing synaptic DA release (Sesack et al., 2003).

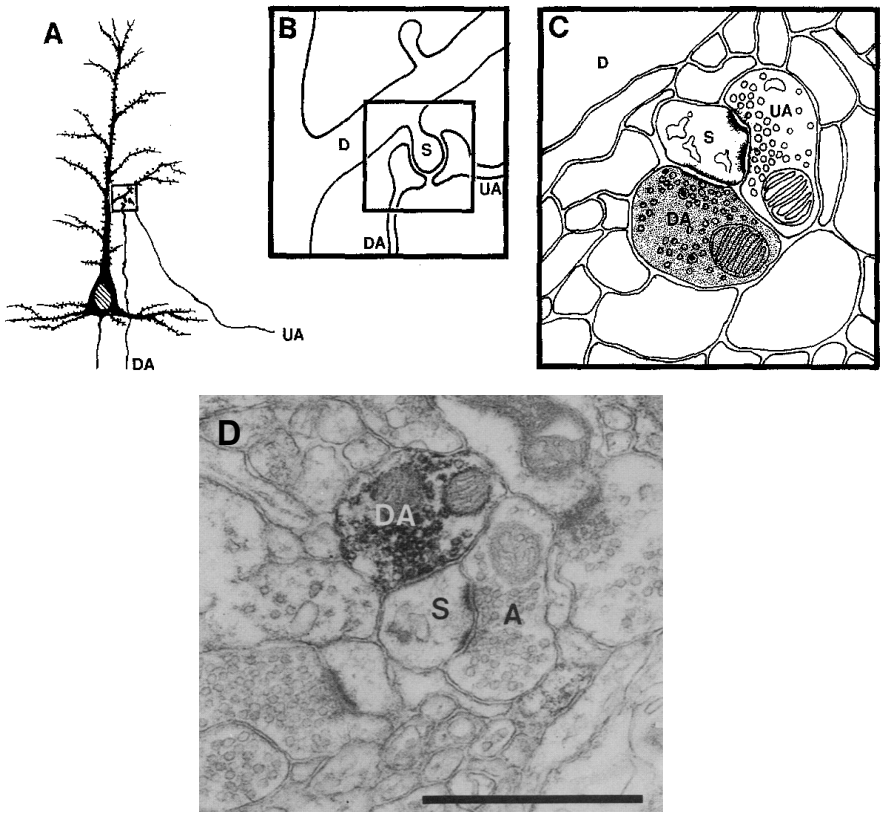

Figure 6. Diagrams of synaptic arrangements involving the dopamine input to the cortical pyramidal neurons. A) DAergic (DA) afferents terminate on the spine of a pyramidal cell in the PFC, together with an unidentified axon (UA). B) Enlargement of axospinous synapses illustrated in (A), showing apposition of the DA input and a presumed excitatory input (UA) that makes an asymmetrical synapse on the same dendritic (D) spine (S). C) Diagram of the ultrastructural features of the axospinous synapses in (B); the dopamine terminal (darkened profile) forms a symmetrical synapse; the unidentified profile forms an asymmetrical synapse with the post-synaptic membrane (from Goldman-Rakic, 1995). D) Electron micrograph from layer II of the monkey PFC, immunostained for DA (DA: dopamine; S: spine; A: non-immunoreactive axon terminal) [Scale bar: 1 μm] (from Goldman-Rakic et al., 1989).

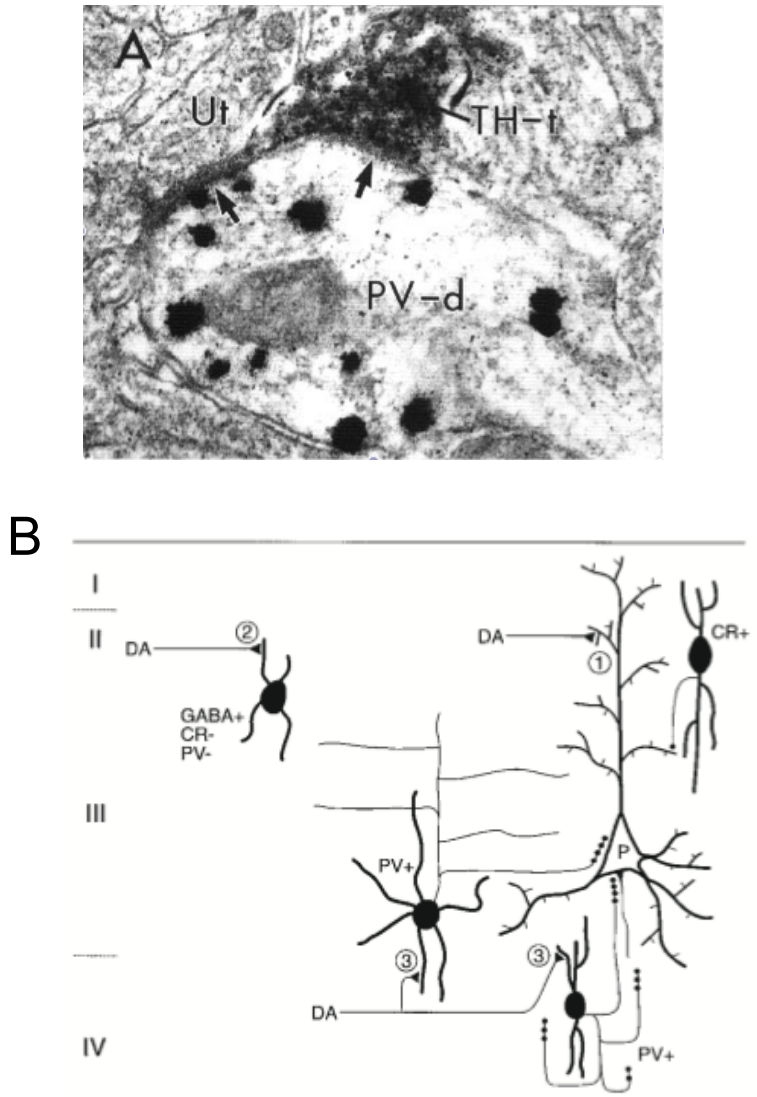

Figure 7. DAergic afferents to cortical interneurons. A) Electron micrograph from the middle layers of monkey PFC: a parvalbumin-positive dendrite (PV-d) is innervated by a TH-positive terminal (TH-t) and an unlabeled terminal (Ut), both forming symmetric synapses. B) Drawing of the selectivity of DA terminal inputs to subclasses of local interneurons. The predominant synaptic contacts of DA terminals are the distal dendrites and spines of pyramidal neurons (1), but they can contact the dendrites of GABAergic neurons in layer I-IIIa (2); in the middle layers IIIb-IV of PFC, DAergic terminals form synapse-like contacts on the dendrites of PV neurons (wide arbor and chandelier cells) (from Sesack et al., 1998).

2.2.3 – DISTRIBUTION OF DOPAMINERGIC RECEPTORS IN THE PFC

The diverse physiological actions of DA are mediated by at least five distinct G protein-coupled receptor subtypes: D_1 and D_5 subtypes, belonging to the D_1-like family, are coupled to $G_\alpha s$ proteins and activate adenylyl cyclase pathway (elevating the cAMP level), whereas the D_2-like family, including D_2, D_3 and D_4 subtypes, inhibits adenylyl cyclase and activates K^+ channels (Missale et al., 1998). In the CNS DAergic receptors are widely expressed, because they are involved in the control of different functions, such as locomotion, cognition, emotion and affect; for this reason, almost two decades of research have produced maps of their cellular and subcellular distribution (Dopamine Handbook, Oxford University Press, 2010).

D_1-LIKE FAMILY IN THE PFC. The D_1-like receptors are the most abundant DAergic receptors in the PFC (almost 20-fold more abundant than D_2 family receptors). Immunoelectron microscopy studies have revealed that D_1 receptors are expressed on distal dendrites and spines of prefrontal pyramidal neurons, in the perisynaptic membranes flanking asymmetric axospinous synapses (Goldman-Rakic et al., 2000). Furthermore, the D_1 receptor is present also on the PV-containing GABAergic interneurons (basket and chandelier cells), preferentially in the distal dendrites, adjacent to asymmetric synapses, as well as in presynaptic terminals (as it is recognized for pyramidal neurons) (Muly et al., 1998). Both in pyramidal neurons and in interneurons D_1 receptors have been found to colocalize and physically and functionally interact with NMDA

receptors, providing evidence for a synergistic action of D_1 and NMDA receptors in the PFC in the modulation of the balance between pyramidal neuron and interneuron firing, to filter weak or irrelevant stimuli (Kruse et al., 2009). D_5 receptors show a rather complementary expression in the PFC: they are present on all somata and throughout the dendrites (including numerous spines) of pyramidal neurons and on somata and proximal dendrites of calretinin (Glausier et al., 2009) and to a lesser extent PV interneurons, where the C-terminal domain of D_5 receptor can contact and modulate $GABA_A$ receptors (Oda et al., 2010).

D_2-LIKE FAMILY IN THE PFC. Compared to D_1 receptors, the distribution of D_2 receptors is poorly understood and not completely clear. D_2 receptors are predominantly expressed on dendritic stems of both pyramidal and non-pyramidal neurons and on axonal varicosities (Paspalas et al., 2006). Despite a predominant non-synaptic distribution, D_2 receptors have been also found in symmetric axodendritic synapses in monkey PFC and rodent neocortex (Dopamine Handbook, Oxford University Press, 2010). Furthermore, they are present on axons, where presynaptic D_2 receptors act as autoreceptors able to regulate DA release, and on glutamatergic varicosities, where they function as heteroreceptors (Paspalas et al., 2006). D_4 receptors show a high affinity for atypical antipsychotics, but little is known about their expression pattern in the PFC: they are expressed mainly by GABAergic interneurons and in a subset of pyramidal neurons in monkey PFC, at the soma and dendritic processes (Mrzljak et al., 1996).

2.3 - DOPAMINERGIC MODULATION OF PFC ACTIVITY

Several cell types exist in the mPFC, including excitatory (glutamate) pyramidal output neurons, cholinergic efferents, inhibitory GABAergic interneurons and cholinergic interneurons. DAergic neurons synapse on at least two cell types, pyramidal neurons and non-pyramidal GABAergic interneurons; these GABAergic cells synapse on pyramidal neurons in the mPFC as well (Steketee, 2003). The actions of DA on cortical circuits have been studied using different approaches and techniques, such as *ex vivo* rodent slice preparations and *in vivo* experiments in anesthetized rats and behaving monkeys; studies in rodents have been useful to identify the mechanisms at the basis of DA influence on intracellular signalling events, while the *in vivo* studies allowed to link DA actions to higher cognitive operations (Dopamine Handbook, Oxford University Press, 2010).

Following the discovery of the mesocortical DA system in 1973 by Thierry and colleagues, there was an incredible growth of functional data on the role of DA in the PFC both *in vivo* and *in vitro*. However, the studies were performed under different experimental conditions and this, combined with the variety of DAergic receptors, their effecter mechanisms, the regional heterogeneity in expression and the species-specific features of PFC architecture, generated controversial findings and opposing interpretations of the results (Seamans and Yang, 2004). Now it is well accepted that DA is not a classical, fast ionotropic neurotransmitter (as glutamate, GABA and acetylcholine),

but it acts as a neuromodulator with differential effects on CNS (Yang et al., 1999).

2.3.1 – DOPAMINE EFFECTS ON PYRAMIDAL NEURONS

While dorsolateral prefrontal cortical areas of macaque monkeys and humans present multiple common characteristics, significant anatomical and functional differences have been found between rat medial PFC and monkey dorsolateral PFC (Preuss, 1995).

In primate PFC, where DA receptors and fibres are present in high density in the superficial layers, layer III pyramidal neurons receive numerous excitatory synaptic connections, such as local and long range projections from pyramidal cells in the same cortical region but in different layers, associational and callosal projections from other cortical regions, and projections from the mediodorsal thalamus (Melchitzky et al., 1998; Melchitzky et al., 2001; Urban et al., 2002). Layer II/III also contain most of the pyramidal cells that originate long-distance intrinsic horizontal connections mediating intrinsic excitation, which is essential to delay-related activity in monkey PFC neurons (Goldman-Rakic, 1995). Thus, the regulation of layer III pyramidal neuron activity by DA could have a significant impact on local excitation in the PFC and its propagation to other regions (Henze et al., 2000). Using PFC slices from male cynomolgus monkeys, Henze et al. (2000) have shown that application of DA at a concentration as low as 500 nM increases the excitability of layer III pyramidal neurons to depolarizing current steps (increase of the

number of spikes, decrease of the voltage threshold of the first action potential and of the inter-spike interval between the first and the second evoked spike) without altering the resting state of these neurons, and that this effect requires activation of D_1-like, but not of D_2-like, receptors (Henze et al., 2000). Although early studies have suggested that pyramidal cells in rat PFC superficial layers are not responsive to DA receptor activation, more recent studies have shown that a proportion of these neurons is able to respond to DA: in fact, bath application of DA to rat PFC slices causes a moderate increase in the glutamate-mediated EPSCs through the activation of D_1 receptors and the involvement of Ca^{2+}-dependent postsynaptic mechanisms (Gonzalez-Islas and Hablitz, 2003; Bandyopadhyay et al., 2005). Furthermore, DA D_1 receptor-mediated enhancement of EPSCs causes alterations of the spatiotemporal spread of activity and it can have a proconvulsant effect: DA can either enhance activity locally or, if the enhancement is strong enough, result in epileptiform events, which are able to propagate across the slice (Bandyopadhyay et al., 2005). Together with the DA-mediated EPSC enhancement, it has been demonstrated that DA is able to cause a synapse-specific reduction of the strength of excitatory synaptic transmission at synapses onto pyramidal cells in layer III of monkey PFC, through a combined action of D_1 and D_2 receptors: in this way, the increased cell excitability previously described together with the selective depression of excitatory synaptic input could increase the relative weight only of specific synaptic inputs (Urban et al., 2002). Thus, dopaminergic modulation of superficial layer cell activity is an effect, which is found in PFC across species, even if it is more robust in

primates than in rodents and it is likely to modulate significantly the interaction between dorsolateral PFC and other neocortical regions (Henze et al., 2000).

The deep layers of rodent PFC receive the strongest DAergic innervation and for this reason the majority of studies of DA action on pyramidal neurons *in vitro* concentrated on layers V and VI (Henze et al., 2000). It has been reported that DA is able to modulate the excitability of layer V pyramidal neurons, in a different manner according to the receptors involved: in fact, bath application of D_1 agonist SKF38393 to rat PFC slices determines a concentration-dependent excitability increase through a facilitation of NMDA receptor currents via PKA activation, while D_2 agonist quinpirole induces a decrease of excitability inhibiting NMDA- and AMPA-mediated responses, without modifying the membrane potential or the action potential threshold (Gulledge and Jaffe, 1998; Gulledge and Stuart, 2003; Tseng and O'Donnell, 2004). This latter effect on NMDA currents requires activation of $GABA_A$ receptors and thus it suggests that it is mediated by an increase in GABAergic transmission (Gulledge and Jaffe, 2001); on the contrary, the D_2 inhibitory action on AMPA responses requires intracellular Ca^{2+} and the PLC-IP_3 and partly the cAMP-PKA cascades (Tseng and O'Donnell, 2004). In detail, DA effect on NMDA responses can act in opposite directions, because it has been demonstrated that at low concentrations DA enhances NMDA currents (Zheng et al., 1999) and inhibitory post-synaptic currents (IPSCs; Trantham-Davidson et al., 2004) via D_1 receptors, while high DA concentrations determine a decrease of NMDA currents (Zheng et al., 1999) and IPSCs (Trantham-Davidson

et al., 2004) through D_2 receptors. Therefore, the amount of DA released may determine the receptor subtype that is activated and that affects the tuning of PFC networks encoding working memory (Trantham-Davidson et al., 2004). Furthermore, in PFC slices, prestimulation of D_1 and D_2 DA receptors with continuous application of a low concentration of DA (priming phase) is able to convert NMDA-independent long-term depression (LTD, described by Otani et al., 1998) to LTP, which depends on NMDA receptor activation during the priming process and mGluRs during the induction, thus suggesting the importance of tonic background DA levels in the regulation of cognitive processes (Matsuda et al., 2006). The excitatory action of DA has been identified also in slices from ferret PFC, where D_2 receptor activation is able to promote bursting in layer V pyramidal neurons in response to minimal extracellular stimulation in layer III (Wang and Goldman-Rakic, 2004). DA is also able to suppress a slowly inactivating outward K^+ conductance (Yang and Seamans, 1996) and an inwardly rectifying K^+ current (IRKC) to facilitate the transition to the up-states (Dong et al., 2004) and to increase the gain of the input-output function of layer V pyramidal neurons, reducing the slow afterhyperpolarization (sAHP) via activation of D_1 receptors and, eventually, of non-DAergic receptors (such as β-adrenergic receptors) at high DA concentrations; this modulation of the input-output function is able to facilitate and stabilize persistent activity in prefrontal pyramidal neurons (Thurley et al., 2008). Various works from different groups have also reported an inhibitory action of DA on the activity of layer V pyramidal neurons: Rotaru et al. (2007) demonstrated that D_1 receptor activation

decreases EPSP amplification down-regulating persistent sodium currents (I_{NaP}) through an enhancement of Na^+ channel slow inactivation, thus attenuating subthreshold responses to slow depolarizing current ramps. In this way, in depolarized pyramidal neurons D_1 receptor activation would decrease the effectiveness of temporal summation, favouring coincidence detection, as opposed to temporal integration (Rotaru et al., 2007). Furthermore, DA is able to decrease the amplitude of EPSPs, evoked by superficial layer stimulation in adult rat PFC slices, through a direct D_2 action on pyramidal neurons and a D_2-mediated upregulation of local GABAergic activity that sustains inhibition; this latter mechanism is absent in prepubertal rat slices, thus suggesting that the periadolescent maturation of the DAergic control of excitatory and inhibitory neurotransmission could be critical to fine-tuning PFC functions and activity, which are fundamental for mature cognitive processes (Tseng and O'Donnell, 2007). The interactions between DA and GABA on PFC pyramidal neurons have also been examined by Seamans et al. (2001): DA produces biphasic effects on $GABA_A$-mediated IPSCs, causing an initial reduction in IPSCs via D_2 receptor activation (determining a presynaptic reduction in GABA release and a small postsynaptic reduction in $GABA_A$ receptor conductance), followed by a delayed and long-lasting increase in IPSC amplitude mainly mediated by D_1 receptors (increase in the intrinsic excitability of interneurons) (Seamans et al., 2001).

One hypothesis for working memory involves the formation of reverberant circuits able to maintain activity for a short period of time. A well described pyramidal neuron feature is the enhanced output

during specific phases of working memory tasks; at the same time, a level of synaptic inhibition is required to constrain firing only to those neurons which provide behaviourally significant output. The acute presence of DA, through inhibition of TTX-sensitive conductances and enhancement of GABAergic transmission, may gate appropriate firing, increasing the signal-to-noise level through the attenuation of weak signals and allowing output only from those neurons receiving the strongest excitatory drive (Gulledge and Jaffe, 1998; Tseng and O'Donnell, 2004). Delayed increases in excitability may regulate tonic levels of excitability. In this way DA release during working memory tasks may not only set the stage for reverberatory activity, but may also constrain such heightened activity to behaviourally relevant neurons, establishing a network state for proper working memory function (Gulledge and Jaffe, 1998 and 2001; Seamans et al., 2001; Gorelova et al., 2002; Fig. 8).

Thus, combined activation of D_1, D_2, GABA and glutamate receptors may allow a "gating with filtering" phenomenon; disruption of these interaction may contribute to abnormal coordination of pyramidal neuron firing and participate to the development of cognitive deficits observed in schizophrenia and related neuropsychiatric disorders (Tseng and O'Donnel, 2004; Matsuda et al., 2006).

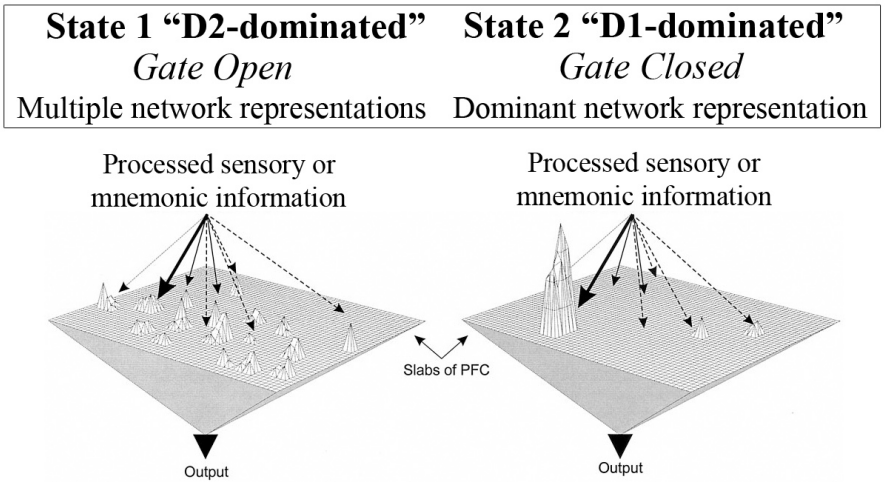

Figure 8. A two-state model of DA action in PFC. Peaks denote up-states, corresponding to sustained recurrent activity required to hold items in working memory. (Left) In state 1, the D2 modulation predominates, and inhibition is reduced. Thus, multiple inputs have access to the working memory buffers, allowing multiple representations to be held in PFC networks nearly simultaneously. (Right) In state 2, the D1 modulation predominates and inhibition increases. Thus, inputs have difficulty accessing PFC networks and only particularly strong inputs, able to overcome the effects of increased inhibition, produce active and stable network representations, even after the offset of the initiating stimulus. In this way, DA may first allow the exploration of the input space (state 1), and then it shuts off the influence of weak inputs and stabilizes one or a limited set of representations, which completely control PFC output (from Seamans et al., 2001 and Seamans and Yang, 2004).

2.3.2 – DOPAMINE EFFECTS ON GABAERGIC NEURONS

DA and GABA interact in a complex manner in the PFC. DA induces an increase of the excitability of fast-spiking (FS) interneurons in layer II, III and V of rat PFC (Zhou and Hablitz, 1999; Gorelova et al., 2002): this effect is mediated by D_1-like receptors, which determine the suppression of Cs^+-sensitive inward rectifying and voltage-independent leak K^+ conductances, responsible to set the resting

membrane potential and input resistance of interneuron membrane, and of slowly inactivating outward rectifying K^+ current, regulating subthreshold synaptic events and repetitive firing (Gorelova et al., 2002; Fig. 9). This excitatory action of DA on interneurons has been reported also by Tseng et al. (2006) using *in vivo* experiments: in response to VTA stimulation, FS interneurons of layers V and VI show an enhanced firing, accompanied by a decrease in pyramidal neuron activity. Thus, these mechanisms might explain the "inhibitory" actions of D_1 receptors on firing of PFC pyramidal neurons (Williams and Goldman-Rakic, 1995).

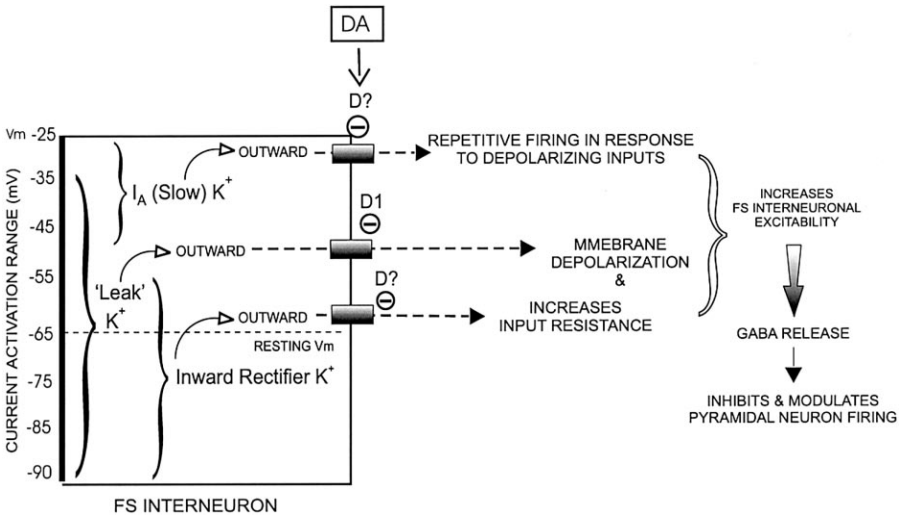

Figure 9. A schematic summary of the mechanisms that mediate DA actions in FS interneurons and that cause an increase of FS interneuron excitability. The voltage ranges through which the three K^+ currents are active are displayed on the left. DA suppresses a voltage-dependent I_A (slow) K^+ current via undefined DA receptor mechanisms to induce repetitive firing. D_1 activation blocks a voltage-independent, outward, leak K^+ current. Through unknown receptor DA also inhibits a voltage-dependent inward-rectifier K^+ current, determining an increase in input resistance (the flow of this current is outward at membrane potentials more positive than its reversal potential) (from Gorelova et al., 2002).

Furthermore, it is known that DA can also act in the opposite direction on GABAergic interneurons, leading to a decreased feedforward inhibition to PFC pyramidal neurons: in fact, activation of D_4 receptors, either by exogenous agonist or endogenous DA, induces a persistent reduction of synaptic AMPA responses in layer I GABAergic interneurons, through a postsynaptic mechanism which causes an alteration in the AMPA receptor trafficking involving the myosin V-mediated transport along actin (Yuen and Yan, 2009). The DA-mediated reduction of interneuron activity has been observed first *in vivo* by Tierney et al. (2008): both iontophoretic application of DA and VTA stimulation determine an inhibition of layer V interneuron firing which is mediated by both D_1 and D_2 receptors; this effect is preceded by a short-latency fast EPSP in pyramidal cells, that is likely the result of DA and glutamate corelease (Lavin et al., 2005; Tierney et al., 2008).

Thus, DA can act through its receptors to modulate different ionic currents (Fig. 10) on different time scales in different cell types to produce different modifications in neuronal excitability and a modulation of the network behaviour (Lapish et al., 2007).

2.3.3 – DOPAMINE EFFECTS ON NETWORKS

It has been demonstrated that DA is able to modulate inhibitory transmission in a circuit-dependent manner: in fact, using paired whole-cell recordings of synaptic connections from adult ferret PFC slices, Gao et al. (2003) have shown that DA decreases the IPSP

amplitude in FS non pyramidal-pyramidal neuron (FS NP-P) connections, while IPSP amplitude in non-FS non pyramidal-pyramidal neuron (non-FS NP-P) pairs is increased by DA. The former effect, which concerns FS interneurons known to target the perisomatic domain of pyramidal cells, involves a pre-synaptic mechanism related to GABA release; instead, the latter one, involving non-FS cells known to synapse on peridendritic regions of pyramidal neurons, occurs via a post-synaptic action (Gao et al., 2003).

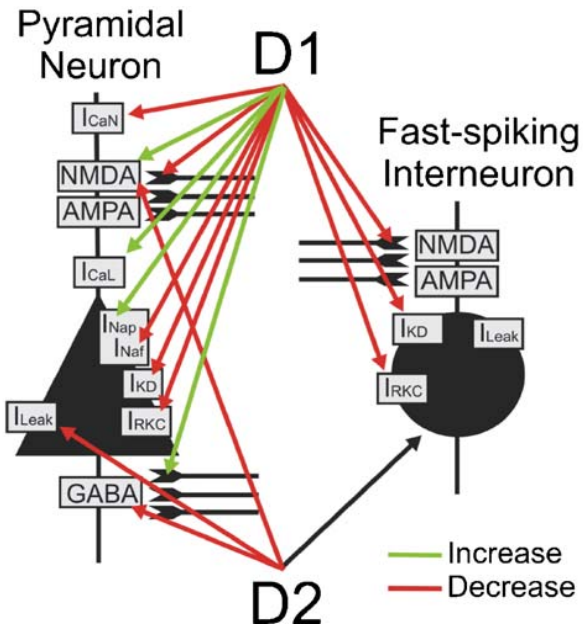

Figure 10. DAergic modulation of currents. Modulation of a variety of intrinsic and synaptic currents by DA has been shown to occur over minutes and hours both *in vivo* and *in vitro*. Activation of D_1- and D_2-like receptors occurs in both pyramidal cells and interneurons, and this makes DA able to modulate network behaviour (from Lapish et al., 2007).

Furthermore, DA directly modulates unitary excitatory synaptic neurotransmission in local pyramidal-to-pyramidal (P-P) circuits that mediate recurrent excitation, but not in pyramidal-to-FS non

pyramidal (P-FS NP) pairs: through activation of D_1 receptors DA decreases the probability of glutamate release, thus attenuating local horizontal excitatory synaptic transmission in layer V neurons (Gao et al., 2001; Gao and Goldman-Rakic, 2003).

PFC functions (i.e. working memory, memory retrieval and selective attention) need coactivation of NMDA and DA D_1 receptors; however, it is known that DAergic modulation follows an inverted-U-shaped profile: too little or too much DAergic receptor activation is detrimental for working memory, with moderate D_1 receptor activation optimizing PFC functions and working memory performance, in the presence of glutamatergic transmission (Fig. 11; Goldman-Rakic et al., 2000; Vijayraghavan et al., 2007; Kroener et al., 2009). This type of modulation of neuronal populations and circuits has been also described by Stewart and Plenz (2006), using multielectrode arrays to record network-level events in slices (the so called 'avalanches', rapidly propagating negative local field potentials with diverse spatiotemporal patterns): DA and NMDA regulate the spontaneous occurrence of neuronal avalanches in PFC superficial layers via an inverted-U pharmacological profile, because optimal avalanche induction is obtained with 30 μM DA, while at higher or lower DA concentrations the avalanches are reduced (Stewart and Plenz, 2006).

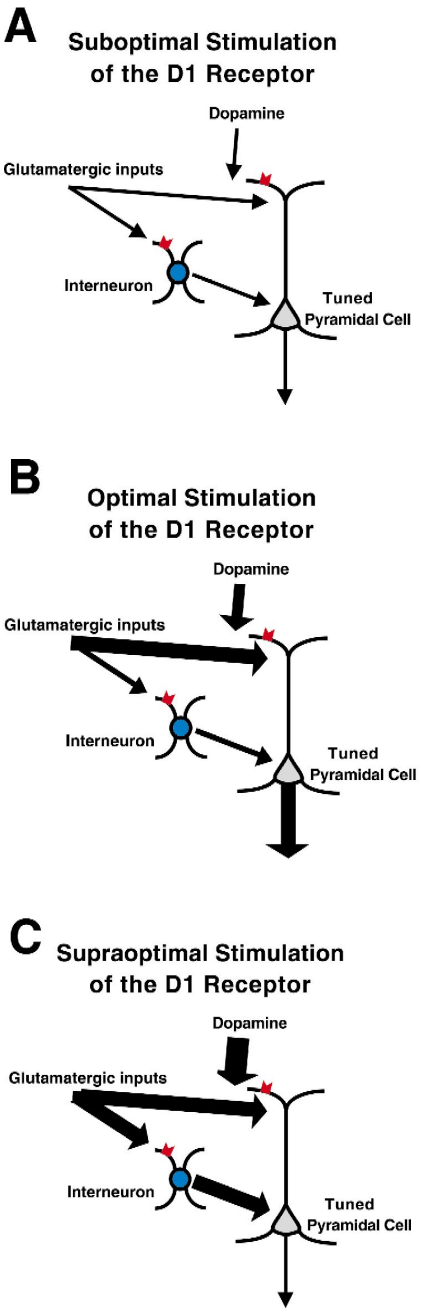

Figure 11. Model to explain the relationship between D_1 receptor stimulation and working memory performance. DA, acting at D_1 receptors (red), enhances glutamatergic inputs to both pyramidal cells (grey) and interneurons (blue). At low levels of DA release (A), the inputs are not enhanced to either pyramidal and GABAergic neurons. At moderate levels of DA release, the glutamatergic inputs to pyramidal cells are primarily enhanced (higher close contacts between DAergic terminals and pyramidal cell dendrites), thus improving working memory function (B). At high levels of DA release, the glutamatergic inputs are enhanced to both pyramidal cells and interneurons, with a resultant impairment of working memory function (C) caused by feedforward inhibition of pyramidal cell activity (from Goldman-Rakic et al., 2000).

2.4 – CONNECTIONS BETWEEN VTA AND PFC

2.4.1 – VTA TO PFC CONNECTIONS

A10 DA-containing fibres consist of small diameter, non-myelinated axons that ascend in the medial forebrain bundle (MFB). The majority of ascending (and descending) connections of the VTA are ipsilateral, while only thalamus, neostriatum and other forebrain areas receive minor contralateral projections; furthermore, it has been shown that some VTA neurons might innervate more than one region (Oades and Halliday, 1987), but the majority of ascending projections originates from non-collateralized cells (Sesack et al., 2003). It is possible to notice a topography of the origin of VTA projections: in fact, the more medial VTA neurons project to the ventral PFC, whereas the more lateral neurons project to the dorsolateral PFC in the monkey; furthermore, mesocortical projections tend to have their origin dorsorostrally in the VTA, while, by contrast, most mesolimbic projections originate in the ventrocaudal VTA (Oades and Halliday, 1987). DAergic cells that send projections to the PFC have unique physiological properties, in comparison with mesoaccumbens DAergic neurons, because they show higher baseline firing rates, more APs in each burst, higher DA metabolism and turnover and higher sensitivity to mild stressful stimuli; this is due to the fact that DAergic neurons that modulate the activity of PFC glutamatergic cells are themselves subject to afferent glutamate regulation within the ventral midbrain (Sesack et al., 2003).

2.4.2 – PFC TO VTA CONNECTIONS

The connections between the VTA and the PFC are reciprocal and there is a strong feedback pathway from the PFC to the VTA; in fact, most areas receiving a projection from the VTA project back to the VTA itself, which can act as a mediator of dialogue with the frontostriatal and limbic/extrapyramidal systems (Oades and Halliday, 1987; Tong et al., 1996). Glutamate PFC afferents to the VTA originate from layer V and VI neurons (Thierry et al., 1983) and exhibit a degree of specificity in their synaptic targets, because they form asymmetric axodendritic synapses on mesoaccumbens GABAergic but not DAergic cells and on mesoprefrontal DAergic but not GABAergic neurons; in this way the PFC selectively slows down the firing of mesoaccumbens neurons and accelerates the activity of mesoprefrontal cells (Sesack and Pickel, 1992; Carr and Sesack, 2000b; Sesack et al., 2003). Furthermore, these PFC to VTA projections have a relatively slow conduction velocity (0.6-5.5 m/s), which suggests that they are thin and poorly myelinated fibers (Thierry et al., 1983; Naito and Kita, 1994), and they can innervate several mesencephalic structures sending collaterals, thus modulating the activity of various cell populations (Thierry et al., 1983).

2.4.3 – FUNCTIONAL COUPLING BETWEEN THE VTA AND THE PFC

DA can affect the activity in the PFC; the effects of DA involve the modulation of the transitions between active glutamate-driven up

states and resting down states of pyramidal neurons. It has been demonstrated that there is a strong interdependence between VTA population activity and PFC up states: in fact, *in vivo* the fluctuations of membrane potentials in PFC pyramidal neurons and PFC local field potentials (LFPs) are correlated with LFP oscillations in the VTA, and when the VTA is transiently blocked with lidocaine, PFC LFPs disappear, the up states have an increased variability in duration and PFC neurons display a decreased firing rate (Peters et al., 2004). Thus, a transient inactivation of the mesocortical system can desynchronize up states in PFC neuronal populations, because VTA firing is able to synchronize a local cortical network; at the same time, DAergic cell burst firing requires NMDA receptor activation, which derives from cortical inputs. In this way, there is a continuous reverberation between a glutamatergic drive of VTA cell firing by the PFC and VTA support of PFC up states (Peters et al., 2004: Seamans et al., 2003). Moreover, a recent work has demonstrated that in PFC-VTA circuits *in vivo* a 4 Hz (2-5 Hz) oscillation appears and becomes the predominant pattern of activity during working memory tasks and it is phase coupled to hippocampal theta oscillations when working memory is in use (Fujisawa and Buzsáki, 2011). Furthermore, it has been shown that in most DAergic neurons the rhythmic bursting is inversely correlated with the degree of PFC depolarization, thus suggesting that part of the PFC information is conveyed to DAergic cells at least partially through inhibitory GABAergic neurons (a subset of which is found to fire in synchrony with the active up states of PFC cells) (Gao et al., 2007; Lodge, 2011).

2.4.4 – *IN VITRO* REGENERATION OF THE MESOCORTICAL PATHWAY

It is known that the extracellular environment of the adult CNS exerts an inhibitory action on the axonal regeneration, but a partial re-growth of axons after CNS injury has been observed. This supports the idea that adult CNS neurons may have an intrinsic capacity to evoke mechanisms that promote spontaneous axonal regeneration after injury (Muramatsu et al., 2009). In this perspective, it has been demonstrated that organotypic co-cultures of the VTA/SN-complex and the PFC can be used as an appropriate model to study the post-injury regeneration of DAergic fibres (Franke et al., 2003).

In fact, the study of the development and regeneration of functional connections in mammaliam CNS requires the use of appropriate model systems. The development and growth of complex connections and functionality within the brain involve processes which cannot be mimicked by neuronal networks of dissociated cells in culture, which represent a relatively simple system to analyze different parameters, as the induction of neurite sprouting. Alternatively, using *in vivo* models, it is difficult to maintain a precise control of the experimental conditions and these models are often time consuming (Hofmann and Bading, 2006). Thus, organotypic brain slices constitute a model, which is closer to the *in vivo* situation than cell cultures, and they allow long-term experiments, unlike acute slice preparations (Stoppini et al., 1991; Papp et al., 1995; Hofmann and Bading, 2006).

Franke et al. (2003) and Heine et al. (2007) have reconstructed the mesocortical system *in vitro* and demonstrated that in co-cultures

containing the VTA/SN-complex and the PFC, dopaminergic mesencephalic neurons are able to innervate the target areas in the PFC (Fig. 12), in a way that resembles the normal appearance of tissue from young rats. In fact, in the co-cultures, TH-positive fibres in PFC layers I and II form a band of parallel terminals that run along the medial cerebral surface, while in deeper layers they are perpendicular to the pial surface (as it has been described for rats *in vivo*) (Franke et al., 2003). It remains unclear whether the observed *in vitro* newborn projections derive from axonal regeneration of the neurons severed by the culture procedure, or from *a priori* outgrowth of undamaged cells, that had not yet sent an axonal process to the target tissue at the time of preparation (Franke et al., 2003). Nevertheless, it seems possible that the mechanisms that regulate fibre outgrowth of DAergic neurons may be the same as those operating during normal ontogenetic development (Franke et al., 2003).

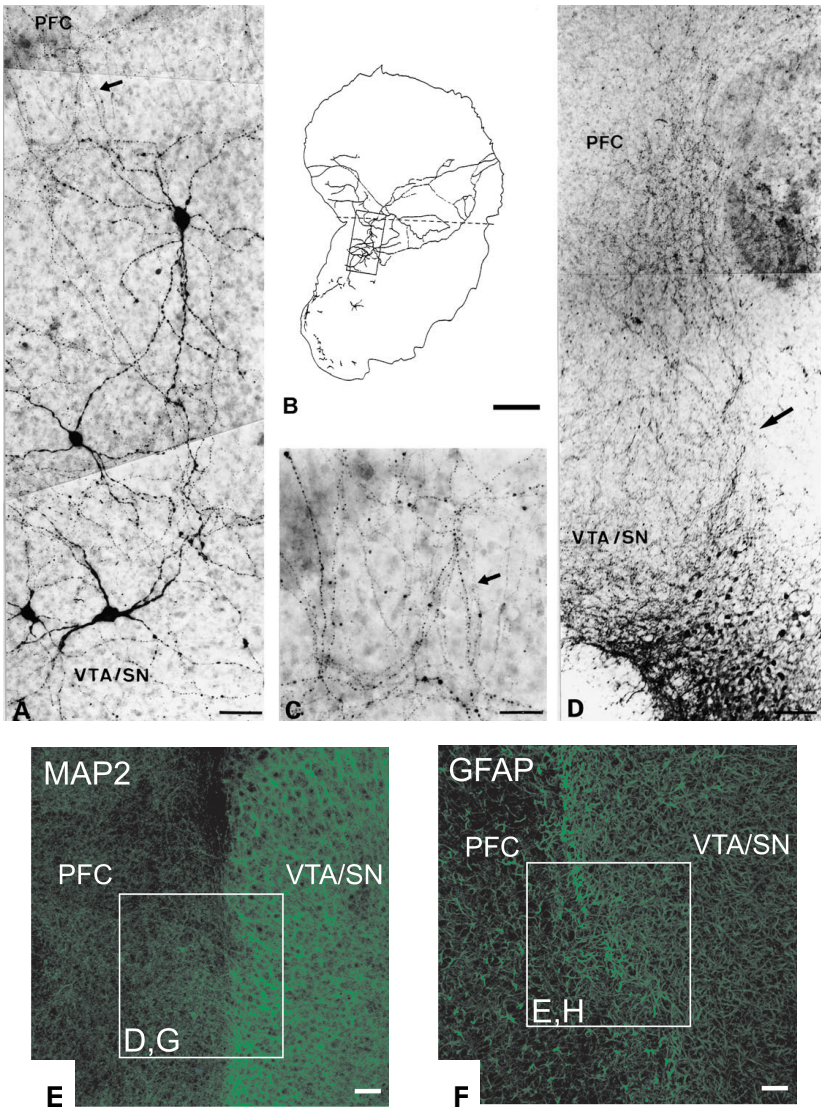

Figure 12. Co-cultures of VTA/SN-complex and PFC. A) Photomicrograph montage of TH-positive neurons and fibres in a co-culture at 21 div. B) Camera lucida drawing of the complete co-culture; the inset indicates the location of (A). C) Fibres (arrow) that had crossed the border, at higher magnification. D) VTA/SN-complex/PFC co-culture (21 div). Note the outgrowth of the TH-positive fibres (arrow) of VTA/SN neurons over long distances in the target region. E-F) Overview about the culture system containing the border region, characterized by immunofluorescence labelling of (E) MAP2 (neuronal marker)- and (F) GFAP (astroglial marker)- (→)

2.5 - PATHOLOGIES

Many psychiatric disorders (such as schizophrenia, addiction and attention-deficit/hyperactivity disorder) show cognitive and emotional alterations, which are related to an abnormal functioning and modulation of the mesocortical system (PFC and anatomically-related brain areas, and VTA) (Artigas, 2010).

2.5.1 – SCHIZOPHRENIA

Schizophrenia is a disorder of cognitive neurodevelopment, which presents deficits in cognition (i.e. impairments in attention and executive functions, abnormalities in working memory) normally appearing and progressing years before the onset of psychosis (Hoftman and Lewis, 2011). This disorder is directly proportional to the degree of genetic relatedness to an affected individual and linked to several identified susceptibility genes (Lewis et al., 2005) and it is characterized by marked anatomical, cellular and neurochemical alterations of the PFC (such as reduced PFC volume and layer thickness, tight packing of pyramidal neurons, reduced neuropil and energy metabolism, alterations of neurotransmitters such as GABA and DA and abnormal pruning of excitatory synapses, which cause lower spine density in deep layer III) (Artigas, 2010; Hoftman and Lewis, 2011).

---

positive cells and fibres (10 div) [Scale bars: 25 μm (A); 500 μm (B); 15 μm (C); 100 μm (D, E, F)] (from Franke et al., 2003; Heine et al., 2007).

It is known that working memory depends on the coordinated and sustained firing of subsets of PFC pyramidal neurons between the presentation of a stimulus cue and the later initiation of a behavioural response; during working memory tasks, inhibition might exert both a spatial role (to control which PFC pyramidal neurons are activated) and a temporal role (to control when they are active during the different phases of working memory). Thus, the reduced level of GAD67 and GAT1 mRNA expression in PFC PV-containing interneurons and the up-regulation of $GABA_A$ receptors at pyramidal neuron axon initial segments found in schizophrenia indicate an impairment in GABA-mediated inhibition, which could provide a mechanism for the disturbances in working memory in schizophrenic patients. In fact, a deficit in the synchronization of pyramidal cells, resulting from impaired perisomatic inhibition, might contribute to deficits in the gamma band oscillation, normally induced and sustained during the delay period of working memory tasks (Lewis et al., 2005). There are indications that this alteration in inhibition could be a consequence of the weakening of pyramidal cell network activity, which happens during development due to genetic and/or environmental insults and is caused by progressive PFC spine loss leading to reduced pyramidal cell network excitation (Arnsten, 2011). All these alterations determine a reduced cortical drive on VTA DAergic neurons projecting to the PFC, causing a functional decrease in the PFC DA levels, which induces the appearance of the negative symptoms of schizophrenia and the increase of the DAergic tone in subcortical sites (responsible of the positive symptoms of the disorder), due to the removal of corticofugal glutamatergic neurons

from tonic DA-mediated inhibition (Glowinski et al., 1984; Goldstein and Deutch, 1992; Yang et al., 1999; Arnsten, 2011).

2.5.2 – ADDICTION

Drug addiction is a complex behavioural phenomenon which is characterized by compulsion to continue seeking and administering drugs, despite the severe consequences to work, social relationships and health (Kauer, 2004). It is widely accepted that addictive drugs cause functional changes in DA-containing neurons, resulting in an increase of neuronal activity and of DA release from their terminals (Bonci et al., 2003; Kauer, 2004). Amphetamine and cocaine determine a depression of the spontaneous firing rate of VTA DAergic neurons because, blocking DA re-uptake by DAT, the higher extracellular DA level activates D_2 autoreceptors; furthermore, it has been recently shown that a single exposure to cocaine or amphetamine is able to induce LTP of AMPA-mediated excitatory transmission in DAergic neurons, thus favouring DA release at synaptic terminals (Bonci et al., 2003; Kauer, 2004). Instead, opioids cause an increase in the firing frequency of DAergic neurons, through the inhibition of afferent GABAergic neurons and reduced GABA release from presynaptic terminals; these acute effects determine an increase of DA release in the PFC and NAcc and have been associated with reward (Bonci et al., 2003). In normal individuals, following the intake of a drug, homeostatic responses tend to re-establish the initial level of neuronal activity, but in a percentage of vulnerable individuals (who have a genetic predisposition, modulated also by developmental and

environmental factors) erroneous responses are established and propagated to various regions of the reward circuit. In this way, a prolonged changed state substitutes the physiological one and the maintenance of the changed state leads to continued drug use. Thus, drug seeking can be seen as a persevering effort of the individual to retain the defective coding of neuronal activity by repeatedly activating drug-induced responses (Bonci et al., 2003).

Recently, preclinical and clinical studies have also discovered and began to clarify the role of PFC in addiction; in fact, on the basis of imaging studies it has been shown that a disrupted function of the PFC leads to a syndrome of impaired response inhibition and salience attribution in addiction, characterized by excessive salience to the drug and drug-related cues, which results in drug seeking and taking (Goldstein and Volkow, 2011).

3. MATERIALS AND METHODS

3.1 – ANIMALS

Neonatal mice pups (CD1® mice, Harlan Laboratories, Italy) of postnatal day (P) 1-3 were used for the preparation of the organotypic dopaminergic slice co-cultures. The animals were housed under standard laboratory conditions, under a 12 h light/dark cycle and allowed access to lab food and water ad libitum.

All the animal use procedures were approved by the Committee of experimental animal protection. The number of animals used was minimized as well as their sufferings.

3.2 - PREPARATION OF THE SLICE CO-CULTURES

Slice co-cultures were prepared from P1-3 mice according to the protocol described by others (Franke et al., 2003; Heine et al., 2007; Fig. 13 I and II), with some modifications. Briefly, mice pups were decapitated and the brains were removed from the skull under sterile conditions. The brains were apposed to an agar block (Serva, Heidelberg, Germany) and tissue blocks containing the VTA/SN-complex or PFC were dissected, fixed onto a specimen stage of a vibratome (Leica, VT 1000S, Nussloch, Germany) with Loctite Super Attack glue (Henkel, Dusseldorf, Germany) and placed in ice-cold (4°C) solution containing the following (in mM): 87 NaCl, 25

$NaHCO_3$, 1.25 NaH_2PO_4, 7 $MgCl_2$, 0.5 $CaCl_2$, 2.5 KCl, 25 D-glucose and 75 sucrose, equilibrated with 95% O_2 and 5% CO_2 (pH 7.4). Coronal sections of 200 μm (Shimono et al., 2002a and 2002b) were cut at the mesencephalic and forebrain levels. In the preparation of organotypic slice cultures we did not attempt to separate the VTA and the SN; for further discussion this area will be named VTA/SN-complex.

The slices were separated into the different brain areas and transferred into Petri dishes filled with the same ice-cold solution. Selected sections were placed on MEA petri dishes (30 μm diameter ITO electrodes 200 μm apart, Multichannel Systems, Germany), pre-treated with Plasma Cleaner (Harrick Plasma, Ithaca, New York) and pre-coated with collagen 3.5 mg/mL (Collagen type I, rat tail, Millipore, Italy; Maeda et al., 2004), to cover the 8 x 8 microelectrode array (Fig. 13 III and IV). The sections of the VTA/SN-complex and the PFC were placed on the MEAs, in the way that the VTA faced the medial PFC (Fig. 13 IV a). We positioned the slices trying to leave the smallest possible distance (< 300-400 μm) between them, with each slice covering almost half of the electrodes. The cultures on MEA dishes were kept at 37°C in 5% CO_2 for 1 h before adding the culture medium up to an interface level (250 μL) and covered with gas permeable covers (MEA-MEM, Ala Scientific Instruments, Inc., USA). The medium contained 25% MEM, 25% Basal Medium Eagle without glutamine (Gibco, Life Technologies), 25% Horse Serum (EuroClone), supplemented with glutamine to a final concentration of 2 mM, 0.6% glucose and Pen/Strep 150 μg/mL (Sigma-Aldrich); the pH was adjusted to 7.2 for the period of incubation. Sterile distilled

water was added around the probe to increase humidity and prevent over-drying of the culture medium in the MEA dish (Shimono et al., 2002b).

All the cultures were maintained at 37°C in 5% CO_2; after two days *in vitro* (DIV) the incubation medium was changed with a serum-free medium, consisting of Neurobasal Medium (NB) supplemented with B27 (Invitrogen, Italy), glutamine 1 mM and Pen/Strep 150 μg/mL (Sigma-Aldrich, Italy). For the co-cultures on MEA dishes the medium was changed with half volume every day.

We maintained the co-cultures up to 4 weeks *in vitro* to study the regeneration and the functional properties of the growing projections between the VTA/SN-complex and the PFC. As described by Stewart and Plenz (2008), the position of the electrodes under both the areas of the co-cultures was established during the culture preparation and checked after 1-2 div and later during the development, because it has been shown that organotypic cultures adhere to the substrate, slightly expand and flatten during postnatal maturation (Stoppini et al., 1991; Stewart and Plenz, 2008).

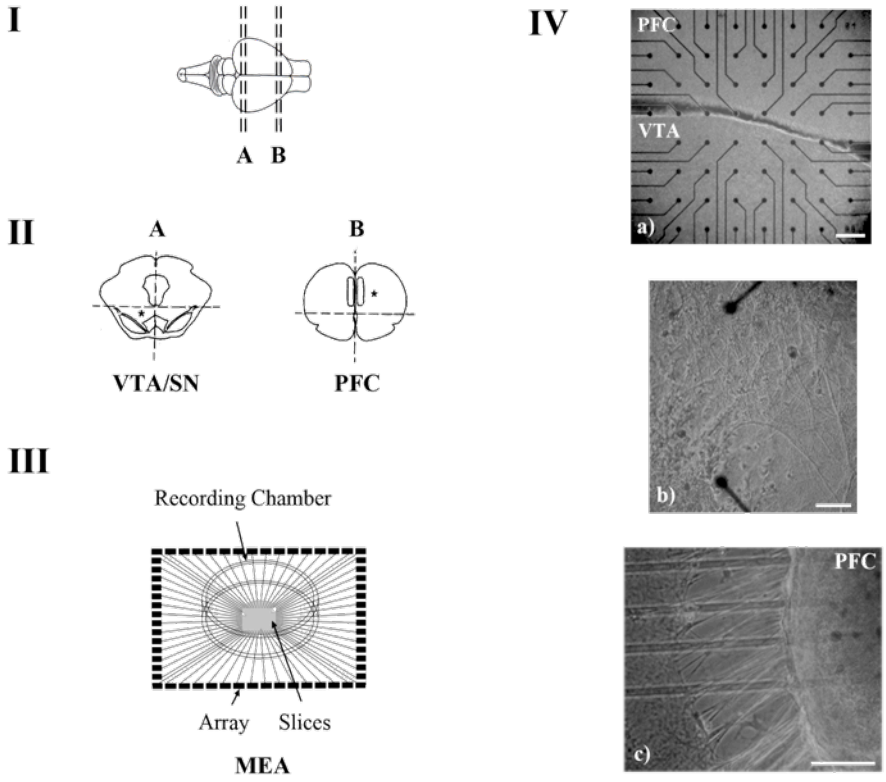

Figure 13. Schematic illustration of the organotypic co-culture preparation procedure from P1-3 mice. (I) Tissue blocks were dissected at the position A and B to obtain the ventral tegmental area/substantia nigra-complex (VTA/SN, A) and the prefrontal cortex (PFC, B). (II) Blocks were trimmed along the dashed lines and coronal sections of the regions of interest (200 µm; asterisks) were selected and incubated as co-cultures on multi-electrode arrays (MEA, III) (modified from Franke et al., 2003 and Heine et al., 2007). (IV) In a-c, pictures of VTA/SN-PFC co-cultures on multi-electrode arrays with an inter-electrode distance of 200 (a, c) or 500 (b) µm, taken at 1 (a), 7 (b) and 14 (c) DIV, respectively. In (b), the border region between VTA/SN and PFC is shown and it is possible to notice the newborn projections grown between the two areas of the co-culture. In (c), detail of the projections originating from the external border of the PFC. It is possible to note the difference between the area where the projections are present (central part of the picture) in which the collagen, used to allow the slices to adhere to the MEA, has been metabolized, and the left side of the picture, where projections are absent [Scale bars: (a) 200 µm; (b, c) 100 µm].

3.3 – MULTI-ELECTRODE ARRAY RECORDINGS

Data recordings were done as described (Gullo et al., 2009; Gullo et al., 2010) with some changes. Briefly, raw analogue signals sampled at 32 kHz were recorded at 36°C in CO_2-controlled incubators, from MEA-1060BC preamplifiers (bandwidth 0.1-8 kHz, Multichannel Systems, Germany) and detected through MC_Rack Software (version 4.0, Multichannel Systems, Germany) by using appropriate filters to separate spikes (0.25-5 kHz) and local field potentials (LFPs, 5-200 Hz; Santos et al., 2010). For the characterization of the firing properties during the development of the cultures, MEA recordings were performed between 3 and 28 days *in vitro* (div); for the other experiments, we used only 12-20 div MEA dishes, because this age interval is considered to be the optimal temporal window for having a fairly stable activity (Wagenaar et al., 2006; Santos et al., 2010).

3.3.1 – SPIKING ACTIVITY

The spike signals were detected through MC_Rack software using a fixed threshold of -5 standard deviations from the background noise of each electrode, and sorted in units through a mixed amplitude-duration criterion in a window of 2 ms (as described in Gullo et al., 2009) and cleaned of artefacts using the OFFline Sorter program (Plexon Inc., USA). The electrodes, which responded irregularly during the experiments, were excluded from the analysis. To perform burst detection and analyze their properties, we used the procedures described in Gullo et al. (2009), with some modifications. Briefly, for

each identified channel unit, we computed the following characteristics: the autocorrelation function (ACF), the time at which the decaying phase of the autocorrelation halved (ACHL), the burst duration (BD), the number of spikes in each burst (SN), the spike rate (SR), the intra-burst spike rate (IBSR), the Fano Factor (FF) and the inter-burst interval (IBI) (Gullo et al., 2010). The data for all the bursts of a specific neuron were averaged in defined time segments corresponding to the control or the presence of different drugs or treatments. We were able to classify neurons on the basis of an Unsupervised Learning Approach, consisting of data reducing principal component analysis (PCA), followed by the K-means clustering procedure (Johnson, 2002; Duda, 2000). In the clustering processing we also used an outliers removing procedure, which discarded from results those units having a Mahalanobis distance from the centroid of its cluster bigger than a fixed threshold (here we used 2; Fig. 14). The procedure identified two statistically different clusters, as previously described (Gullo et al., 2010), which were named with the subscript "e" (excitatory) and "i" (inhibitory), respectively. The two identified clusters obeyed all the following rules at the same time (in control conditions): $ACHL_e << ACHL_i$; $BD_e << BD_i$; $SN_e << SN_i$; $SR_e << SR_i$; $IBSR_e >> IBSR_i$; $FF_e << FF_i$; $IBI_e \leq IBI_i$; $NN_e \approx NN_i \times 4$. To analyze the burst structure we applied a scanning window of variable duration (5-30 ms) in order to search the start of the up states, collect the spikes and identify the major burst leaders (MBLs, which are those neurons able to trigger al least 4 % of the total recorded bursts; Ham et al., 2008). From the two clusters

defined above it was possible to identify how the spikes belonging to each clusters are elicited during the burst time-course.

Furthermore, we applied a new procedure described in Gullo et al. (2012), that consists in a PCA-based classification of network states, performed by using the following features: i) the shape of the spike number time histograms (SNTH); ii) the number of engaged neurons (NN); iii) burst duration (BD). The statistical significance of the classification was evaluated using a 2-sample paired *t* test ($p < 0.05$) and the states, which included less than 4 % of the total recorded bursts in the considered time segment, were discarded. After the identification of the statistically different states, the programme output consisted in a series of files, associated to the two clusters of neurons, that described: i) the probability density function of finding 1, 2, 3, i-th spikes (FSH) and its cumulative probability (cFSH) in order to investigate the mode of firing of these neurons; ii) the time histograms of the number of spikes (SNTH), of the neurons engaged in the activity (for each time bin, NNTH) and its ratio, called excitability (EXTH) (Gullo et al., 2012).

3.3.2 – LOCAL FIELD POTENTIAL ACTIVITY

Recordings of LFPs were captured simultaneously by positive and negative thresholds (± 5 standard deviations from the background noise of each electrode) and filtered in the 5-200 Hz frequency band. For each electrode, LFPs were further sorted by PCA analysis into 2 clusters. Data were averaged during time segments of 600 s or more.

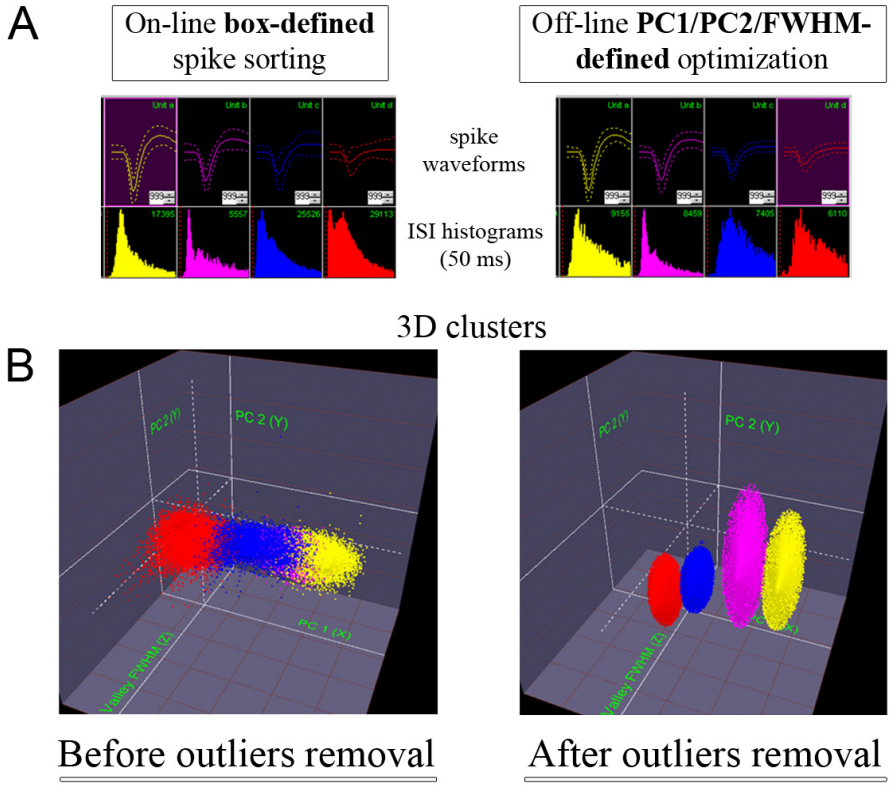

Figure 14. Optimization and identification of units in the same electrode. Left and right graphs represent data obtained before and after outliers removal (during on-line acquisition and off-line analysis, respectively). In A, plots of average spike waveforms (1.2 ms) in each defined unit and, below, the corresponding inter-spike interval histograms (ISI histograms, 50 ms full scale). Notice that in the upper-right corner of these rectangles the number of spikes of the specific unit is indicated. In B, 3D plots in the feature space of PCA1, PCA2 and full-width at half valley maximum (FWHM) dimensions (same colours as in the upper panels). It is possible to note that the outliers of yellow and blue units completely inhibit the view of the purple cluster only before the procedure. The total *p*-value of the MANOVA-test changed from 10-5 to 10-30 before and after the outliers removal with a Mahalanobis threshold of 2. This data have been obtained from a recording which lasted more than 5 h. Notice that the outliers removal determines a strong decrease in the number of spikes in each unit (modified from Gullo et al., 2009).

3.4 – DRUG APPLICATION

As previously described (Gullo et al., 2009), all the findings reported here in presence of different drugs were obtained in just a few hours and so they can be considered at steady state. All the experiments with the MEA technique were performed by adding the drugs in volumes that were always less than 1% of the total volume of the solution bathing the co-cultures. The drugs (Gabazine, also known as SR95531, and Eticlopride) were purchased from Sigma and Tocris (UK) and kept as frozen stock solutions in distilled water at -20 °C until diluted to their appropriate concentrations.

3.5 – DATA ANALYSIS

We used OriginPro 7.0 (OriginLab Co., Northampton, MA, USA) to analyze data and Corel Draw 15.1 (Corel Corporation, Ottawa, Canada) to prepare the figures. All the results are indicated as mean ± SEM and *n* indicates the number of experiments performed; drug effects were calculated as percentage of change from control values. Statistical analysis was performed with OriginPro 7.0 software package using paired Student's *t*-Test and ANOVA, if necessary, at the indicated significance level (*p*). If the data normality test was not satisfied, the Kolmogorov-Smirnov test was used.

4. RESULTS

Through the MEA platforms, we recorded two different types of spontaneous activity from the VTA/SN-PFC co-cultures: i) a very fast activity (250 Hz-5 kHz), namely bursts of action potentials and ii) local field potentials (LFPs), which are characterized by frequencies ranging from 5 to 200 Hz and represent population synaptic potentials, afterpotentials of somatodendritic spikes and voltage-gated membrane oscillations, thus reflecting the input to a given brain area and its internal processing (Juergens et al., 1999; Belitski et al., 2008; Rasch et al., 2008). In Fig. 15A, an exemplificative burst, recorded from a co-culture at 5 div and interesting both the VTA/SN-complex and the PFC, is shown. Different neurons from both the slices participated to the burst, with a variable number of action potentials. Fig. 15B shows some examples of LFPs, recorded from the PFC (upper row) and the VTA/SN-complex (lower row). The waveforms shown in the graphs are represented as average ± sem of 900 s recording periods.

We followed the VTA/SN-PFC co-cultures during their *in vitro* development and we characterized the developmental profile of single-neuron properties and network firing patterns, in order to evaluate the functionality of the newborn projections between the VTA/SN-complex and the PFC.

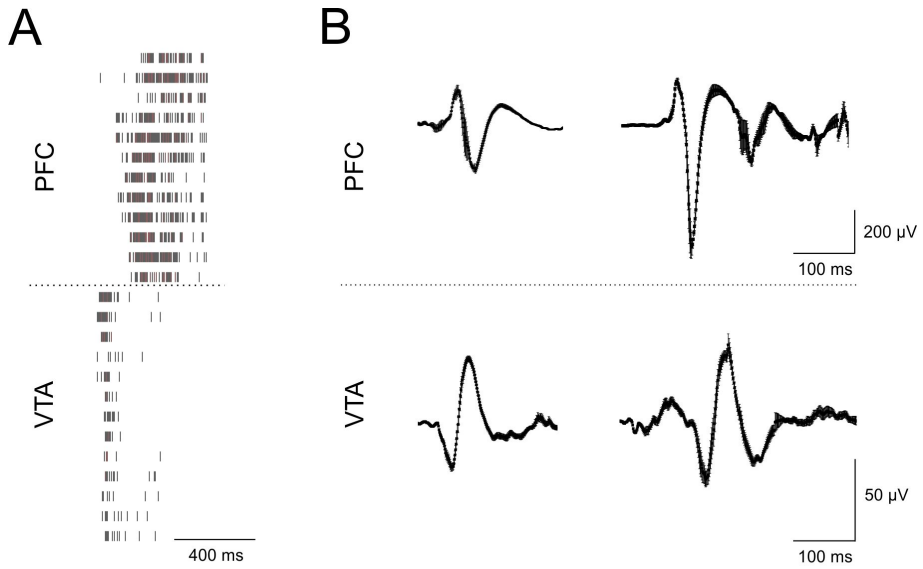

Figure 15. Types of activity recorded from VTA/SN-PFC co-cultures. (A) Example of a burst of action potentials (bandwidth 250 Hz-5 kHz) recorded from a co-culture at 5 div. Each row shows the activity of a neuron, while each vertical line represents the timestamp of an action potential; the dashed line separates neurons belonging to the VTA (n = 13, bottom) from those belonging to the PFC (n = 12, upper part). (B) Example of local field potentials (bandwidth 5-200 Hz) recorded from the VTA/SN- complex (bottom part) and the PFC (upper part). The waveforms shown in the graphs are represented as average ± sem of 900 s recording periods.

4.1 – CHARACTERIZATION OF THE DEVELOPMENT OF VTA/SN-PFC CO-CULTURES

The first step for the characterization of VTA/SN-PFC co-culture development consisted in the quantification of the following properties of VTA/SN-complex and PFC neuron spontaneous bursting activity during the time in culture: burst rate (bursts/min), intra-burst spike rate (IBSR, Hz), burst duration (BD, s), spike number (SN), inter-spike interval in burst (ISI in burst, ms), peak IBSR (Hz) and the

percentage of spikes in bursts (%). We observed a gradual but significant increase of the burst frequency both in the VTA/SN-complex (black) and in the PFC (grey) from 10 different co-cultures (Fig. 16A, left); in fact, while after the first three days *in vitro* the VTA/SN-complex and the PFC showed a very low average burst rate (1.3 ± 0.2 and 0.5 ± 0.3 bursts/min, respectively), the frequency of the bursts increased up to 5.1 ± 0.7 and 3.9 ± 0.6 bursts/min in the VTA/SN-complex and the PFC, respectively, after two weeks of culture (p-value < 0.01). Differently, IBSR changed during the development only in the VTA/SN-complex (Fig. 16B, left): in fact, while the average IBSR of PFC neurons remained constant throughout all the *in vitro* maturation, VTA/SN-complex neurons showed an increase of IBSR values from 18.4 ± 3.2 Hz during the first days of culture to 40 ± 3.6 Hz at 13-15 div (p-value < 0.01), then remaining stable and not statistically different from PFC values. Furthermore, we observed that both BD and SN did not undergo a significant change during the development *in vitro*: in fact, BD of PFC neurons displayed a trend towards increase without reaching statistical significance, while VTA/SN-complex activity showed stable BD values (Fig. 16C, left); on the contrary, VTA/SN-complex and PFC neurons differed in their SN values only in the first days of development (10.6 ± 2.4 and 26.3 ± 3.4 spikes in burst, in the VTA/SN-complex and in the PFC, respectively), with similar SN averages during the remaining *in vitro* maturation (18.1 ± 4.4 in the VTA/SN-complex and 15.7 ± 3.7 in the PFC at 13-15 div; Fig. 16D, left).

Using our software for the discrimination of excitatory and inhibitory neurons (Gullo et al., 2009), we analysed the previously described

parameters in the PFC of the co-cultures, distinguishing between the excitatory (red) and the inhibitory (black) clusters of neurons. For both the clusters, the burst rate increased from 1.4 ± 0.4 and 1.9 ± 0.6 bursts/min at 1-3 div to 5.1 ± 0.7 and 6.3 ± 0.2 bursts/min at 13-15 div (p-value < 0.05), for excitatory and inhibitory neurons, respectively (Fig. 16A, right). At the same time, we observed that IBSR significantly increased after two weeks of culture only for the excitatory cluster (77.1 ± 4 Hz at 1-3 div and 108 ± 8.9 Hz at 13-15 div, p-value < 0.05; Fig. 16B, right) and that excitatory neuron IBSR was statistically different and higher than inhibitory cluster value (77.1 ± 4 and 43.3 ± 2.9 Hz at 1-3 div, p-value < 0.01; 108 ± 8.9 and 53.5 ± 7.6 Hz at 13-15 div, p-value < 0.01, for excitatory and inhibitory neurons, respectively), in agreement with the well known high spike frequency inside the bursts of excitatory neurons, compared to the low IBSR of interneurons (Csicsvari et al., 1999; Barthó et al., 2004). Contrarily, during the first days of culture, BD and SN of excitatory and inhibitory neurons were similar and they differed only later in the development: in fact, both BD and SN of inhibitory neurons were higher than the corresponding values of the excitatory cluster at 13-15 div (BD: 0.25 ± 0.11 s and 0.59 ± 0.14 s, Fig. 16C, right; SN: 5.2 ± 0.7 and 13.4 ± 3.5, p-value < 0.05, Fig. 16D, right, for excitatory and inhibitory neurons, respectively), as expected from the known firing properties of principal cells and interneurons.

In Fig. 16E, F and G, the developmental trend of ISI, peak IBSR and the percentage of spikes in burst (%) are represented. We observed a progressive decrease of ISI in the VTA/SN-complex (black) from 94.3

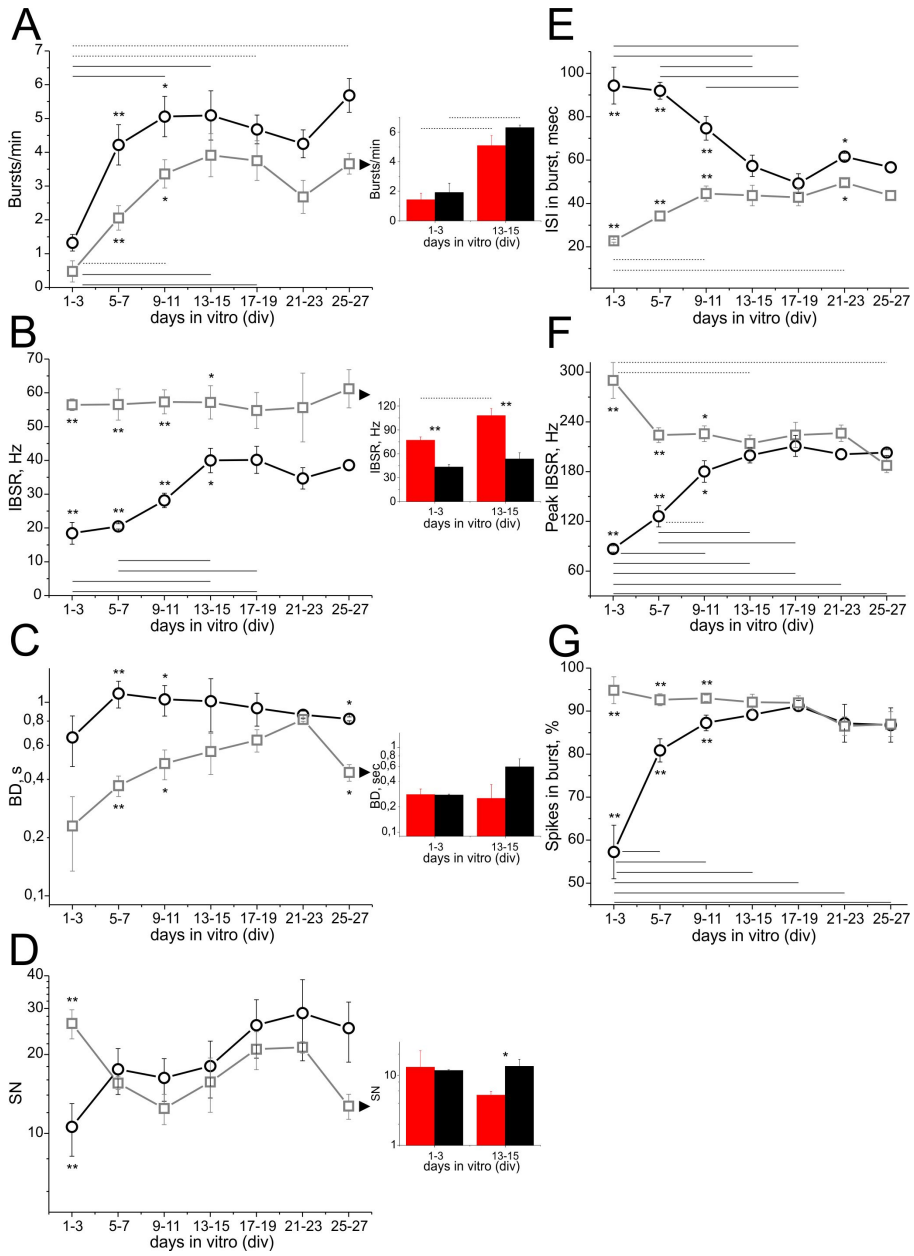

Figure 16. Characterization of the developmental features of the VTA/SN-PFC co-cultures. (A) On the left, burst rate (bursts/min) of the PFC (grey line, empty squares) and of the VTA/SN-complex (black line, empty circles) during the development of the co-cultures. On the right, histograms of the burst rate for the excitatory (red) and inhibitory (black) neurons recorded from the PFC at 1-3 (early development) and 13-15 (→)

± 8.5 ms at 1-3 div to 57.3 ± 5 ms at 13-15 div (p-value < 0.01) and an increase of PFC ISI (grey) from 22.8 ± 0.6 ms at 1-3 div to 43.7 ± 4.8 ms at 13-15 div (p-value < 0.05, Fig. 16E). An opposite trend was identified for the peak IBSR (Fig. 16F): in fact, while this parameter significantly decreased in the PFC (290 ± 21.6 Hz at 1-3 div and 214

(advanced development) div. (B) On the left, intra-burst spike rate (IBSR, Hz) measured in the PFC (grey line with empty squares) and in the VTA/SN-complex (black line with empty circles) during the development. On the right, IBSR histograms of excitatory (red) and inhibitory (black) neurons belonging to the PFC at 1-3 and 13-15 div. (C) On the left, burst duration (BD, s) during the development of the PFC (grey line, empty squares) and the VTA/SN-complex (black line, empty circles) of the co-cultures. On the right, as in A and B, burst duration histograms of PFC excitatory (red) and inhibitory (black) neurons at 1-3 and 13-15 div. (D) On the left, number of spikes in burst (SN) during the development of the VTA/SN-complex (black line with empty circles) and of the PFC (grey line with empty squares). On the right, SN for excitatory (red) and inhibitory (black) neurons of the PFC at the beginning (1-3 div) and after two weeks of development. (E) Inter spike interval (ISI) in burst (ms) in the VTA/SN-complex (black, empty circles) and in the PFC (grey, empty squares) during the development. (F) Peak firing frequency in burst (peak IBSR, Hz) in the co-cultures (VTA/SN-complex and PFC, indicated by a black line with empty circles and by a grey line with empty squares, respectively) during the development. (G) Percentage of spikes in burst, on the total number of spikes recorded from the VTA/SN-complex (black line, empty circles) and the PFC (grey line, empty squares) during development. The data shown in A-G clearly indicate that during the development of the co-cultures the VTA/SN-complex and the PFC go towards a similar mature condition with comparable firing properties, due to the progressive growth of new projections, which are able to link the two areas and allow a continuous communication. In all the graphs, data are obtained following the development of 10 co-cultures; the continuous and dashed lines indicate a p-value of 0.01 and 0.05, respectively, for the PFC or the VTA/SN-complex; the double and the single asterisks indicate a p-value of 0.01 and 0.05, respectively, in the comparison between the PFC and the VTA/SN-complex at each developmental stage (ANOVA followed by Bonferroni test).

± 10.1 Hz at 13-15 div, *p*-value < 0.05), the VTA/SN-complex showed a gradual increase in the peak IBSR values during the first two weeks of development (86.8 ± 3.8 Hz at 1-3 div and 199.5 ± 9.1 Hz at 13-15 div, *p*-value < 0.01). Finally, we quantified the percentage of spikes, which are organized in bursts, on the total number of the recorded spikes. We observed that while in the PFC the amount of spikes being part of bursts remained constant and high throughout the development (94.9 ± 3.1 % and 92.1 ± 1.9 % at 1-3 and 13-15 div, respectively), with few spikes occurring out of the identified bursts, in the VTA/SN-complex the burst firing pattern matured during the development, as indicated by the progressively increasing percentage of spikes encompassed in bursts (57.3 ± 6.2 and 89.1 ± 1.2 at 1-3 and 13-15 div, respectively; Fig. 16G). After 13-15 div the percentage of spikes in burst remained stable for both the PFC and the VTA/SN-complex. The data shown in Fig. 16 A-G clearly indicate that during the *in vitro* development the VTA/SN-complex and the PFC tend to reach a similar mature condition, with homogeneous firing properties, in parallel with the progressive growth of new projections, which are able to link the two areas and allow a continuous communication.

From Fig. 16 it is also possible to note that the characteristics of VTA/SN-complex and PFC firing reached a stable condition within two weeks of culture and then remained stable during the late development.

To characterize the developmental features of the activity in the VTA/SN-complex and in the PFC of the co-cultures, we also recorded the local field potentials, representing population synaptic events.

With the progressive maturation of the co-cultures, we observed a gradual increase in the amplitude of the LFPs, recorded either from the VTA/SN-complex and the PFC. In Fig. 17 exemplificative LFP waveforms (mean ± sem, obtained averaging the LFPs captured during 900 s recording periods; thick black lines) recorded from a co-culture are represented; the thin black lines show the correspondent spike rate (Hz). It is possible to note the gradual LFP amplitude increase at 6 (a), 10 (b), 14 (c) and 17 (d) div, together with an increase of the spike rate, both in the PFC (first row) and in the VTA/SN-complex (second row); later in the development the LFP amplitude remained almost stable (data not shown).

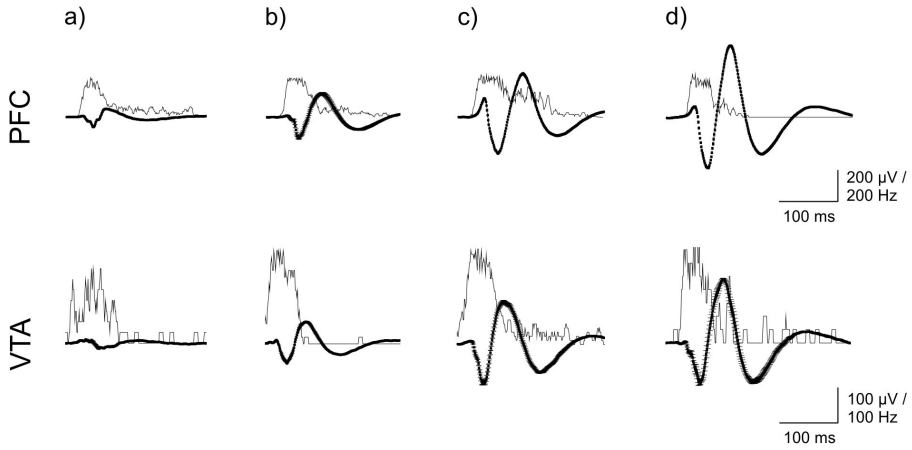

Figure 17. Developmental changes of local field potentials. Exemplificative average waveforms recorded from a VTA/SN-PFC co-culture (LFPs from the PFC in the first row and those from the VTA/SN-complex in the second row) during the development *in vitro*. The thick black lines represent the average waveform (mean ± sem) of a 900 s recording period at 6 (a), 10 (b), 14 (c) and 17 (d) days *in vitro*, while the thin black lines show the corresponding spike rate histograms [bin = 0,001 s].

4.2 – EXCITATORY AND INHIBITORY NEURONS IN THE VTA/SN-PFC CO-CULTURES

To further characterize the VTA/SN-PFC co-cultures we investigated the distribution of excitatory and inhibitory cells. For this aim, we calculated the number of excitatory and inhibitory neurons recorded from the PFC through the MEA technique during the development of the VTA/SN-PFC co-cultures. We observed a progressive increase of the average number of excitatory (red) and inhibitory (black) neurons (Fig. 18), recorded from each culture and successively identified through the software for the analysis of the electrophysiological data, from 1-3 div to 9-15 div (excitatory cluster: 3 ± 1.2 and 22.1 ± 3 neurons at 1-3 and 13-15 div, respectively; inhibitory cluster: 1.1 ± 0.5 and 8.1 ± 1.3 neurons at 1-3 and 13-15 div, respectively). In this analysis, we considered the maturation of the co-cultures up to 17-19 div, because from the previous data illustrated in Fig. 16 it was clear that after this developmental stage the co-cultures maintained a stable condition. From these data it is possible to note that the excitatory/inhibitory ratio in mature VTA/SN-PFC co-cultures at 13-15 div is ≈ 3.

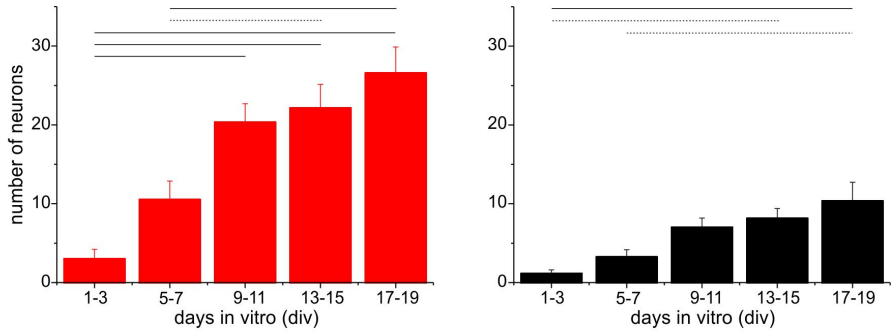

Figure 18. Increase of the number of excitatory and inhibitory neurons recorded from the PFC during the development of the VTA/SN-PFC co-cultures. Histograms of the average number of excitatory (red, left) and inhibitory (black, right) neurons recorded from the PFC during the development of 10 co-cultures. These values indicate an excitatory/inhibitory neuron ratio of about 3. The continuous and dashed lines in the graphs indicate a *p*-value of 0.01 and 0.05, respectively (ANOVA followed by Bonferroni test).

4.3 – APPEARANCE OF DIFFERENT FIRING PATTERNS IN THE VTA/SN-PFC CO-CULTURES DURING DEVELOPMENT

From all the parameters previously described in Fig. 16 it is possible to note that the differences in the firing between the VTA/SN-complex and the PFC of the co-cultures tended to disappear during the first two weeks *in vitro*, parallel to the progressive growth of the newborn projections between the two areas. Thus, we evaluated how the network firing patterns of the whole VTA/SN-PFC co-cultures changed during the *in vitro* development. We collected the starts of network bursts in the VTA/SN-complex and in the PFC of 10 different co-cultures and then we compared them to look for different propagation patterns of activity. Four patterns of network bursts were

observed during the development (Fig. 19A): i) bursts restricted to the VTA/SN-complex, while the PFC remained silent (named VTA-only bursts); ii) bursts confined in the PFC, without activation of the VTA/SN-complex (called PFC-only bursts); iii) bursts which started in the VTA/SN-complex and rapidly propagated to the PFC (indicated as VTA-to-PFC bursts) and iv) bursts which arose in the PFC and back-propagated to the VTA/SN-complex (namely, PFC-to-VTA bursts). Furthermore, we quantified the percentage incidence of these burst patterns during the development of the co-cultures. The VTA-only bursts were the predominant firing pattern during the early development, at 1-3 div (78.2 ± 14.5 %), when we could also observe PFC-only bursts (21.8 ± 14.5 %) but no propagating bursts between the VTA/SN-complex and the PFC (Fig. 19A, right). This can be explained by the fact that, after 1-3 div, the growth of new projections is still at the very beginning: thus, the connection between the two areas of the co-cultures is limited, and not sufficient to let the activity propagate, or absent. After 5-7 div, the percentage of VTA-only bursts significantly decreased to 29.8 ± 10.7 % (p-value <<< 0.01), less PFC-only bursts were observed (even if the decrease was not significant), but there was the remarkable appearance of VTA-to-PFC bursts (61.7 ± 10.8 %, p-value <<< 0.01 in comparison with the previous developmental phase). At this developmental stage we also recorded a very limited number of PFC-to-VTA bursts (2.2 ± 1.7 %). After 9-11 div this trend was maintained: we observed a further reduction in the incidence of VTA-only bursts (13 ± 6.1 %), the disappearance of PFC-only bursts (Fig. 19A, left, inset) and an additional increase in VTA-to-PFC bursts (86.3 ± 6 %, Fig. 19A,

right). The developmental profile of the firing patterns reached a stable condition after two weeks in cultures: in fact, the incidence of VTA-to-PFC bursts remained almost stable (80-90 %), the VTA-only bursts and the PFC-to-VTA bursts were less than 15 % each, while no PFC-only bursts were recorded (Fig. 19A). Then, we analyzed the propagating bursts (VTA-to-PFC and PFC-to-VTA bursts) and we characterized the developmental changes of the propagation delays. We observed a progressive reduction in the VTA-to-PFC burst propagation delays: the delay significantly decreased from 99.6 ± 10.8 ms at 5-7 div, when this type of firing patterns first appeared, to 47.4 ± 4.7 ms at 17-19 div (p-value < 0.05); then, the delay remained constant during the subsequent week of culture (Fig. 19B, left). On the contrary, we could not distinguish a clear developmental profile for the PFC-to-VTA burst delays: at 5-7 and 9-11 div the incidence of PFC-to-VTA bursts was too low (< 2.5 %) to allow the quantification of the delay; from 13-15 div throughout the remaining development, when this propagation pattern represented > 5 % of the total recorded network bursts, we calculated the delays, but the variability was too high to identify a clear developmental trend (Fig. 19B, right). In fact, the PFC-to-VTA propagation delay significantly decreased from 28.7 ± 9.5 ms at 13-15 div to 9.8 ± 1.1 ms at 17-19 div (p-value < 0.01), but then we observed a successive increment during the last week *in vitro*.

Furthermore, we analyzed how network bursts are triggered in the VTA/SN-complex and in the PFC, during all the four previously identified firing patterns, quantifying the major burst leaders (MBLs),

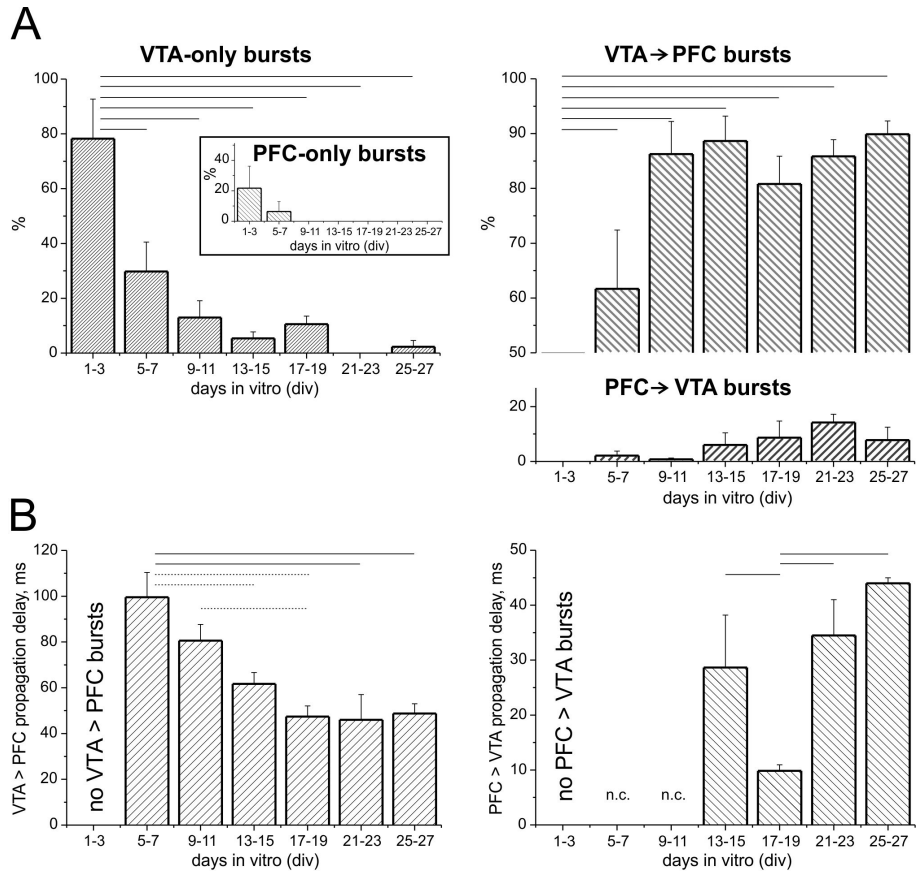

Figure 19. Patterns of activity during development and propagation delays. (A) Percentage incidence (mean ± sem) of different patterns of activity recorded during the development of the co-cultures (n = 10): bursts restricted to the VTA (VTA-only bursts, left) or to the PFC (PFC-only bursts, left, inset), bursts originating in the VTA and propagating to the PFC (VTA-to-PFC bursts, top right) and bursts starting in the PFC and back-propagating to the VTA (PFC-to-VTA bursts, bottom right). (B) Propagation delays (mean ± sem) of VTA-to-PFC (left) and PFC-to-VTA (right) bursts during the development of the co-cultures (n = 10). At 5-7 and 9-11 div the percentage of PFC-to-VTA bursts is too low to allow the computation of the average delay (n.c. = not calculated). The continuous and dashed lines in A and B indicate a *p*-value of 0.01 and 0.05, respectively (ANOVA followed by Bonferroni test).

according to a procedure described by Ham et al. (2008). As described by these authors, we classified a neuron as a MBL if it triggered at least 4% of the network bursts in the VTA/SN-complex or in the PFC. We calculated the percentage of MBLs and the percentage of network bursts triggered by MBLs for each of the 10 co-cultures previously used for the analysis of the propagation patterns and delays during the development *in vitro* (we did not consider the 21-23 div interval because it is clear, from the previous analysis, that the development of the firing patterns did not change at this time point) and then we averaged the results. We observed that both in the VTA/SN-complex and in the PFC there was a progressive decrease of MBLs during the development (Fig. 20A): while at 1-3 div 51.1 ± 10.3 % of the neurons in the PFC (grey) and 56.8 ± 9.5 % of those in the VTA/SN-complex (black) were classified as MBLs, this incidence significantly decreased after 9-11 div to 21.9 ± 2 % in the PFC and 22.6 ± 3 % in the VTA/SN-complex (p-value < 0.01 for both, while the VTA/SN-complex and the PFC did not significantly differ one from the other at each developmental stage). This means that during the development of the co-cultures there was a gradual increase in the potential initiation sites of activity in the networks, revealing an enrichment in the propagation pathways of synaptic activity inside each area of the co-cultures. This result was accompanied by a slight reduction in the percentage of network bursts triggered by MBLs (Fig. 20B), but this change was not statistically significant.

In Fig. 20C, the data from an exemplificative VTA/SN-PFC co-culture are shown. From these histograms (which represent four

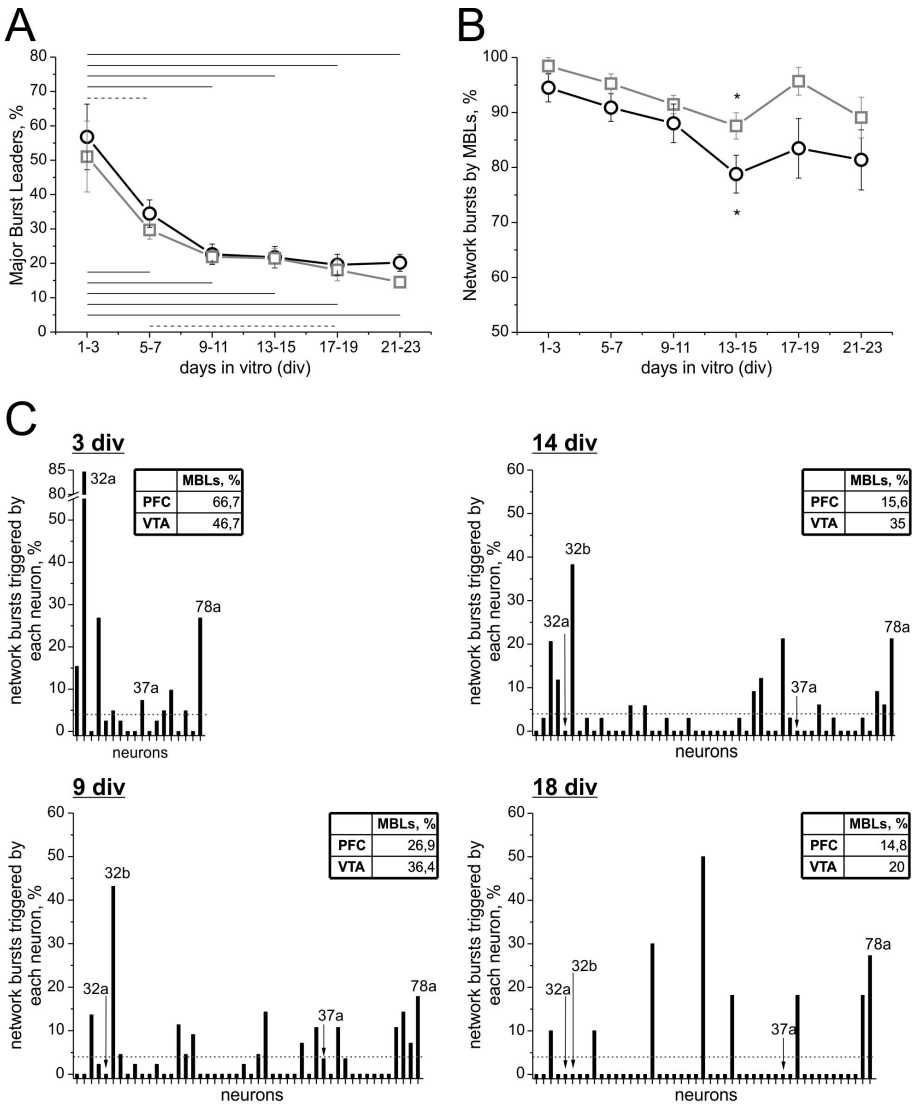

Figure 20. Increase in the variety of initiation sites for the spontaneous activity of the VTA/SN-PFC co-cultures during the development. (A) Major Burst Leaders (MBLs, measured as the percentage of the total number of neurons recorded at each stage of the maturation) during the development of the VTA/SN-complex (black line with empty circles) and the PFC (grey line with empty squares) of 10 co-cultures. A neuron is considered a MBL if it leads at least 4 % of all the recorded network bursts (according to Ham et al., 2008). It is possible to note that during the development, the percentage of MBLs decreased: this implies that there was a gradual increase of the (→)

different stages of the maturation of the co-cultures, namely 3, 9, 14 and 18 div) it is possible to note some previously described features of the development: i) the number of neurons recorded from the co-cultures progressively increased during the days *in vitro*, as evident from the x-axis; ii) the percentage of MBLs in the VTA/SN-complex and in the PFC decreased during the development (the values for the co-culture in analysis are shown in the inset tables in each panel of the graph); iii) neurons could change their behaviour during the time in culture. In fact, it is possible to note that they can behave as MBLs only during the early stage of development (at 3 div, as neurons 32a and 37a) or in the central phase of the maturation of co-cultures (at 9-15 div, like neuron 32b) or they can have a predominant role in

---

potential initiation sites of activity in the co-cultures. The continuous and dashed lines indicate a *p*-value of 0.01 and 0.05, respectively (ANOVA followed by Bonferroni test). The lines in the upper part of the graph refer to the statistics of the VTA/SN-complex (black), while those in the lower part concern the PFC (grey). There is not a difference between the VTA/SN-complex and the PFC during development. (B) Percentage of network bursts triggered by MBLs during development. The asterisks indicate a *p*-value of 0.05 (ANOVA followed by Bonferroni test). (C) Histograms of the percentage of network bursts leaded by each neuron recorded at different stages of the development (3, 9, 14 and 18 div) for one representative VTA/SN-PFC co-culture. The neurons indicated on the x-axis include those belonging both to the VTA/SN-complex and the PFC. The grey dotted line in each of the four graphs represents the threshold for a neuron to be considered a MBL ($\geq$ 4 % of the network bursts leaded). The insets (top right of each graphs) indicate the percentage of MBLs in the VTA/SN-complex and in the PFC at each time point. It is possible to note that neurons can have different behaviours during development: they can act as MBLs only during the early stage of development (see neurons 32a and 37a in the graphs) or in the central phase of the maturation of the co-cultures (like neuron 32b) or they can have a very predominant role in triggering activity steadily during the development (as neuron 78a).

initiating network bursts steadily throughout the development (see neuron 78a).

Therefore, during the time in culture we assisted to a progressive maturation of the activity of the VTA/SN-PFC co-cultures, which showed complex firing propagation patterns appearing concomitantly with the growth of projections from one area of the co-cultures to the other.

4.4 – DISRUPTION OF THE NEWBORN PROJECTIONS COMPLETELY ABOLISHES THE CORRELATED ACTIVITY OF THE VTA/SN-PFC CO-CULTURES

To test whether the correlated activity recorded in the VTA/SN-PFC co-cultures was due to the newborn projections grown between the two areas of the cultures during the *in vitro* development, these connections were cut in the middle of the border region between the two slices, using the tip of a needle and without making the slices detach. Before and after the cutting procedure, the spontaneous activity was recorded for 1 hour, in order to evaluate the changes caused by the disruption of the projections. At first, we computed the single neuron properties before and after the cut. In Fig. 21A and B, exemplificative auto-correlograms of an excitatory (red) and an inhibitory (black) neuron from the PFC of a co-culture, recorded from the electrodes indicated by the dashed circles, are shown in presence of intact projections (Fig. 21A) and after their cut along the red dashed line (Fig. 21B). The disruption of the newborn projections did not

change the single neuron properties of the two clusters: in fact BD, SN, IBSR, FF and ACF of both excitatory (red) and inhibitory (black) neurons of the PFC did not show a significant change in response to the cut of the projections (Fig. 21C and D). Then, we analyzed the network properties of the VTA/SN-PFC co-cultures; the two panels in Fig. 21E and F show the raster plots of the spiking activity in the VTA/SN-complex (14 neurons) and in the PFC (15 neurons) in presence of intact (Fig. 21E) and disrupted (Fig. 21F) projections between the slices. It is clear that the disruption of the projections between the two areas of the co-cultures caused the complete loss of the highly correlated activity, which was observed in control. To verify this change, the cross-correlograms of the spiking activity (shown in Fig. 21G as normalized spike frequency) in the VTA/SN-complex and in the PFC was calculated in control and after the cut of the projections, using a neuron of the PFC as the reference. When the projections were eliminated, there was the loss of correlation in the network activity, as shown by the flat profile of the cross-correlogram of the VTA (Fig. 21G, right). In fact, while in control the propagation delays of VTA-to-PFC and of PFC-to-VTA bursts were in the order of tenths of milliseconds (Fig. 21G, middle), indicating a high level of correlation (as shown also by the cross-correlogram in Fig. 21G, left), in absence of intact projections the delays of the activity appeared to be randomly distributed in the order of tenths of seconds. This means that when the VTA/SN-complex and the PFC were linked by the projections, there could be propagation of activity from the VTA/SN-complex to the PFC and vice-versa; on the contrary, when the projections were not continuous but interrupted by the cut, the

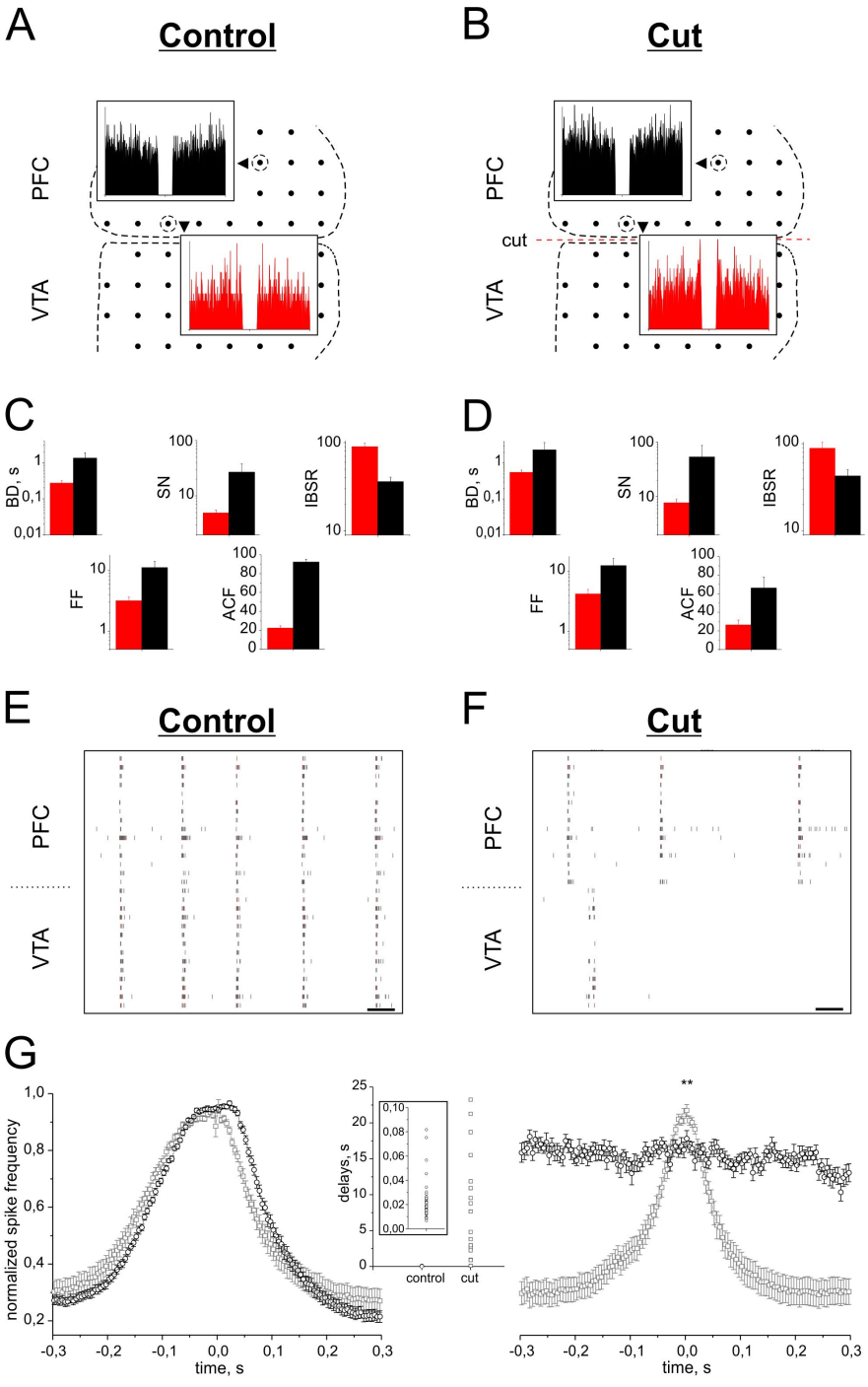

Figure 21. Functional role of the new-born projections for the correlated activity between the VTA/SN-complex and the PFC. (→)

propagation of activity was blocked and both the VTA/SN-complex and the PFC continued to fire spontaneously according to their intrinsic frequency, each independently from the other.

4.5 – PHARMACOLOGICAL DISINHIBITION OF THE ACTIVITY: GABAZINE-MEDIATED EFFECTS ON VTA/SN-PFC CO-CULTURES

To demonstrate that the model of organotypic VTA/SN-PFC co-

(A-D) Single neuron properties are not changed cutting the newborn projections in the border region between the VTA/SN-complex and the PFC. In A and B, exemplificative auto-correlograms of an excitatory (red) and an inhibitory (black) neuron, recorded from the electrodes indicated by the dashed circles, are shown in control condition (A) and after the cut of the projections (B; the red dashed line indicates the cut). Each plot has the same x-axis of ± 20 ms and the y-axis (spikes/s) has maximum values ranging from 70 to 150 [Time bin for auto-correlograms: 0.1 ms]. In C and D, properties of all the excitatory (red) and inhibitory (black) neurons recorded in the PFC of a co-culture in presence of intact (C) and cut (D) projections. It is possible to note that the disruption of the newborn projections did not change the properties (BD, SN, IBSR, FF and ACF) of the neuron clusters. (E-G) Network properties of the co-cultures before and after the cutting of the projections. In E and F, raster plots of the activity of neurons belonging to the VTA/SN-complex (n = 14) and the PFC (n = 15) in presence of intact (E) and disrupted (F) projections. It is evident that when the projections between the two areas of the co-cultures were destroyed, the highly correlated activity was completely lost [Scale bar: 1 s]. In G, cross-correlograms of the activity (shown as normalized spike frequency) in the VTA/SN-complex (black circles) and in the PFC (grey squares), computed using a neuron of the PFC as the reference, in control (left) and after the cut of the projections (right). The panel in the middle shows the distribution of the propagation delays (absolute values) between the areas of the co-cultures; the inset presents a magnification of the delays in control condition at a higher temporal resolution [Time bin for cross-correlograms: 5 ms].

cultures can be used to test the effects of different pharmacological agents (such as modulators of the activity or potentially interesting neuroregenerative substances), we applied gabazine (GZ or SR95531), a blocker of GABA-A receptors, at two different concentrations (200 nM and 10 μM), known to act on phasic and both phasic and tonic inhibition, respectively (Stell and Moody, 2002). In order to allow GZ to enter the slice tissue properly, we recorded the spontaneous activity at each concentration for 30 min and we considered the second half of the recording sessions to evaluate the drug effects and calculate the firing parameters (expressed as percentage change relative to control, which is indicated as 100%). In Fig. 22A, the single neuron properties of the excitatory (red) and inhibitory (black) clusters of PFC cells are shown (average data of 5 experiments, with a total number of 263 excitatory and 93 inhibitory neurons): BD of excitatory neurons increased almost two-fold (180.1 ± 24.2 %, p-value < 0.05) with 200 nM GZ in comparison with control and further with 10 μM GZ (up to 337.3 ± 39.7 %, p-value < 0.01), while there was no change in BD of inhibitory neurons; SN and SR of the excitatory and inhibitory clusters increased with both the concentrations of GZ (SN: 168.2 ± 17.7 % and 145 ± 17.8 % at 200 nM GZ and 284.7 ± 40.2 % and 229.4 ± 40.9 % at 10 μM GZ, with p-values < 0.01 and 0.05, for excitatory and inhibitory neurons, respectively; SR: 336.6 ± 93.9 % and 279.6 ± 60.1 % at 200 nM GZ, with p-value < 0.05, and 732 ± 175.4 % and 416.6 ± 82.8 % at 10 μM GZ, with p-values < 0.01 and 0.05, for excitatory and inhibitory neurons, respectively); finally, the excitability (calculated as the spike number/neuron number ratio) of both the clusters of neurons significantly increased with the high GZ

concentration (260.2 ± 48 % and 230.6 ± 25.6 %, with *p*-values < 0.05 and 0.01, for excitatory and inhibitory neurons, respectively), while with 200 nM GZ the effect was visible only for the excitatory cluster (174.3 ± 28.2 %, *p*-value < 0.05). We also evaluated the interval between successive network bursts (network burst-inter burst interval, NB-IBI) both in the VTA/SN-complex and the PFC (Fig. 22B): we observed a reduction of the NB-IBI, corresponding to an increase in the frequency of network bursts, in both the areas of the co-cultures when we blocked phasic and tonic inhibition through 10 μM GZ (47.8 ± 6.2 % and 61.8 ± 11.1 % in the PFC and the VTA/SN-complex, respectively; *p*-value < 0.01), while the block of phasic inhibition with 200 nM GZ caused only a small but not significant change.
Furthermore, we considered the VTA-to-PFC bursts, which represent the most frequent identified propagation pattern, and we analyzed if the treatment with GZ caused a change in the propagation delay. We observed that the propagation delay of VTA-to-PFC bursts significantly decreased to 73.7 ± 8.1 % in presence of 200 nM GZ (*p*-value < 0.05) and to 43.8 ± 6.4 % with 10 μM GZ (*p*-value < 0.01), in comparison with control (Fig. 22C).

Fig. 22D shows the properties of PFC network states from one exemplificative experiment performed with GZ. We have calculated the FSH (first column) in control and in presence of 200 nM and 10 μM GZ: the treatment with GZ caused an increase of the probability of having bursts with a high number of spikes (> 10), both for excitatory (red) and inhibitory (black) neurons; this effect appeared first on inhibitory neurons, being evident already with 200 nM GZ and further enhancing with 10 μM GZ, while the increase in the

spikes/burst probability of excitatory neurons was evident mainly in presence of 10 μM GZ. Furthermore, the cFSHs (Fig. 22D, second column) indicate that, in addition to an increase of the spikes per burst (evident from the shift towards the right of the cFSH profile compared to control), GZ caused an increase of the average percentage of excitatory (red) and inhibitory (black) neurons, which are engaged during the network bursts. Finally, in order to study how these two clusters of neurons are progressively recruited during the bursts, we have computed the NNTHs (Fig. 22D, third column), which allowed the identification of different network states (short and long bursts). In particular, while in control only one significant network state (short bursts) was found to be predominant (94.4 % on the total recorded bursts), the treatment with GZ caused the appearance of a second, longer network state (36.9 % and 25.4 % of all the recorded bursts in presence of 200 nM and 10 μM GZ, respectively) and the increase of the excitatory (red) and inhibitory (black) neurons engaged in the activity in each time bin (5 ms).

The disinhibition expected and observed as a consequence of the treatment with GZ on the spiking activity of VTA/SN-PFC co-cultures was also evident in the local field potential activity, simultaneously recorded with the MEAs. In Fig. 22E, exemplificative average traces (mean ± sem) of LFPs (black thick lines) from the PFC of an experiment are shown with the corresponding instantaneous spike rates (black thin lines). It is evident that 200 nM GZ caused an increase in the amplitude of LFPs, which was accompanied by the appearance of an oscillatory activity in presence of 10 μM GZ. This is

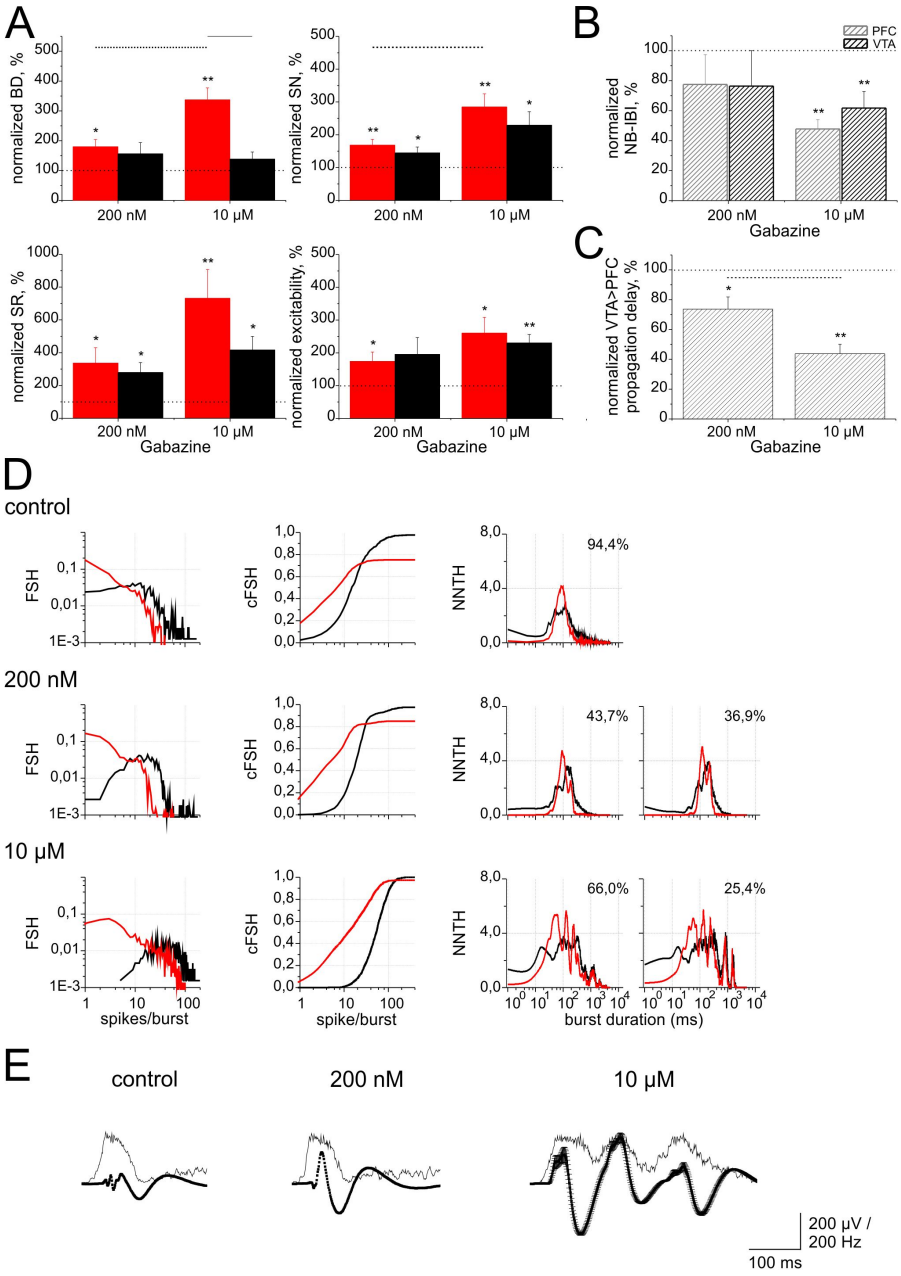

Figure 22. Effects of gabazine (GZ) on the activity of the VTA/SN-PFC co-cultures. (A) Histograms of single neuron properties (first row: burst duration, BD, on the left and spike number in burst, SN, on the right; second row: spike rate, SR, on the left and excitability, measured as the spike (→)

number/neuron number ratio, on the right) in the PFC in presence of 200 nM or 10 μM of gabazine (SR95531). Excitatory and inhibitory neurons are indicated in red and black, respectively (5 experiments, with a total number of 263 excitatory and 93 inhibitory neurons). (B) Gabazine effect on the inter-burst interval for network bursts (NB-IBI), recorded in the PFC (grey) and in the VTA (black) of the same experiments used in A. (C) Gabazine-induced changes on the propagation delay of VTA-to-PFC bursts at low (200 nM) and high (10 μM) concentrations. All the data (mean ± sem) shown in A-C are obtained normalizing all the values of 5 experiments to the value found in the control condition of each experiment and then averaging the normalized values. In A-C, the dotted line indicates the control level; the continuous and dashed lines indicate a *p*-value of 0.01 and 0.05, respectively, in the comparison between values at different concentrations of gabazine or between values of the two clusters of neurons at the same GZ concentrations; the double and the single asterisks indicate a *p*-value of 0.01 and 0.05, respectively, in the comparison with the control (ANOVA followed by Bonferroni test). (D) Properties of network states in control (first row) and in presence of 200 nM (middle row) or 10 μM (lower row) GZ from the PFC of an exemplificative experiment (46 excitatory and 11 inhibitory neurons). In the first and the second column, probability histograms of having a certain number of spikes in each burst (firing spike histograms, FSH) and cumulative probabilities (cFSH), respectively. For cumulative data, the full scale represents the totality of the identified neurons in each cluster. The third column shows the time histograms of the number of neurons engaged during the bursts (neuron number time histograms, NNTH, measured as the number of neurons NN per bin) during short bursts (on the left) and long bursts (on the right). The percentages indicate the relative amount of the two network states (short and long bursts) among the recorded bursts during control and in presence of 200 nM or 10 μM gabazine. It is possible to note that gabazine is able to modify the network states and the relative amounts of the two identified ones. In all the graphs in D, the red and the black lines indicate excitatory and inhibitory neurons, respectively. (E) Effect of gabazine on local field potentials recorded from an electrode under the PFC of a co-culture. The thick black lines represent the average waveforms (mean ± sem) of 900 s recording periods in control (left) and in presence of 200 nM (middle) and 10 μM (right) GZ, while the thin black lines show the corresponding spike rate histrograms [bin: 0.001 s]. It is possible to note that gabazine caused an increase in the average amplitude of LFPs and the appearance of an oscillatory activity at high concentrations.

consistent with the previously observed increase in the spiking activity, which was the consequence of the block of phasic and tonic inhibition through the blockade of $GABA_A$ receptors.

4.6 – D2 RECEPTOR-MEDIATED MODULATION OF THE VTA/SN-PFC CO-CULTURE ACTIVITY

Since the VTA/SN-complex contains DAergic neurons, which physiologically project to the PFC, and that the PFC contains DA receptors, we decided to test whether the spontaneous activity of the VTA/SN-PFC co-cultures could be modulated by DA receptor blockade. We applied 10 μM eticlopride, a D2 receptor blocker, in the co-cultures on MEAs, as we did with GZ, and we evaluated the firing parameters in the PFC. In Fig. 23A, the effects of eticlopride on BD, SR and excitability (expressed here as normalized values) of PFC excitatory (red) and inhibitory (black) neurons are shown (average data of 4 experiment, with a total number of 112 excitatory and 37 inhibitory neurons). The treatment with 10 μM eticlopride caused a significant decrease of BD and excitability of inhibitory neurons (48.5 ± 13.9 % and 54.8 ± 12.6 % for BD and excitability, respectively, where the control is referred as 100 %, p-value < 0.01), while excitatory neurons did not show a modification of their BD and displayed a slight but not significant decrease in their excitability. Differently, both PFC excitatory and inhibitory neurons showed a marked SR decrease (42.5 ± 17.8 % and 37 ± 13.9 %, p-value < 0.05 and 0.01, for excitatory and inhibitory clusters, respectively). Furthermore, we evaluated the NB-IBI (Fig. 23B) for both the

VTA/SN-complex (black) and the PFC (grey) in presence of the D2 receptor antagonist: 10 μM eticlopride caused a marked increase in the interval between successive network bursts in both the regions of the VTA/SN-PFC co-cultures (197.1 ± 38.2 % and 496.1 ± 120.1 %, *p*-value < 0.05, for the PFC and the VTA/SN-complex, respectively), thus indicating that D2 receptor blockade caused an inhibition of the activity (evident from the lower burst rate and spike rate, Fig. 23A and B).

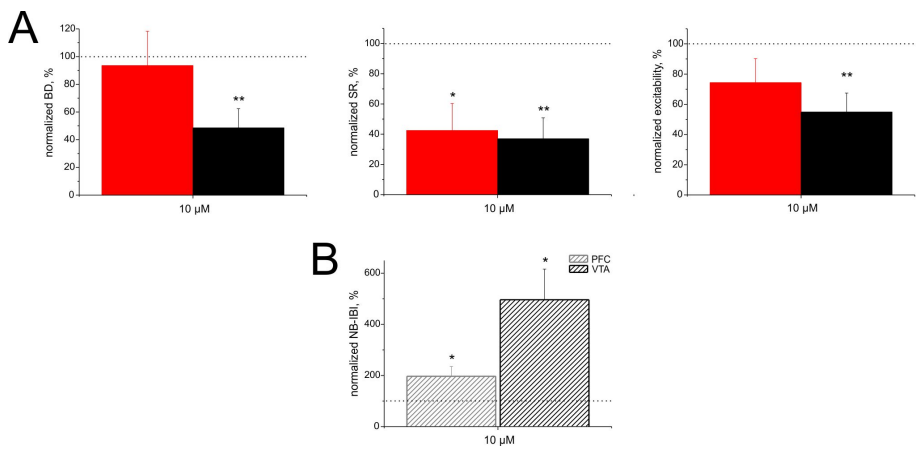

Figure 23. Effects of eticlopride on the activity of the VTA/SN-PFC co-cultures. (A) Histograms of single neuron properties (burst duration, BD, on the left; spike rate, SR, in the middle; excitability, measured as the spike number/neuron number ratio, on the right) in the PFC in presence of 10 μM eticlopride. Excitatory and inhibitory neurons are indicated in red and black, respectively (4 experiments, with a total number of 112 excitatory and 37 inhibitory neurons). (B) Eticlopride effect on the inter-burst interval for network bursts (NB-IBI), recorded in the PFC (grey) and in the VTA (black) of the same experiments used in A. All the data (mean ± sem) shown in A and B are obtained normalizing all the values of 4 experiments to the value found in the control condition of each experiment and then averaging the normalized values; the dotted line indicates the control level; the double and the single asterisks indicate a *p*-value of 0.01 and 0.05, respectively, in the comparison with the control (ANOVA followed by Bonferroni test).

5. DISCUSSION

The aim of the present study was to characterize the developmental features of the VTA/SN-PFC co-cultures maintained on multielectrode array platforms, in order to study the functionality of the neuronal projections which have been demonstrated to grow *in vitro* (Franke et al., 2003; Heine et al., 2007) between the two areas of the cultures, the VTA/SN-complex and the PFC. We have followed the development of the co-culture spontaneous activity up to four weeks *in vitro*, and we have demonstrated that the newborn projections are functional, because they allow the activity to propagate from the VTA/SN-complex to the PFC and in the opposite direction and in their absence the propagation is lost, and that the progressive development of the connections is accompanied by the appearance of different activity patterns. Furthermore, through our pharmacological experiments with the GABA-A receptor blocker gabazine and the D2 receptor antagonist eticlopride, we have proven that the VTA/SN-PFC co-cultures can be used as an appropriate model to study the effects of different pharmacological agents (such as modulators of the activity or potentially interesting neuroregenerative substances).

5.1 – THE IMPORTANCE OF REGENERATION

It is known that spontaneous functional recovery after injuries to the adult CNS, such as brain contusion and spinal cord injuries, which

cause neuronal cell death and a loss of axonal connections, rarely occurs, thus causing permanent functional deficits as a consequence of CNS neuron inability to spontaneously regenerate (Muramatsu et al., 2009). The failure of axonal regeneration after injury to the adult CNS, in contrast with the regenerative potential of embryonic and peripheral nervous system, has been attributed to different factors (Huebner and Strittmatter, 2009), such as the presence of a tissue environment and of inhibitory molecules in myelin which inhibit the growth of axons (McDonald, 1999; He and Koprivica, 2004; Schwab et al., 2006), the inhibiting effect of the astroglial scar (Silver and Miller, 2004; Fitch and Silver, 2008), and the lack of a sufficient trophic support which leads to the retrograde death of injured neurons (Fernandez er al., 1999; Hains er al., 2003). In recent years, many studies have been done to face the problem of CNS regeneration and these works have found that a form of naturally occurring regeneration of axons exists also in animal models of CNS injury; in fact, spontaneous axon sprouting of the corticospinal tract (CST) was identified *in vivo* at the proximal sites of injury in spinal cord injury (Harel and Strittmatter, 2006) and few damaged CST axons regrew beyond the lesion site (Steward et al., 2008). Furthermore, many *in vitro* studies have analysed the regenerative abilities of different CNS pathways, such as the serotoninergic raphe-hippocampal pathway (Papp et al., 1995), the corticostriatal (Plenz and Aertsen, 1996a and 1996b) and the thalamocortical connections (Rennie et al., 1994), the perforant pathway (Hofmann et al., 2004; Hofmann and Bading, 2006), the nigrostriatal system (Snyder-Keller et al., 2008) and the meso-cortico-limbic dopaminergic pathway (Franke et al., 2003;

Maeda et al., 2004; Heine et al., 2007). Here we have reconstructed the meso-cortico-limbic system *in vitro* in the form of organotypic co-cultures and we have demonstrated that the projections between the VTA/SN-complex and the PFC, which are able to regenerate in the slice cultures following an innervation pattern that is similar to what occurs *in vivo* (as described by Franke et al., 2003), are able to propagate the electrical activity between the two areas of the reconstructed dopaminergic system, thus allowing a continuous and reciprocal communication. Therefore, not only the neuronal connections regenerate, but they are also functional.

5.2 – NEURONAL SPONTANEOUS ACTIVITY

Although many studies using organotypic cultures on MEAs concentrated on evoked activity (Egert et al., 1998; Jahnsen et al., 1999; Shimono et al., 2002b; Van Bergen et al., 2003; Hofmann et al., 2004; Cater et al., 2007), many other groups focused on the spontaneous activity of the cultures (Beggs and Plenz, 2003 and 2004; Plenz and Thiagarajan, 2007; Gireesh and Plenz, 2008; Stewart and Plenz, 2008; Santos et al., 2010) or both (Darbon et al., 2002; Shew et al., 2009). In this work we have recorded and analysed the spontaneous activity of VTA/SN-PFC co-cultures, in the form of bursts of spikes and local field potentials. In fact, spontaneous synchronous activity, which is the ongoing activity in the absence of intentional sensory input such as during sleep or anesthesia (Sanchez-Vives and McCormick, 2000), is an emerging property of many central networks and it is originated by the interactions of many

relatively simple network component, such as chemical and electrical synapses between neurons, ion channels and transporters (Corlew et al., 2004; Fellin et al., 2004; Dupont et al., 2006). Besides, the complex dynamics of the ongoing activity in cortical circuits in absence of and preceeding sensory stimulation play an important role in development (Thompson, 1997; Sur et al., 1999), in shaping neural activity during stimulus presentation and to ensure the reliability of synaptic trasmission, plasticity and information processing (Harris, 2005), and they may reflect an "off-line" mode of information processing (Steriade et al., 1993; Hoffman and McNaughton, 2002; Luczak et al., 2007). Furthermore, there is growing evidence that the dynamics underlying spontaneous depolarizing events, also called up states, are strikingly similar to those of sensory-evoked activity (Sanchez-Vives and McCormick, 2000; Kenet et al., 2003), due to the presence of common constraints on both the order in which neurons fire and the possible combinations of neural firing rates and patterns, which determine the activity temporal structure (Luczak et al., 2009). In this way, the firing patterns which can be expressed by neuronal circuits are restricted to a limited "vocabulary", with spontaneous events widely sampling it, and responses to sensory stimuli reproducing smaller subsets of it (Luczak et al., 2009; Harris et al., 2011). Thus, these data suggest that spontaneous activity patterns may be an useful experimental model to understand the mechanisms which regulate the connectivity and the flow of activation within neuronal networks, both in slice and in dissociated cultures, in the absence of stimuli (Luczak et al., 2007; Gullo et al., 2009). In particular, the principal feature of developing neuronal networks on MEAs is the

spontaneous reverberating activity, generated and modulated by sets of excitatory and inhibitory synaptic transmission systems (Eytan and Marom, 2006; Baltz et al., 2010), which has been described as spikes during synchronous bursting in cortical cultures (Keefer et al., 2001; Gramowski et al., 2004; Tateno et al., 2005; Van Pelt et al., 2004; Wagenaar et al., 2006; Baltz et al., 2010) and as LFPs in organotypic slices (Beggs and Plenz, 2003 and 2004; Hofmann et al., 2004; Sun and Luhmann, 2007). We have observed the activity of the VTA/SN-PFC organotypic co-cultures and recorded both spikes (high-frequency range, 250-5000 Hz), organized in bursts which characterized both the VTA/SN-complex and the PFC and whose patterns varied during the *in vitro* development, and LFPs (low-frequency range, 5-200 Hz) (Fig. 15). It is known that these two types of electrical activity reflect different aspects of information processing: in fact, single-unit spikes are attributable to the spiking activity of pyramidal and inhibitory neurons, thus reflecting the cortical output, while LFPs reflect the complex summation of synaptic currents and other types of slow activity, such as voltage-dependent membrane oscillations, produced by multiple inputs onto cells of all layers (Belitski et al., 2008; Rasch et al., 2008; Harris et al., 2011). We were able to correlate the spike rate with the correspondent simultaneous local field potential (Fig. 17) and we found that, as described by Pouille et al. (2009), Harris et al. (2011) and Isaacson and Scanziani (2011), LFPs anticorrelate with the instantaneous firing rate of local neurons, with negative LFP deflections, which correspond to pyramidal neuron firing, occurring at the times of

increased firing rate, and positive deflections, characterized by the activity of interneurons, occurring when the firing rate decreases.

5.3 – THE COMBINATION OF ORGANOTYPIC CULTURES WITH MULTIELECTRODE ARRAY RECORDINGS

The analysis of the formation of functional connections in the CNS requires appropriate model systems to study its mechanisms; while cultures of dissociated neuronal cells are a relatively simple model to study phenomena such as neuroprotection and toxicity and *in vivo* studies are often time consuming and difficult to interpret, organotypic brain slices are closer to the *in vivo* situation than cell cultures and combine the advantages of experiments performed in cell cultures with the analysis of complex systems such as those studied *in vivo* (Stoppini et al., 1991; Gähwiler et al., 1997; Hofmann and Bading, 2006). In fact, in these cultures the cytoarchitecture of the tissue is maintained and the neurons retain a high degree of morphological and electrophysiological similarities when compared with the same cell types *in vivo* (Karpiak and Plenz, 2002). Moreover, the organotypic co-culture of brain regions is diffusing as an effective and powerful means to reconstruct brain circuitry in a simplified and easily manipulated model. On the other hand, electrophysiological recordings are necessary to demonstrate the formation and the functionality of projections and synapses, but traditional single-cell recording techniques are limited to the analysis of few cells per day and for periods not longer than 10-12 h. However, the combination of organotypic culture technique with multielectrode array recordings

allows to perform extracellular non-invasive multi-site recordings from electrodes covering the whole slice preparation, simultaneously and repeatedly, and to analyse the firing patterns at an integrated level (Egert et al., 1998; Shimono et al., 2002a and 2002b; Hofmann et al., 2004). Here we combined the VTA/SN-PFC organotypic co-cultures with MEA recordings to monitor the electrical activity over extended periods of time (up to four week *in vitro*). We were able to monitor the developmental changes of spontaneous spiking activity and LFPs in the VTA/SN-complex and in the PFC (Fig. 16 and 17) and we evaluated the single neuron parameters, such as burst duration, intra-burts spike rate, burst rate and spike number; we noticed that the differences in the firing between the two regions of the co-cultures tended to disappear in the first two weeks of culture, in parallel with the growth of projections between the areas, thus leading the VTA/SN-complex and the PFC to have similar firing properties. Furthermore, we were able to characterize the developmental increase in the number of excitatory and inhibitory neurons recorded from the PFC and identified through our software of analysis, and we found an excitatory/inhibitory neuron ratio of about 3 (Fig. 18). These data have been confirmed by immunolabelling experiments performed in collaboration with Prof. Peter Illes' and Prof. Heike Franke's group at the Rudolf-Boehm Institute for Pharmacology and Toxicology, University of Leipzig (Leipzig, Germany) and with Prof. Alida Amadeo at the University of Milan (Milan, Italy); in fact, these experiments demonstrated that already at 8-9 div the VTA/SN-complex and the PFC were strictly connected by neuronal and glial newborn projections (data not shown, but see also Heine et al., 2007),

which allow a continuous communication between them, and that also in the physiological condition there is a ratio of ≈ 3 between the number of excitatory and inhibitory neurons in the PFC. It is important to remind that the *in vitro* grown projections have been demonstrated to be target-specific, because while also in co-cultures of the VTA and hippocampus, which is a minor target of DAergic fibres, a growth of fibres is present, in co-culturing the VTA with the cerebellum, which is not a physiological target of DAergic projections, no growth of fibres into the cerebellar slices has been described (Østergaard et al., 1990; Holmes et al., 1995).

In addition to the developmental profile of single neuron properties in the two areas of the co-cultures, we also evaluated if activity patterns involving simultaneously the whole co-cultures were present, in order to study the functionality of the newborn projections in the propagation of activity. We observed a correlated activity between the VTA/SN-complex and the PFC (Fig. 19) in the form of bursts which originated in the VTA/SN-complex and propagated to the PFC (VTA-to-PFC bursts) and bursts which arose in the PFC and back-propagated to the VTA/SN-complex (PFC-to-VTA bursts); both these two types of communication between the two areas disappeared when the newborn projections were destroyed, thus proving their functional role (Fig. 21). The presence of this bidirectional propagation of activity is in agreement with *in vivo* experiments, which have demonstrated the functional coupling and the reciprocal modulation between the VTA and the PFC electrical activity (Sesack and Pickel, 1992; Seamans et al., 2003; Peters et al., 2004; Tseng et al., 2006; Gao et al., 2007; Fujisawa and Buzsáki, 2011). Furthermore, we have also

analysed the propagation delays of the correlated activity and we have seen that during the *in vitro* development of the VTA/SN-PFC co-cultures there was a progressive decrease of the VTA-to-PFC burst propagation delay from 99.6 ± 10.8 ms at 5-7 div, when we started to observe this firing pattern, to 47.4 ± 4.7 ms at 17-19 div, when the co-cultures have fully developed (Fig. 19). Given that the two slices have been placed on MEAs in the way that each of them covered about half of the electrodes and that we have observed that activity could start from different neurons in the network (Fig. 20, as described by Ham et al., 2008), we can assume that the distance, which neuronal signals have to cover to propagate from one slice to the other, is of about 800 μm, which corresponds to the distance between the central points of the two slices, perpendicularly to their juxtaposed borders. Under this assumption, we can calculate a VTA-to-PFC burst propagation velocity of ≈ 0.02 m/s when the VTA/SN-PFC co-cultures are mature.

Deniau and co-workers (1980) and Thierry and colleagues (1980) have reported that the conduction velocity of VTA-cortical fibres, based on antidromic activation, ranges between 0.55 and 11.5 m/s. It is also known that the fibres with high conduction velocity (11.5 m/s) are not DAergic fibres, but myelinated non-DAergic projections, given that they are not affected by 6-OHDA lesions (Thierry et al., 1980; Glowinski et al., 1984). Instead, the low value of 0.55 m/s reported for mesolimbic DAergic fibres, which are normally thin and unmyelinaed in the rat (Naito et al., 1994), is comparable with the value of 0.58 m/s reported for nigrostriatal DAergic fibres (Guyenet and Aghajanian, 1978; Lapish et al., 2007). The value of VTA-to-PFC burst propagation velocity that here we have obtained (0.02 m/s) is

twenty times slower than the slowest fibres reported by Deniau et al. (1980) and Thierry et al. (1980); therefore, the latency of the VTA-to-PFC bursts is much longer compared to what is expected for monosynaptic events, but this can be explained considering that the projections linking the VTA/SN-complex and the PFC in the co-cultures have re-grown *in vitro* after the slicing procedure and assuming that the bursts were polysinaptically generated (Overton and Clark, 1997).

5.4 – THE VTA/SN-PFC CO-CULTURES AS AN USEFUL PHARMACOLOGICAL TOOL

The organotypic cultures, maintained both on semiporous membranes (Stoppini et al., 1991) or on multielectrode arrays, have been widely used to study the effects of different substances on various processes: i.e., agonists or antagonists of purinergic receptors have been tested on enthorinal cortex-dentate gyrus (EC-DG) and on VTA/SN-PFC co-cultures to study their effects on the regeneration of neuronal projections (Heine et al., 2006; Heine et al., 2007). Modulators of excitatory and inhibitory receptors and synapses have been used to study the mechanisms involved in the regulation of the activity of EC-DG, hippocampal and cortical organotypic cultures (Shimono et al., 2002b; Hofmann et al., 2004; Shew et al., 2009) and activators and blockers of DAergic receptors were useful to understand the DAergic modulation of NAcc activity in VTA-Nacc-PFC triple cultures (Maeda et al., 1995). In this work we verified how dishinibition obtained through the application of two different concentrations of

gabazine (GABA-A receptor antagonist), known to act on phasic and both phasic and tonic inhibition (Stell and Moody, 2002), and blockade of D2 receptors with eticlopride were able to modify the activity of VTA/SN-PFC co-cultures.

The treatment with GZ (Fig. 22) caused a strong dishinibition of the activity in both the areas of the co-cultures, as it is possible to note from the observed increase of burst duration, spike number, spike rate, and excitability and decrease of the network burst inter-burst interval of the VTA/SN-complex and PFC neurons, in agreement with the dishinibitory effect previously described on primary dissociated cultures (Gullo et al., 2009; Gullo et al., 2010). Furthemore, using the procedure described by Gullo et al. (2012), we were also able to distinguish different PFC network states and to study the effects of GZ on them, computing the FSH, cFSH and NNTH. We observed that the dishinibition obtained with the application of GZ determined the appearance of new network states and the increase of the average number of neurons that are engaged during the network bursts.

On the contrary, D2 receptor blockade with eticlopride (Fig. 23) caused a decrease of VTA/SN-PFC co-culture activity, as it results clear from the increase in the inter-burst interval both in the VTA/SN-complex and in the PFC. This effect was also accompanied by a decrease of BD, SR and excitability of PFC excitatory and inhibitory neurons. These data are in agreement with whole-cell patch-clamp experiments on VTA/SN-PFC co-cultures performed by Dr. Ilenio Servettini at the University of Milano-Bicocca (now working at the University of Perugia), which showed that the treatment with

eticlopride causes a decrease of the VTA-evoked AMPA- and NMDA-mediated currents in PFC pyramidal neurons (data not shown). Thus, the patch-clamp results provide the mechanisms at the basis of the D2 receptor blockade inhibitory effect, which has been observed through the MEA experiments. However, the effects, here reported, observed with eticlopride contrast with other evidences indicating that the activation, and not the inhibition, of D2 receptors causes a decrease of neuronal excitability through the inhibition of AMPA- and NMDA-mediated responses (Gulledge and Jaffe, 1998 and 2001; Gulledge and Stuart, 2003; Tseng and O'Donnell, 2004), but this can be attributed to differences in the experimental conditions, as it has been observed for other aspects of the DAergic neuromodulatory action (Seamans and Yang, 2004).

.

6. CONCLUSIONS

In this work we have characterized the developmental features of VTA/SN-PFC co-culture spontaneous activity through the multielectrode array recording technique, which allowed us to demonstrate that the neuronal projections, which grow *in vitro* between the two areas of the co-cultures, are functional. In fact, we detected a correlated activity between the VTA/SN-complex and the PFC, expressed as bursts of activity of the whole co-cultures which were able to propagate from one area to the other and back and which disappeared when the newborn projections were interrupted. Furthermore we studied how the spontaneous activity of the *in vitro* reconstructed meso-cortico-limbic system could be modulated and we found that the treatment with the GABA-A receptor antagonist gabazine caused a dishinibition of the neuronal firing, while the blockade of D2 receptors with eticlopride determined a decrease in VTA/SN-PFC co-culture activity.

Thus, the VTA/SN-PFC co-cultures on MEAs represent a good model and an useful and powerful tool to study the neuronal regenerative processes and their functionality over time; moreover, it enables us to analyse how these processes can be influenced by neuromodulators or potentially interesting novel neuroreparative substances and affected by detrimental (toxic/hypoxic) stimuli.

7. BIBLIOGRAPHY

Adell A, Artigas F (2004) The somatodendritic release of dopamine in the ventral tegmental area and its regulation by afferent transmitter systems. Neurosci and Biobehav Rev 28:415-431

Afonso-Oramas D, Cruz-Muros I, Alvarez de la Rosa D, Abreu P, Giráldez T, Castro-Hernández J, Salas-Hernández J, Lanciego JL, Rodríguez M, González-Hernández T (2009) Dopamine transporter glycosylation correlates with the vulnerability of midbrain dopaminergic cells in Parkinson's disease. Neurobiol Dis 36:494-508

Arnsten AFT (2011) Prefrontal cortical network connections: key site of vulnerability on stress and schizophrenia. Int J Dev Neurosci 29:215-223

Artigas F (2010) The prefrontal cortex: a target for antipsychotic drugs. Acta Psychiatr Scand 121:11-21

Baltz T, de Lima AD, Voigt T (2010) Contribution of GABAergic interneurons to the development of spontaneous activity patterns in cultured neocortical networks. Fron Cell Neurosci 4:15

Bandyopadhyay S, Gonzalez-Islas C, Hablitz JJ (2005) Dopamine enhances spatiotemporal spread of activity in rat prefrontal cortex. J Neurophysiol 93:864-872

Barthó P, Hirase H, Monconduit L, Zugaro M, Harris KD, Buzsáki G (2004) Characterization of neocortical principal cells and interneurons

by network interactions and extracellular features. J Neurophysiol 92:600-608

Bayer HM, Lau B, Glimcher PW (2007) Statistics of midbrain dopamine neuron spike trains in the awake primate. J Neurophysiol 98(3):1428-1439

Bean BP (2007) Stressful pacemaking. Nature 447:1059-1060

Beggs JM, Plenz D (2003) Neuronal avalanches in neocortical circuits. J Neurosci 23:11167-11177

Beggs JM, Plenz D (2004) Neuronal avalanches are diverse and precise activity patterns that are stable for many hours in cortical slice cultures. J Neurosci 24:5216-5229

Belitski A, Gretton A, Magri C, Murayama Y, Montemurro MA, Logothetis NK, Panzeri S (2008) Low-frequency local field potentials and spikes in primary visual cortex convey independent visual information. J Neurosci 28(22):5696-5709

Bonci A, Malenka RC (1999) Properties and plasticity of excitatory synapses on dopaminergic and GABAergic cells in the ventral tegmental area. J Neurosci 19(10):3723-3730

Bonci A, Bernardi G, Grillner P, Mercuri NB (2003) The dopamine-containing neuron: maestro or simple musician in the orchestra of addiction? Trends Pharmacol Sci 24(4):172-177

Carr DB, Sesack SR (2000a) GABA-containing neurons in the rat ventral tegmental area project to the prefrontal cortex. Synapse 38:114-123

Carr DB, Sesack SR (2000b) Projections from the rat prefrontal cortex to the ventral tegmental area: target specificity in the synaptic associations with mesoaccumbens and mesocortical neurons. J Neurosci 20(10):3864-3873

Cater HL, Gitterman D, Davis SM, Benham CD, Morrison B, Sundstrom LE (2007) Stretch-induced injury in organotypic hippocampal slice cultures reproduces *in vivo* post-traumatic neurodegeneration: role of glutamate receptors and voltage-dependent calcium channels. J Neurochem 101:434-447

Chan CS, Guzman JN, Ilijic E, Mercer JN, Rick C, Tkatch T, Meredith GE, Surmeier DJ (2007) 'Rejuvenation' protects neurons in mouse models of Parkinson's disease. Nature 447:1081-1086

Chergui K, Suaud-Chagny MF, Gonon F (1994) Nonlinear relationship between impulse flow, dopamine release and dopamine elimination in the rat brain *in vivo*. Neuroscience 62(3):641-645

Corlew R, Bosma MM, Moody WJ (2004) Spontaneous, synchronous electrical activity in neonatal mouse cortical neurones. J Physiol 560(2):377-390

Csicsvari J, Hirase H, Czurkó A, Mamiya A, Buzsáki G (1999) Oscillatory coupling of hippocampal pyramidal cells and interneurons in the behaving rat. J Neurosci 19(1):274-287

Dal Bo G, St-Gelais F, Danik M, Williams S, Cotton M, Trudeau LE (2004) Dopamine neurons in culture express VGLUT2 explaining their capacity to release glutamate at synapses in addition to dopamine. J Neurochem 88:1398-1405

Darbon P, Scicluna L, Tscherter A, Streit J (2002) Mechanisms controlling bursting activity induced by dishinibition in spinal cord networks. Eur J Neurosci 15:671-683

Deniau JM, Thierry AM, Feger J (1980) Electrophysiological identification of mesencephalic ventromedial tegmental (VMT) neurons projecting to the frontal cortex, septum and nucleus accumbens. Brain Res 189(2):315-326

Descarries L, Bérubé-Carrière N, Riad M, Dal Bo G, Mendez JA, Trudeau LE (2008) Glutamate in dopamine neurons: synaptic versus diffuse transmission. Brain Res Brain Res Rev 58:290-302

Dobi A, Margolis EB, Wang HL, Harvey BK, Morales M (2010) Glutamatergic and nonglutamatergic neurons of the ventral tegmental area establish local synaptic contacts with dopaminergic and nondopaminergic neurons. J Neurosci 30(1):218-229

Dong Y, Cooper D, Nasif F, Hu XT, White FJ (2004) Dopamine modulates inwardly rectifying potassium currents in medial prefrontal cortex pyramidal neurons. J Neurosci 24(12):3077-3085

Duda OR, Hart PE, Stork DG (2000) Pattern classification. New York, NY: Wiley InterScience

Dupont E, Hanganu IL, Kilb W, Hirsch S, Luhmann HJ (2006) Rapid developmental switch in the mechanisms driving early cortical columnar networks. Nature 439:79-83

Egert U, Schlosshauer B, Fennrich S, Nisch W, Fejtl M, Knott T, Muller T, Hämmerle H (1998) A novel organotypic long-term culture of the rat hippocampus on substrate-integrated multielectrode arrays. Brain Res Brain Res Protoc 2:229-242

Eytan D, Marom S (2006) Dynamics and effective topology underlying synchronization in networks of cortical neurons. J Neurosci 26(33):8465-8476

Fellin T, Pascual O, Gobbo S, Pozzan T, Haydon PG, Carmignoto G (2004) Neuronal synchrony mediated by astrocytic glutamate through activation of extrasynaptic NMDA receptors. Neuron 43:729-743

Fernandes KJL, Fan DP, Tsui BJ, Cassar SL, Tetzlaff W (1999) Influence of the axotomy to cell body distance in rat rubrospinal and spinal motoneurons: differential regulation of GAP-43, tubulins, and neurofilament. J Comp Neurol 414:495-510

Fitch MT, Silver J (2008) CNS injury, glial scars, and inflammation: inhibitory extracellular matrices and regeneration failure. Exp Neurol 209(2):294-301

Floresco SB, West AR, Ash B, Moore H, Grace AA (2003) Afferent modulation of dopamine neuron firing differentially regulates tonic and phasic dopamine transmission. Nat Neurosci 6(9):968-973

Franke H, Schelhorn N, Illes P (2003) Dopaminergic neurons develop axonal projections to their target areas in organotypic co-cultures of the ventral mesencephalon and the striatum/prefrontal cortex. Neurochem Int 42:431-439

Fujisawa S, Buzsáki G (2011) A 4 Hz oscillation adaptively synchronizes prefrontal, VTA, and hippocampal activities. Neuron 72:153-165

Fuster JM (2001) The prefrontal cortex – An update: time is the essence. Neuron 30:319-333

Gähwiler BH, Capogna M, Debanne D, McKinney RA, Thompson SM (1997) Organotypic slice cultures: a technique has come of age. Trends Neurosci 20(10):471-477

Gao M, Liu CL, Yang S, Jin GZ, Bunney BS, Shi WX (2007) Functional coupling between the prefrontal cortex and dopamine neurons in the ventral tegmental area. J Neurosci 27(20):5414-5421

Gao WJ, Krimer LS, Goldman-Rakic PS (2001) Presynaptic regulation of recurrent excitation by D1 receptors in prefrontal circuits. Proc Natl Acad Sci 98(1):295-300

Gao WJ, Wang Y, Goldman-Rakic PS (2003) Dopamine modulation of perisomatic and peridendritic inhibition in prefrontal cortex. J Neurosci 23(5):1622-1630

Gao WJ, Goldman-Rakic PS (2003) Selective modulation of excitatory and inhibitory microcircuits by dopamine. Proc Natl Acad Sci 100(5):2836-2841

Gentet LJ, Williams SR (2007) Dopamine gates action potential back-propagation in midbrain dopaminergic neurons. J Neurosci 27(8):1892-1901

Gireesh ED, Plenz D (2008) Neuronal avalanches organize as nested theta- and beta/gamma-oscillations during development of cortical layer 2/3. Proc Natl Acad Sci 105(21):7576-7581

Glausier JR, Khan ZU, Muly EC (2009) Dopamine D_1 and D_5 receptors are localized to discrete populations of interneurons in primate prefrontal cortex. Cereb Cortex 19:1820-1834

Glowinski J, Tassin JP, Thierry AM (1984) The mesocortico-prefrontal dopaminergic neurons. Trends Neurosci 7(11):415-418

Goldman-Rakic PS, Leranth C, Williams SM, Mons N, Geffard M (1989) Dopamine synaptic complex with pyramidal neurons in primate cerebral cortex. Proc Natl Acad Sci 86:9015-9019

Goldman-Rakic PS, Lidow MS, Smiley JF, Williams MS (1992) The anatomy of dopamine in monkey and human prefrontal cortex. J Neural Transm Suppl 36:163-177

Goldman-Rakic PS (1995) Cellular basis of working memory. Neuron 14:477-485

Goldman-Rakic PS, Muly EC, Williams GV (2000) D_1 receptors in prefrontal cells and circuits. Brain Res Brain Res Rev 31:295-301

Goldstein M, Deutch AY (1992) Dopaminergic mechanisms in the pathogenesis of schizophrenia. FASEB J 6:2413-2421

Goldstein RZ, Volkow ND (2011) Dysfunction of the prefrontal cortex in addiction: neuroimaging findings and clinical implications. Nature 12:652-669

González-Hernández T, Barroso-Chinea P, Acevedo A, Salido E, Rodríguez M (2001) Colocalization of tyrosine hydroxylase and GAD65 mRNA in mesostriatal neurons. Eur J Neurosci 13:57-67

Gonzalez-Islas C, Hablitz JJ (2003) Dopamine enhances EPSCs in layer II-III pyramidal neurons in rat prefrontal cortex. J Neurosci 23(3):867-875

Gorelova N, Seamans JK, Yang CR (2002) Mechanisms of dopamine activation of fast-spiking interneurons that exert inhibition in rat prefrontal cortex. J Neurophysiol 88:3150-3166

Gorelova N, Mulholland PJ, Chandler LJ, Seamans K (2011) The glutamatergic component of the mesocortical pathway emanating from different subregions of the ventral midbrain. Cereb Cortex doi:10.1093/cercor/bhr107

Goto Y, Otani S, Grace AA (2007) The Yin and Yang of dopamine release: a new perspective. Neuropharmacology 53:583-587

Grace AA, Bunney BS (1983a) Intracellular and extracellular electrophysiology of nigral dopaminergic neurons-I. Identification and characterization. Neuroscience 10(2):301-315

Grace AA, Bunney BS (1983b) Intracellular and extracellular electrophysiology of nigral dopaminergic neurons-II. Action potential

generating mechanisms and morphological correlates. Neuroscience 10(2):317-331

Grace AA, Bunney BS (1984a) The control of firing pattern in nigral dopamine neurons: single spike firing. J Neurosci 4(11):2866-2876

Grace AA, Bunney BS (1984b) The control of firing pattern in nigral dopamine neurons: burst firing. J Neurosci 4(11):2877-2890

Grace AA, Onn SP (1989) Morphology and electrophysiological properties of immunocytochemically identified rat dopamine neurons recorded *in vitro*. J Neurosci 9:3463-3481

Gramowski A, Jügelt K, Weiss DG, Gross GW (2004) Substance identification by quantitative characterization of oscillatory activity in murine spinal cord networks on microelectrode arrays. Eur J Neurosci 19:2815-2825

Grenhoff J, Ugedo L, Svensson TH (1988) Firing patterns of midrain dopamine neurons: differences between A9 and A10. Acta Physiol Scand 134:127-132

Groenewegen HJ, Uylings HBM (2000) The prefrontal cortex and the integration of sensory, limbic and autonomic information. Prog Brain Res 126:3-28

Gulledge AT, Jaffe DB (1998) Dopamine decreases the excitability of layer V pyramidal cells in the rat prefrontal cortex. J Neurosci 18(21):9139-9151

Gulledge AT, Jaffe DB (2001) Multiple effects of dopamine on layer V pyramidal cell excitability in rat prefrontal cortex. J Neurophysiol 86:586-595

Gulledge AT, Stuart GJ (2003) Action potential initiation and propagation in layer 5 pyramidal neurons of the rat prefrontal cortex: absence of dopamine modulation. J Neurosci 23(36):11363-11372

Gullo F, Maffezzoli A, Dossi E, Wanke E (2009) Short-latency cross- and autocorrelation identify clusters of interacting cortical neurons recorded from multi-electrode array. J Neurosci Methods 181:186-198

Gullo F, Mazzetti S, Maffezzoli A, Dossi E, Lecchi M, Amadeo A, Krajewski J, Wanke E (2010) Orchestration of "*presto*" and "*largo*" synchrony in up-down activity of cortical networks. Front Neural Circuits 4:11

Gullo F, Maffezzoli A, Dossi E, Lecchi M, Wanke E (2012) Classifying heterogeneity of spontaneous up-states: a method for revealing variations in firing probability, engaged neurons and Fano factor. J Neurosci Methods 203:407-417

Guyenet PG, Aghajanian GK (1978) Antidromic identification of dopaminergic and other output neurons of the rat substantia nigra. Brain Res 150:69-84

Hains BC, Black JA, Waxman SG (2003) Primary cortical motor neurons undergo apoptosis after axotomizing spinal cord injury. J Comp Neurol 462:328-341

Ham MI, Bettencourt LM, McDaniel FD, Gross GW (2008) Spontaneous coordinated activity in cultured networks: analysis of multiple ignition sites, primary circuits, and burst phase delay distributions. J Comput Neurosci 24:346-357

Harel NY, Strittmatter SM (2006) Can regenerating axons recapitulate developmental guidance during recovery from spinal cord injury? Nat Rev Neurosci 7:603-616

Harris KD (2005) Neural signatures of cell assembly organization. Nat Rev Neurosci 6(5):399-407

Harris KD, Barthó P, Chadderton P, Curto C, de la Rocha J, Hollender L, Itskov V, Luczak A, Marguet SL, Renart A, Sakata S (2011) How do neurons work together? Lessons from auditory cortex. Hear Res 271:37-53

Hausser M, Stuart G, Racca C, Sakmann B (1995) Axonal initiation and active dendritic propagation of action potentials in substantia nigra neurons. Neuron 15(3):637-647

He Z, Koprivica V (2004) The Nogo signaling pathway for regeneration block. Annu Rev Neurosci 27:341-368

Heine C, Heimrich B, Vogt J, Wegner A, Illes P, Franke H (2006) P2 receptor-stimulation influences axonal outgrowth in the developing hippocampus *in vitro*. Neuroscience 138:303-311

Heine C, Wegner A, Grosche J, Allgaier C, Illes P, Franke H (2007) P2 receptor expression in the dopaminergic system of the rat brain during development. Neuroscience 149:165-181

Henze DA, González-Burgos GR, Urban NN, Lewis DA, Barrionuevo G (2000) Dopamine increases excitability of pyramidal neurons in primate prefrontal cortex. J Neurophysiol 84:2799-2809

Hnasko TS, Chuhma N, Zhang H, Goh GY, Sulzer D, Palmiter RD, Rayport S, Edwards RH (2010) Vesicular glutamate transport promotes dopamine storage and glutamate corelease *in vivo*. Neuron 65(5):643-656

Hoffman KL and McNaughton BL (2002) Coordinated reactivation of distributed memory traces in primate neocortex. Science 297:2070-2072

Hofmann F, Guenther E, Hämmerle H, Leibrock C, Berezin V, Bock E, Volkmer H (2004) Functional re-establishment of the perforant pathway in organotypic co-cultures on microelectrode arrays. Brain Res 1071:184-196

Hofmann F, Bading H (2006) Long term recordings with microelectrode arrays: studies of transcription-dependent neuronal plasticity and axonal regeneration. J Physiol Paris 99:125-132

Hoftman GD, Lewis DA (2011) Postnatal developmental trajectories of neural circuits in the primate prefrontal cortex: identifying sensitive periods for vulnerability to schizophrenia. Schizophr Bull 37(3):493-503

Holmes C, Jones SA, Greenfield SA (1995) The influence of target and non-target brain regions on the development of mid-brain

dopaminergic neurons in organotypic slice culture. Dev Brain Res 88:212-219

Huebner EA, Strittmatter SM (2009) Axon regeneration in the peripheral and central nervous systems. Results Probl Cell Diff 48:339-351

Hur EE, Zaborszky L (2005) Vglut2 afferents to the medial prefrontal and primary somatosensory cortices: a combined retrograde tracing in situ hybridization study. J Comp Neurol 483:351-373

Isaacson JS, Scanziani M (2011) How inhibition shapes cortical activity. Neuron 72:231-243

Iversen LL, Iversen SD, Dunnet SB, Björklund A (2010) Dopamine Handbook. Ion channels and regulation of dopamine neuron activity (3.4). Oxford University Press, Inc. 198 Madison Avenue New York, New York 10016

Jahnsen H, Kristensen BW, Thiébaud P, Noraberg J, Jakobsen B, Bove M, Martinoia S, Koudelka-Hep M, Grattarola M, Zimmer J (1999) Coupling of organotypic brain slice cultures to silicon-based arrays of electrodes. Methods 18:160-172

Johnson RA, Wichern DW (2002) Applied Multivariate Statistical Analysis, 5th Edn. Upper Saddle River, NJ: Prentice-Hall

Johnson SW, North RA (1992) Two types of neurone in the rat ventral tegmental area and their synaptic inputs. J Physiol 450:455-468

Juergens E, Guettler A, Eckhorn R (1999) Visual stimulation elicits locked and induced gamma oscillations in monkey intracortical- and EEG-potentials, but not in human. Exp Brain Res 129:247-259

Karpiak VC, Plenz D (2002) Preparation and maintenance of organotypic cultures for multi-electrode arrays recordings. In: Current Protocols in Neuroscience (John Wiley & Sons, Inc.) pp 6.15.1-6.15.8, New York

Kauer JA (2004) Learning mechanisms in addiction: synaptic plasticity in the ventral tegmental area as a result of exposure to drugs of abuse. Annu Rev Physiol 66:447-475

Kawano M, Kawasaki A, Sakata-Haga H, Fukui Y, Kawano H, Nogami H, Hisano S (2006) Particular subpopulations of midbrain and hypothalamic dopamine neurons express vesicular glutamate transporter 2 in the rat brain. J Comp Neurol 498:581-592

Keefer EW, Gramowski A, Gross GW (2001) NMDA receptor-dependent periodic oscillations in cultured spinal cord networks. J Neurophysiol 86:3030-3042

Kenet T, Bibitchkov D, Tsodyks M, Grinvald A, Ariell A (2003) Spontaneously emerging cortical representations of visual attributes. Nature 425:954-956

Khaliq ZM, Bean BP (2010) Pacemaking in dopaminergic ventral tegmental area neurons: depolarizing drive from background and voltage-dependent sodium conductances. J Neurosci 30(21):7401-7413

Korotkova TM, Sergeeva OA, Eriksson KS, Haas HL, Brown RE (2003) Excitation of ventral tegmental area dopaminergic and nondopaminergic neurons by orexins/hypocretins. J Neurosci 23(1):7-11

Korotkova TM, Ponomarenko AA, Brown RE, Haas HL (2004) Functional diversity of ventral midbrain dopamine and GABAergic neurons. Mol Neurobiol 29(3):243-259

Koyama S, Kanemitsu Y, Weight FF (2005) Spontaneous activity and properties of two types of principal neurons from the ventral tegmental area of rat. J Neurophysiol 93:3282-3293

Kroener S, Chandler LJ, Phillips PEM, Seamans JK (2009) Dopamine modulates persistent synaptic activity and enhances the signal-to-noise ratio in the prefrontal cortex. PloS ONE 4(8):e6507

Kruse MS, Prémont J, Krebs MO, Jay TM (2009) Interaction of dopamine D1 with NMDA NR1 receptors in rat prefrontal cortex. Eur Neuropsychopharmacol 19:296-304

Lammel S, Hetzel A, Häckel O, Jones I, Liss B, Roeper J (2008) Unique properties of mesoprefrontal neurons within a dual mesocorticolimbic dopamine system. Neuron 57:760-773

Lapish CC, Kroener S, Durstewitz D, Lavin A, Seamans JK (2007) The ability of mesocortical dopamine system to operate in distinct temporal modes. Psychopharmacology 191:609-625

Lavin A, Nogueira L, Lapish CC, Wightman RM, Phillips PEM, Seamans JK (2005) Mesocortical dopamine neurons operate in

distinct temporal domains using multimodal signalling. J Neurosci 25(20):5013-5023

Lewis DA, Sesack SR, Levey AI, Rosemberg DR (1998) Dopamine axons in primate prefrontal cortex: specificity of distribution, synaptic targets and development. In: Advances in pharmacology, Vol. 42 (Goldstein D, Eisenhofer G, McCarty R, ed) pp 703-706. San Diego: Academic Press

Lewis DA, Hashimoto T, Volk DW (2005) Cortical inhibitory neurons and schizophrenia. Nature 6:312-324

Liss B, Franz O, Sewing S, Bruns R, Neuhoff H, Roeper J (2001) Tuning pacemaker frequency of individual dopaminergic neurons by Kv4.3L and KChip3.1 transcription. EMBO J 20:5715-5724

Liss B, Haeckel O, Wildmann J, Miki T, Seino S, Roeper J (2005) K-ATP channels promote the differential degeneration of dopaminergic midbrain neurons. Nat Neurosci 8(12):1742-1751

Liss B, Roeper J (2008) Individual dopamine midbrain neurons: functional diversity and flexibility in health and disease. Brain Res Brain Res Rev 58:314-321

Lodge DJ (2011) The medial prefrontal and orbitofrontal cortices differentially regulate dopamine system function. Neuropsychopharmacology 36:1227-1236

Luczak A, Barthó P, Marguet SL, Buzsáki G, Harris KD (2007) Sequential structure of neocortical spontaneous activity *in vivo*. Proc Natl Acad Sci 104(1):347-352

Luczak L, Barthó P, Harris KD (2009) Spontaneous events outline the realm of possible sensory responses in neocortical populations. Neuron 62(3):413-425

Maeda T, Fukazawa Y, Shimizu N, Ozaki M, Yamamoto H, Kishioka S (2004) Electrophysiological characteristic of corticoaccumbens synapses in rat mesolimbic system reconstructed using organotypic slice cultures. Brain Res 1015:34-40

Margolis EB, Lock H, Chefer VI, Shippenberg TS, Hjelmstad GO, Fields HL (2006a) Kappa opioids selectively control dopaminergic neurons projecting to the prefrontal cortex. Proc Natl Acad Sci U S A 103:2938-2942

Margolis EB, Lock H, Hjelmstad GO, Fields HL (2006b) The ventral tegmental area revisited: is there an electrophysiological marker for dopaminergic neurons? J Physiol 577(3):907-924

Margolis EB, Mitchell JM, Ishikawa J, Hjelmstad GO, Fields HL (2008) Midbrain dopamine neurons: projection target determines action potential duration and dopamine D_2 receptor inhibition. J Neurosci 28(36):8908-8913

Matsuda Y, Marzo A, Otani S (2006) The presence of background dopamine signal converts long-term synaptic depression to potentiation in rat prefrontal cortex. J Neurosci 26(18):4803-4810

McDonald JW (1999) Repairing the damaged spinal cord. Sci Am 281:64-73

Melchitzky DS, Sesack SR, Pucak ML, Lewis DA (1998) Synaptic targets of pyramidal neurons providing intrinsic horizontal connections in monkey prefrontal cortex. J Comp Neurol 390:211-224

Mechitzky DS, González-Burgos G, Barrionuevo G, Lewis DA (2001) Synaptic targets of the intrinsic axon collaterals of supragranular pyramidal neurons in monkey prefrontal cortex. J Comp Neurol 430:209-221

Miller EK, Freedman DJ, Wallis JD (2002) The prefrontal cortex: categories, concepts and cognition. Phil Trans R Soc Lond C, 357:1123-1136

Missale C, Nash R, Robinson SW, Jaber M, Caron MG (1998) Dopamine receptors: from structure to function. Physiol Rev 78(1):189-225

Mrzljak L, Bergson C, Pappy M, Huff R, Levenson R, Goldman-Rakic PS (1996) Localization of dopamine D4 receptors in GABAergic neurons of the primate brain. Nature 381:245-248

Muly EC, Szigeti K, Goldman-Rakic PS (1998) D1 receptor in interneurons of macaque prefrontal cortex: distribution and subcellular localization. J Neurosci 18(24):10553-10565

Muramatsu R, Ueno M, Yamashita (2009) Intrinsic regenerative mechanisms of central nervous system neurons. Biosci Trends 3(5):179-183

Naito A, Kita H (1994) The cortico-nigral projection in the rat: an anterograde tracing study with biotinylated dextran amine. Brain Res 637:317-322

Neuhoff H, Neu A, Liss B, Roeper J (2002) I_h channels contribute to the different functional properties of identified dopaminergic subpopulations in the midbrain. J Neurosci 22:1290-1302

Oades RD, Halliday GM (1987) Ventral tegmental (A10) system: neurobiology. 1. Anatomy and connectivity. Brain Res Brain Res Rev 12:117-165

Oda S, Funato H, Adachi-Akahane S, Ito M, Okada A, Igarashi H, Yokofujita J, Kuroda M (2010) Dopamine D5 receptor immunoreactivity is differentially distributed in GABAergic interneurons and pyramidal cells in rat medial prefrontal cortex. Brain Res 1329:89-102

Østergaard K, Schou JP, Zimmer J (1990) Rat ventral mesencephalon grown as organotypic slice cultures and co-cultured with striatum, hippocampus, and cerebellum. Exp Brain Res 82:547-565

Otani S, Blond O, Desce JM, Crépel F (1998) Dopamine facilitates long-term depression of glutamatergic transmission in rat prefrontal cortex. Neuroscience 85:669-676

Overton PG, Clark D (1997) Burst firing in midbrain dopaminergic neurons. Brain Res Brain Res Rev 25:312-334

Papp ECS, Heimrich B, Freund TF (1995) Development of the raphe-hippocampal projection *in vitro*. Neurosci 69:99-105

Paspalas CD, Rakic P, Goldman-Rakic PS (2006) Internalization of D2 dopamine receptors is clathrin-dependent and select to dendro-axonic appositions in primate prefrontal cortex. Eur J Neurosci 24:1395-1403

Pearson J, Goldstein M, Markey K, Brandeis L (1983) Human brainstem catecholamine neuronal anatomy as indicated by immunocytochemistry with antibodies to tyrosine hydroxylase. Neuroscience 8:3-32

Peter Y, Barnhardt NE, O'Donnell P (2004) Prefrontal cortical up states are synchronized with ventral tegmental area activity. Synapse 52:143-152

Pickel VM, Garzón M, Mengual E (2002) Electron microscopic immunolabeling of transporters and receptors identifies transmitter-specific functional sites envisioned in Cajal's neuron. Prog Brain Res 136:145-155

Plenz D, Aertsen A (1996a) Neural dynamics in cortex-striatum co-cultures-I. Anatomy and electrophysiology of neuronal cell types. Neuroscience 70(4):861-891

Plenz D, Aertsen A (1996b) Neural dynamics in cortex-striatum co-cultures-II. Spatiotemporal characteristics of neuronal activity. Neuroscience 70(4):893-924

Plenz D, Thiagarajan TC (2007) The organizing principles of neuronal avalanches: cell assemblies in the cortex? Trends Neurosci 30(3):101-110

Pouille F, Marin-Burgin A, Adesnik H, Atallah BV, Scanziani M (2009) Input normalization by global feedforward inhibition expands cortical dynamic range. Nat Neurosci 12(12):1577-1585

Preuss TM (1995) Do rats have prefrontal cortex? The Rose-Woolsey-Akert program reconsidered. J Cognit Neurosci 7:1-24

Rasch MJ, Gretton A, Murayama Y, Maass W, Logothetis NK (2008) Inferring spike trains from local field potentials. J Neurophysiol 99:1461-1476

Rennie S, Lotto RB, Price DJ (1994) Growth-promoting interactions between the murine neocortex and thalamus in organotypic co-cultures. Neuroscience 61(3):547-564

Rotaru DC, Lewis DA, Gonzalez-Burgos G (2007) Dopamine D1 receptor activation regulates sodium channel-dependent EPSP amplification in rat prefrontal cortex pyramidal neurons. J Physiol 581(3):981-1000

Salthun-Lassalle B, Hirsch E, Wolfart J, Ruberg M, Michel PP (2004) Rescue of mesencephalic dopaminergic neurons in culture by low-level stimulation of voltage-gated sodium channels. J Neurosci 24(26):5922-5930

Sanchez-Vives MV, McCormick DA (2000) Cellular and network mechanisms of rhythmic recurrent activity in neocortex. Nat Neurosci 3(10):1027-1034

Santos GS, Gireesh ED, Plenz D, Nakahara H (2010) Hierarchical interaction structure of neural activities in cortical slice cultures. J Neurosci 30:8720-8733

Schultz W (1986) Responses of midbrain dopamine neurons to behavioural trigger stimuli in the monkey. J Neurophysiol 56(5):1439-1461

Schwab JM, Brechtel K, Mueller CA, Failli V, Kaps HP, Tuli SK, Schluesener HJ (2006) Experimental strategies to promote spinal cord regeneration—an integrative perspective. Prog Neurobiol 78:91-116

Seamans JK, Gorelova N, Dustewitz D, Yang CR (2001) Bidirectional dopamine modulation of GABAergic inhibition in prefrontal cortical pyramidal neurons. J Neurosci 21(10):3628-3638

Seamans JK, Nogueira L, Lavin A (2003) Synaptic basis of persistent activity in prefrontal cortex *in vivo* and in organotypic cultures. Cereb Cortex 13:1242-1250

Seamans JK, Yang CR (2004) The principal features and mechanisms of dopamine modulation in the prefrontal cortex. Prog Neurobiol 74:1-57

Sesack SR, Pickel VM (1992) Prefrontal cortical efferents in the rat synapse on unlabeled neuronal targets of catecholamine terminals in the nucleus accumbens septi and on dopamine neurons in the ventral tegmental area. J Comp Neurol 320:145-160

Sesack SR, Hawrylak VA, Melchitzky DS, Lewis DA (1998) Dopamine innervation of a subclass of local circuit neurons in

monkey prefrontal cortex: ultrastructural analysis of tyrosine hydroxylase and parvalbumin immunoreactive structures. Cereb Cortex 8:614-622

Sesack SR, Carr DB, Omelchenko N, Pinto A (2003) Anatomical substrates for glutamate-dopamine interactions. Evidence for specificity of connections and extrasynaptic actions. Ann N Y Acad Sci 1003:36-52

Shew WL, Yang H, Petermann T, Roy R, Plenz D (2009) Neuronal avalanches imply maximum dynamic range in cortical networks at criticality. J Neurosci 29(49):15595-15600

Shimono K, Baudry M, Ho L, Taketani M, Lynch G (2002a) Long-term recordings of LTP in cultured hippocampal slices. Neural Plasticity 9:249-254

Shimono K, Baudry M, Panchenko V, Taketani M (2002b) Chronic multichannel recordings from organotypic hippocampal slice cultures: protection from excitotoxic effects of NMDA by non-competitive NMDA antagonists. J Neurosci Methods 120:193-202

Silver J, Miller JH (2004) Regeneration beyond the glial scar. Nat Rev Neurosci 5:146-156

Simeone A, Di Salvio M, Di Giovannantonio LG, Acampora D, Omodei D, Tomasetti C (2011) The role of Otx2 in adult mesencephalic-diencephalic dopaminergic neurons. Mol Neurobiol 43:107-113

Smiley JF, Goldman-Rakic PS (1993) Heterogeneous targets of dopamine synapses in monkey prefrontal cortex demonstrated by serial section electron microscopy: a laminar analysis using the silver-enhanced diaminobenzidine sulfide (SEDS) immunolabeling technique. Cereb Cortex 3(3):223-238

Snyder-Keller A, Tseng KY, Lyng GD, Graber DJ, O'Donnell P (2008) Afferent influences on striatal development in organotypic cocultures. Synapse 62:487-500

Steffensen SC, Svingos AL, Pickel VM, Henriksen SJ (1998) Electrophysiological characterization of GABAergic neurons in the ventral tegmental area. J Neurosci 18(19):8003-8015

Steketee JD (2003) Neurotransmitter systems of the medial prefrontal cortex: potential role in sensitization to psychostimulants. Brain Res Rev 41:203-228

Steriade M, Nuñez A, Amzica F (1993) A novel slow (< 1 Hz) oscillation of neocortical neurons *in vivo*: depolarizing and hyperpolarizing components. J Neurosci 13(8):3252-3265

Steward O, Zheng B, Tessier-Lavigne M, Hofstadter M, Sharp K, Yee KM (2008) Regenerative growth of corticospinal tract axons via the ventral column after spinal cord injury in mice. J Neurosci 28:6836-6847

Stewart CV, Plenz D (2006) Inverted-U profile of dopamine-NMDA-mediated spontaneous avalanche recurrence in superficial layers of rat prefrontal cortex. J Neurosci 26(31):8148-8159

Stewart CV, Plenz D (2008) Homeostasis of neuronal avalanches during postnatal cortex development *in vitro*. J Neurosci Methods 169:405-416

Stoppini L, Buchs PA, Muller D (1991) A simple method for organotypic cultures of nervous tissue. J Neurosci Methods 37:173-182

Stuber GD, Hnasko TS, Britt JP, Edwards RH, Bonci A (2010) Dopaminergic terminals in the nucleus accumbens but not the dorsal striatum corelease glutamate. J Neurosci 30(24):8229-8233

Sullivan RM, Brake WG (2003) What the rodent prefrontal cortex can teach us about attention-deficit/hyperactivity disorder: the critical role of early developmental events on prefrontal function. Behav Brain Res 146:43-55

Sulzer D, Joyce MP, Lin L, Geldwert D, Haber SN, Hattori T, Rayport S (1998) Dopamine neurons make glutamatergic synapses *in vitro*. J Neurosci 18(12):4588-4602

Sulzer D, Schmitz Y (2007) Parkinson's disease: return of an old prime suspect. Neuron 55:8-10

Sun JJ, Luhmann HJ (2007) Spatio-temporal dynamics of oscillatory network activity in the neonatal mouse cerebral cortex. Eur J Neurosci 26:1995-2004

Sur M, Angelucci A, Sharma J (1999) Rewiring cortex: the role of patterned activity in development and plasticity of neocortical circuits. J Neurobiol 41:33-43

Tateno T, Jimbo Y, Robinson HPC (2005) Spatio-temporal cholinergic modulation in cultured networks of rat cortical neurons: spontaneous activity. Neuroscience 134:425-437

Thierry AM, Deniau JM, Herve D, Chevalier G (1980) Electrophysiological evidence for non-dopaminergic mesocortical and mesolimbic neurons in the rat. Brain Res 201(1):210-214

Thierry AM, Chevalier G, Ferron A, Glowinski J (1983) Diencephalic and mesencephalic efferents of the medial prefrontal cortex in the rat: electrophysiological evidence for the existence of branched axons. Exp Brain Res 50:275-282

Thompson I (1997) Cortical development: a role for spontaneous activity? Curr Biol 7:R324-R326

Thurley K, Senn W, Lüscher HR (2008) Dopamine increases the gain of the input-output response of rat prefrontal pyramidal neurons. J Neurophysiol 99:2985-2997

Tierney PL, Thierry AM, Glowinski J, Deniau JM, Gioanni Y (2008) Dopamine modulates temporal dynamics of feedforward inhibition in rat prefrontal cortex *in vivo*. Cereb Cortex 18:2251-2262

Tong ZY, Overton PG, Clark D (1996) Stimulation of the prefrontal cortex in the rat induces patterns of activity in midbrain dopaminergic neurons which resemble natural burst events. Synapse 22:195-208

Trantham-Davidson H, Neely LC, Lavin A, Seamans JK (2004) Mechanisms underlying differential D1 versus D2 dopamine receptor

regulation of inhibition in prefrontal cortex. J Neurosci 24(47):10652-10659

Tseng KY, O'Donnell P (2004) Dopamine-glutamate interactions controlling prefrontal cortical pyramidal cell excitability involve multiple signalling mechanisms. J Neurosci 24(22):5131-5139

Tseng KY, Mallet N, Toreson KL, Le Moine C, Gonon F, O'Donnell P (2006) Excitatory response of prefrontal cortical fast-spiking interneurons to ventral tegmental area stimulation *in vivo*. Synapse 59(7):412-417

Tseng KY, O'Donnell P (2007) D_2 dopamine receptors recruit a GABA component for their attenuation of excitatory synaptic transmission in the adult rat prefrontal cortex. Synapse 61:843-850

Urban NN, González-Burgos G, Henze DA, Lewis DA, Barrionuevo G (2002) Selective reduction by dopamine of excitatory synaptic inputs to pyramidal neurons in primate prefrontal cortex. J Physiol 539(3):707-712

Van Bergen A, Papanikolaou T, Schuker A, Möller A, Schlosshauer B (2003) Long-term stimulation of mouse hippocampal slice culture on microelectrode array. Brain Res Brain Res Protoc

Van den Heuvel DMA, Pasterkamp RJ (2008) Getting connected in the dopamine system. Prog Neurobiol 85:75-93

Van De Werd HJJM, Rajkowska G, Evers P, Uylings HBM (2010) Cytoarchitectonic and chemoarchitectonic characterization of the prefrontal cortical areas in the mouse. Brain Struct Funct 214:339-353

Van Pelt J, Corner MA, Wolters PS, Rutten WLC, Ramakers GJA (2004) Longterm stability and developmental changes in spontaneous network burst firing patterns in dissociated rat cerebral cortex cell cultures on multielectrode arrays. Neurosci Lett 361:86-89

Vijayraghavan S, Wang M, Birnbaum SG, Williams GV, Arnsten AFT (2007) Inverted-U dopamine D1 receptor actions on prefrontal neurons engaged in working memory. Nat Neurosci 10(3):376-384

Wagenaar DA, Pine J, Potter SM (2006) An extremely rich repertoire of bursting patterns during the development of cortical cultures. BMC Neurosci 7:11

Wang Y, Goldman-Rakic PS (2004) D2 receptor regulation of synaptic burst firing in prefrontal cortical pyramidal neurons. Proc Natl Acad Sci 101(14):5093-5098

Williams GV, Goldman-Rakic PS (1995) Modulation of memory fields by dopamine D1 receptors in prefrontal cortex. Nature 376:572-575

Williams SM, Goldman-Rakic PS (1998) Widespread origin of the primate mesofrontal dopamine system. Cereb Cortex 8:321-345

Yamaguchi T, Sheen W, Morales M (2007) Glutamatergic neurons are present in the rat ventral tegmental area. Eur J Neurosci 25:106-118

Yamaguchi T, Wang HL, Li X, Ng TH, Morales M (2011) Mesocorticolimbic glutamatergic pathway. J Neurosci 31(23):8476-8490

Yang SR, Seamans JK (1996) Dopamine D1 receptor actions in layer V-VI rat prefrontal cortex neurons *in vitro*: modulation of dendritic-somatic signal integration. J Neurosci 16(5):1922-1935

Yang CR, Seamans JK, Gorelova N (1999) Developing a neuronal model for the pathophysiology of schizophrenia based on the nature of electrophysiological actions of dopamine in the prefrontal cortex. Neuropsychopharmacology 21(2):161-194

Yuen EY, Yan Z (2009) Dopamine D_4 receptors regulate AMPA receptor trafficking and glutamatergic transmission in GABAergic interneurons of prefrontal cortex. J Neurosci 29(2):550-562

Zheng P, Zhang XX, Bunney BS, Shi WX (1999) Opposite modulation of cortical *N*-methyl-D-aspartate receptor-mediated responses by low and high concentrations of dopamine. Neuroscience 91(2):527-535

Zhou FM, Hablitz JJ (1999) Dopamine modulation of membrane and synaptic properties of interneurons in rat cerebral cortex. J Neurophysiol 81:967-976

8. PUBLICATIONS

Gullo F, Maffezzoli A, Dossi E, Wanke E (2012) Classifying heterogeneity of spontaneous up-states: a method for revealing variations in firing probability, engaged neurons and Fano factor. J Neurosci Methods 203:407-417

Gullo F, Mazzetti S, Maffezzoli A, Dossi E, Lecchi M, Amadeo A, Krajewski J, Wanke E (2010) Orchestration of '*presto*' and '*largo*' synchrony in up-down activity of cortical networks. Front Neural Circuits 4:11

Gullo F, Maffezzoli A, Dossi E, Wanke E (2009) Short-latency cross- and autocorrelation identify clusters of interacting cortical neurons recorded from multi-electrode array. J Neurosci Methods 181:186–198.

9. ACKNOWLEDGEMENTS

A special thank to…

…Prof. Enzo Wanke, for his precious help and support during these three years of the PhD program, during which I could learn and travel a lot.

…Prof. Heike Franke and Dr. Claudia Heine, for their help in learning the organotypic co-culture technique, but, above all, for their friendship and support. I wish you all the best in your life and many congratulations to Claudia for your baby and your new life. I wish I will come back to Leipzig one day to see you again and to enjoy a tempting piece of German cake with you!

…Prof. Peter Illes, for his help during the period in Leipzig.

…Fra, a colleague and, above all, a faithful friend. You have to promise me that you will come to visit me wherever I will go to work! And I promise you that wherever I will go, I will find the best places for a healthy, satisfactory and rewarding shopping! The same is for you Marzia, you should come together with Fra and we will consume our credit card. It has been very nice to work with you on our reconstructed visual system, I always have my fingers crossed about it. Eli, even if almost a year has passed since you have left the lab, it is like you are still here with us; all the best for you, Stefano, Giulia and the two babies Sara and Emma. Fra, Marzia, Eli.. I know that I will miss you so much when I will be in another place…

…Antonella, Giuseppe, Simone and all the students that I have met during these three PhD years in the lab. Good luck for your degree and your future biologist carreer.

…Anna, Sara, Barbara, Marina, Diana… my university friends… Even if we cannot meet together often, remind that I always keep you in my best thoughts!

…Clara, Claudio, Francesco, Giovanni, Isabella, Miriam, Riccardo, who have been my "colleagues" in the PhD adventure (PhD course in Biology, XXIV cycle, University of Milano-Bicocca). Good luck for our "discussion day"!

…all the people of the U3 third floor, who are still there or have searched their way somewhere else… including Paola, Patrizia, Marcella, Claudia, Riccardo, Alice, Luca.

…all the friends of a life.. Cla, Cinzia, Fede, Mary, Micky, Cero, Bene, Gaia.. This thesis is dedicated also to everyone of you, for your precious friendship and support!

…Vadym (with his Maya and Sasha), Laura and Laura, with whom I have spent very beautiful days in Washington at the Neuroscience Meeting 2011.

…Davide and Fede, my little (only for the age) brother and my cousin who always root for me, together with grandmothers Olga and Emma (in the kingdom of heaven with my grandfathers), Claudia and Sergio, Auri, Franco and Antonia, Chiara with Mario, Tommaso and Martina.

…Mum and Dad, two fundamental points of reference of my life, two sources of infinite love and support, two people who are always present when a help is needed or desired. Every written word in this thesis wouldn't be possible without you. I will always be your "Bimba".

…Davide… I will always remember when I first met you in Germany, at the congress that changed my life forever. Since that moment a lot of time has passed, one year and a half ago we started our new life together and I couldn't ever imagine my future without you. You always lied by me during these years, you helped me when I needed help, you supported me when I felt down, you advised me when I was hesitant, you listened to me when I was angry or nervous. Life wouldn't be life without you.

A huge hug to everyone,

Elena